



Phase B

Electrical Power System (EPS)

Report of Diploma

Prepared by:
Fabien Jordan

Checked by:

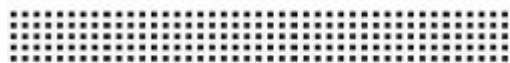
Approved by:

•
HEIG-VD
Yverdon
Switzerland
•
20/12/2006
•

heig-vd

Haute Ecole d'Ingénierie et de Gestion
du Canton de Vaud

Institut d'
Automatisation
Industrielle



Université
Neuchâtel

unine Hes-SO

Haute Ecole Spécialisée
de Suisse occidentale



ÉCOLE POLYTECHNIQUE
FÉDÉRALE DE LAUSANNE



RECORD OF REVISIONS

ISS/REV	Date	Modifications	Created/modified by
1/0	15.12.06	Initial Issue	Fabien Jordan
1/1			
1/2			



PREFACE

This present report is a part of the ongoing design of the first Swiss CubeSat satellite, under the project name SwissCube. The project is a consortium of Swiss schools – made up of EPFL, the University of Neuchâtel, and the HES-SO – to build competences in space related fields.

The report studies the use of an existing power system concept designed by the European Space Agency's technical center for a microsatellite, to be used on SwissCube picosatellite.

The use of the CubeSat standard limits the satellite's size and weight. This requires the electrical power system to be as much efficient and robust as possible taking in account the very low mass and space available. This study is a project assignment performed at the Swiss engineer's school of Yverdon (HEIG-VD) department of Industrial Automation, for an engineering diploma.

This work has been realised with the help of several people. First I would like to thank my wife for her full support. Then I would like to thank my advisor, Professor Marc Correvon, for his valuable feedback through this autumn, and for enriching my knowledge of electronics. Finally, I would also like to thank Professor Muriel Noca and Renato Krpoun at EPFL as well as all students of SwissCube for a positive and motivating work environment.

Yverdon December 19, 2006

Fabien Jordan



TABLE OF CONTENTS

1	INTRODUCTION.....	12
1.1	BACKGROUND	13
1.1.1	<i>CubeSat concept</i>	13
1.1.2	<i>P-POD Interface.....</i>	14
1.1.3	<i>Launch Vehicle</i>	15
1.1.4	<i>Science mission Objectives</i>	16
1.1.5	<i>Electrical Power System Role.....</i>	17
1.2	PROJECT OBJECTIVES.....	18
1.2.1	<i>Solar Cells</i>	18
1.2.2	<i>Batteries.....</i>	18
1.2.3	<i>Power management.....</i>	18
1.2.4	<i>Design of electronics</i>	18
1.2.5	<i>Kill-switches</i>	18
1.3	BASELINE DESIGN	19
1.3.1	<i>Architecture</i>	19
1.3.2	<i>Basic Principle.....</i>	19
1.3.3	<i>Voltage Control</i>	20
2	POWER SYSTEM REQUIREMENTS	21
2.1	SUMMARY OF POWER SYSTEM REQUIREMENTS.....	22
2.2	VACUUM	23
2.3	TEMPERATURE	25
2.4	DERATING	26
2.5	RADIATION.....	26
2.6	ACCELERATION AND VIBRATION	27
3	SUMMARY OF ARCHITECTURE SELECTION	28
3.1	ARCHITECTURE WITH MPPT	29
3.1.1	<i>Solar cells in series – Batteries in series</i>	30
3.1.2	<i>Solar cells in series – Batteries in parallel</i>	30
3.1.3	<i>Solar cells in parallel – Batteries in parallel.....</i>	31
3.1.4	<i>Synthesized comparison</i>	31
3.2	ARCHITECTURE WITHOUT MPPT	33
4	SOLAR CELL: MODELLING AND MEASUREMENTS.....	35
4.1	GENERAL DESCRIPTION	36
4.1.1	<i>Electrical functioning</i>	36
4.1.2	<i>Models</i>	36
4.1.3	<i>Measurements</i>	36
4.2	CLASSICAL MODEL	37
4.3	SIMPLIFIED MODEL	40
4.3.1	<i>Parameters definition</i>	42
4.3.2	<i>Iterative Algorithm $I_{SC}=f(V_{SC})$</i>	42
4.3.3	<i>Variations of the Insolation</i>	45
4.3.4	<i>Variations of the Temperature</i>	47
4.3.5	<i>Series connection</i>	48
4.3.6	<i>Protection Diode.....</i>	48
4.3.7	<i>I-V characteristic of two cells in series with a protection diode.....</i>	48
4.3.8	<i>Comparison with measurements</i>	50
4.3.9	<i>Experimental Installation</i>	50
5	BATTERY CONSIDERATION	52
5.1	LITHIUM-ION POLYMER TECHNOLOGY	53

5.2	BATTERY SELECTION	54
5.2.1	<i>Importance of Thermal Design</i>	54
5.2.2	<i>VARTA PoLiFlex</i>	55
5.2.3	<i>PLF503759</i>	57
5.2.4	<i>Protection Circuit Module (PCM)</i>	61
5.3	SYNTHESIZED POWER BUDGET	64
6	BASELINE DESIGN	65
6.1	GENERAL DESCRIPTION.....	66
6.2	SPECIFICATIONS	67
6.3	BATTERY CHARGE CIRCUIT	68
6.3.1	<i>Step-up converter</i>	68
6.3.2	<i>Voltage Control</i>	68
6.3.3	<i>Burst Mode Control</i>	73
6.3.4	<i>Oscillator frequency</i>	75
6.3.5	<i>Inductor selection</i>	76
6.3.6	<i>Internal Current Limitation</i>	77
6.3.7	<i>Shut-Down the converter</i>	77
6.3.8	<i>Other passive components</i>	78
6.4	CHARGE CURRENT CONTROL.....	79
6.4.1	<i>Charging current measure</i>	79
6.4.2	<i>Voltage at terminals of the battery</i>	81
6.4.3	<i>Current regulator</i>	81
6.5	BATTERY DISCHARGE CIRCUIT	83
6.5.1	<i>Step-down converter</i>	83
6.5.2	<i>Voltage Control</i>	83
6.5.3	<i>Burst Mode Control</i>	87
6.5.4	<i>Oscillator frequency</i>	88
6.5.5	<i>Inductor selection</i>	89
6.5.6	<i>Output Capacitor</i>	90
6.5.7	<i>Shut-Down the converter</i>	92
6.5.8	<i>Other passive components</i>	92
6.6	DISCHARGE CURRENT CONTROL.....	93
6.6.1	<i>Discharging current measure</i>	93
6.6.2	<i>Current regulator</i>	94
6.7	POWER BUS VOLTAGE CONTROL	96
6.7.1	<i>Sum of currents</i>	96
6.7.2	<i>Relationship between the current and the voltage of the bus capacitor</i>	96
6.7.3	<i>Voltage Regulator</i>	96
6.8	CONTROL BLOCK DIAGRAM	101
6.9	CHARGE AND DISCHARGE SECURITIES	102
6.9.1	<i>Introduction</i>	102
6.9.2	<i>Design of protections with the LTC1442</i>	102
6.9.3	<i>Discharge protection switch</i>	104
6.10	DISSIPATION SYSTEM	105
6.10.1	<i>Electronic design</i>	106
6.10.2	<i>Calculation of the power dissipation</i>	107
6.10.3	<i>Choice of components</i>	108
6.10.4	<i>Control of the bus voltage with the dissipation system</i>	113
6.10.5	<i>Control Block diagram of the dissipation system</i>	116
6.11	LAYOUT OF THE PCB	118
7	SIMULATIONS OF THE POWER SYSTEM	120
7.1	CHARGE CURRENT CONTROL LOOP	121
7.1.1	<i>Step-up converter</i>	121
7.1.2	<i>Battery</i>	122
7.1.3	<i>Measure System</i>	124
7.1.4	<i>Gain of correction (input of the PI)</i>	124
7.1.5	<i>System to control (open loop, without the regulator)</i>	124

7.1.6	<i>Synthesis of the PI Regulator</i>	126
7.1.7	<i>Results of the simulation with Simulink</i>	128
7.2	DISCHARGE CURRENT CONTROL LOOP	129
7.2.1	<i>Step-down converter</i>	129
7.2.2	<i>Bus Capacitor</i>	129
7.2.3	<i>Measure System</i>	130
7.2.4	<i>Gain of correction (input of PI)</i>	130
7.2.5	<i>System to control (open loop, without the regulator)</i>	130
7.2.6	<i>Synthesis of the PI Regulator</i>	131
7.2.7	<i>Results of the simulation with Simulink</i>	134
7.3	BUS VOLTAGE CONTROL LOOP	135
8	PRELIMINARY TESTS	136
8.1	TEST OF KILL-SWITCHES.....	137
8.1.1	<i>Test 1: DC current through the kill-switch in vacuum</i>	137
8.1.2	<i>Test 2: DC current limit (without commutation)</i>	137
8.1.3	<i>Test 3: DC current limit (with commutation)</i>	138
8.2	TEST OF BATTERIES	139
8.2.1	<i>Test 1: Vacuum chamber (mechanical test)</i>	139
8.2.2	<i>Electrical tests (Vacuum + Temperature variations)</i>	140
8.3	IDENTIFICATION OF THE PARAMETERS OF THE DC/DC CONVERTERS	141
8.3.1	<i>Step-up converter</i>	141
8.3.2	<i>Step-down converter</i>	143
9	CONCLUSION AND FUTURE WORK.....	145
9.1	RESULTS AND DIFFICULTIES.....	146
9.1.1	<i>Solar Cells</i>	146
9.1.2	<i>Batteries</i>	146
9.1.3	<i>Power management</i>	146
9.1.4	<i>Design of electronics</i>	146
9.1.5	<i>Kill-switches</i>	147
9.2	FUTURE WORK.....	147
10	REFERENCES.....	149
10.1	NORMATIVE REFERENCES.....	149
10.2	INFORMATIVE REFERENCE.....	149
11	TERMS, DEFINITIONS AND ABBREVIATED TERMS	150
11.1	ABBREVIATED TERMS.....	150
11.1.1	<i>Subsystems abbreviations</i>	150
11.1.2	<i>Technical abbreviations</i>	150
11.1.3	<i>Definitions</i>	151
DATE AND SIGNATURE.....		152
ANNEXES.....		153



1 INTRODUCTION

Abstract

This present project deals with practical design and implementation of a power supply for CubeSat picosatellite. The introduction presents the SwissCube's project background. Then the objectives and the requirements of the projects are treated. Finally the baseline design is explained in a synthesized manner.

1.1 Background

SwissCube project aims to design a picosatellite according to the conventional standard provided by CubeSat. The design and the development of the SwissCube picosatellite are carried out by students of the Swiss Federal Institute of Technology in Lausanne (EPFL) and other Swiss engineer schools and universities.

1.1.1 CubeSat concept

The CubeSat's concept developed by CalPoly is an international collaboration of over 40 universities, high schools, and private firms developing picosatellites containing scientific, private, and government payloads.

The primary mission of this program is to provide access to space for small payloads.

The CubeSat's program gives students the opportunity to work in the space technologies field. This opportunity is possible by reducing the cost and development time generally associated with satellite design. To reduce these costs and time constraints it is necessary to drastically reduce the dimensions of the satellite.

It is the reason why the fundamental defining feature of the CubeSat standard is its dimensions of **10 x 10 x 10 cm** and its mass of no more than **1 kg**.

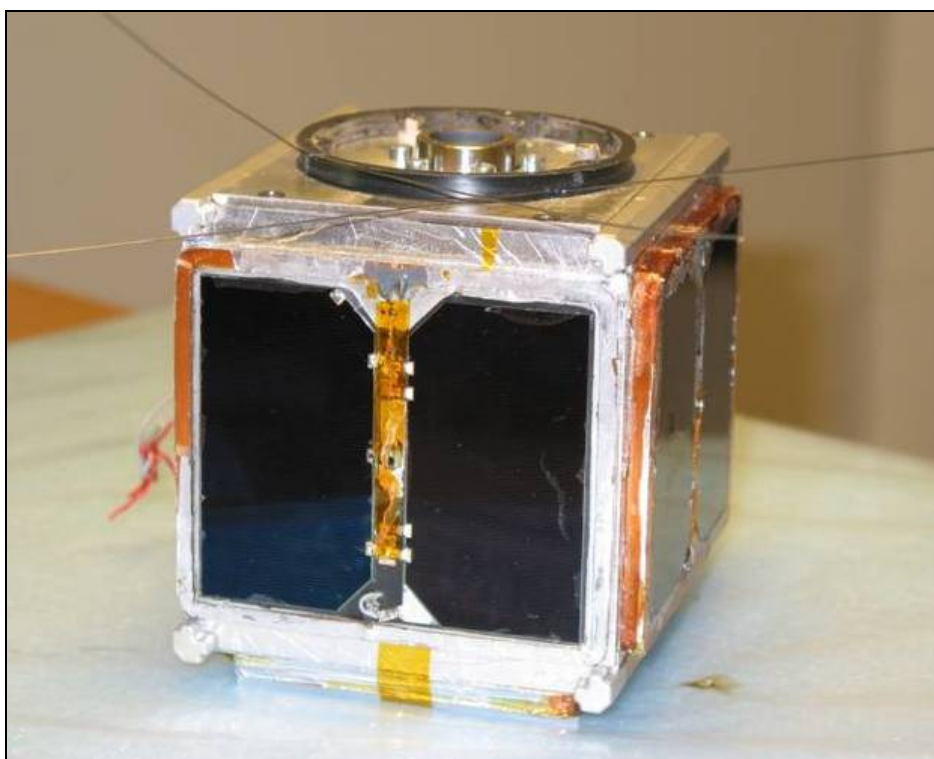


Figure 1-1 : Example: AAUSAT-1 CubeSat

1.1.2 P-POD Interface

The Poly Picosatellite Orbital Deployer (P-POD) is Cal Poly's standardized CubeSat deployment system. It is capable of carrying three standard CubeSats and serves as the interface between the CubeSats and LV (Launch Vehicle). The P-POD is an aluminium rectangular box with a door and a spring mechanism. CubeSats slide along a series of rails during ejection into orbit. CubeSats must be compatible with the P-POD to ensure safety and success of the mission.

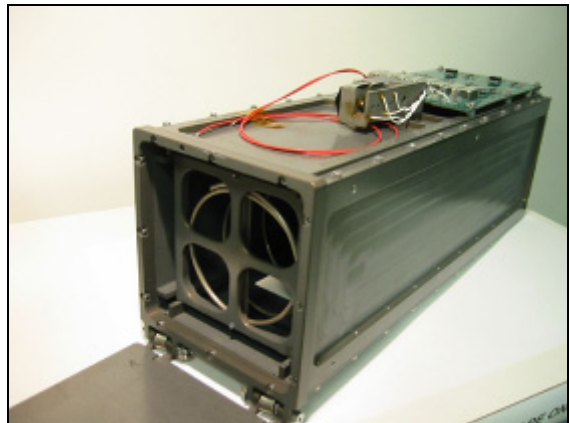


Figure 1-2 : Poly Picosatellite Orbital Deployer (P-POD)

1.1.3 Launch Vehicle

The principal mission of the Vega launcher is to inject payloads of between 600 kg and 2,500 kg into a low polar orbit (300 km to 1,500 km). Vega is in the ‘small launchers’ class with a mass at lift-off (excluding payload) of about 136 tonnes and a length of about 30 metres. Its three first stages have solid propellant, a fourth storable bi-propellant stage and a fairing for housing the payloads [R3].



Figure 1-3 : VEGA LV

Total length:	30 m
Diameter (1 st stage):	3 m
Mass:	136 tonnes

SwissCube will be launched by a VEGA LV but it will of course not be the main payload.

1.1.4 Science mission Objectives

The science Payload objective is taking comprehensive measurements of the Nightglow Phenomenon. This luminous phenomenon occurs in the earth atmosphere (at approximately 100 km altitude) and can be observed by satellite during the eclipse period because it generates a green luminous glow, as shown below. It is principally due to the recombination of the atomic oxygen, which is dissociated during the day.

The SwissCube will be able to take optical measurements and characterize the Nightglow for at least a period of three months.

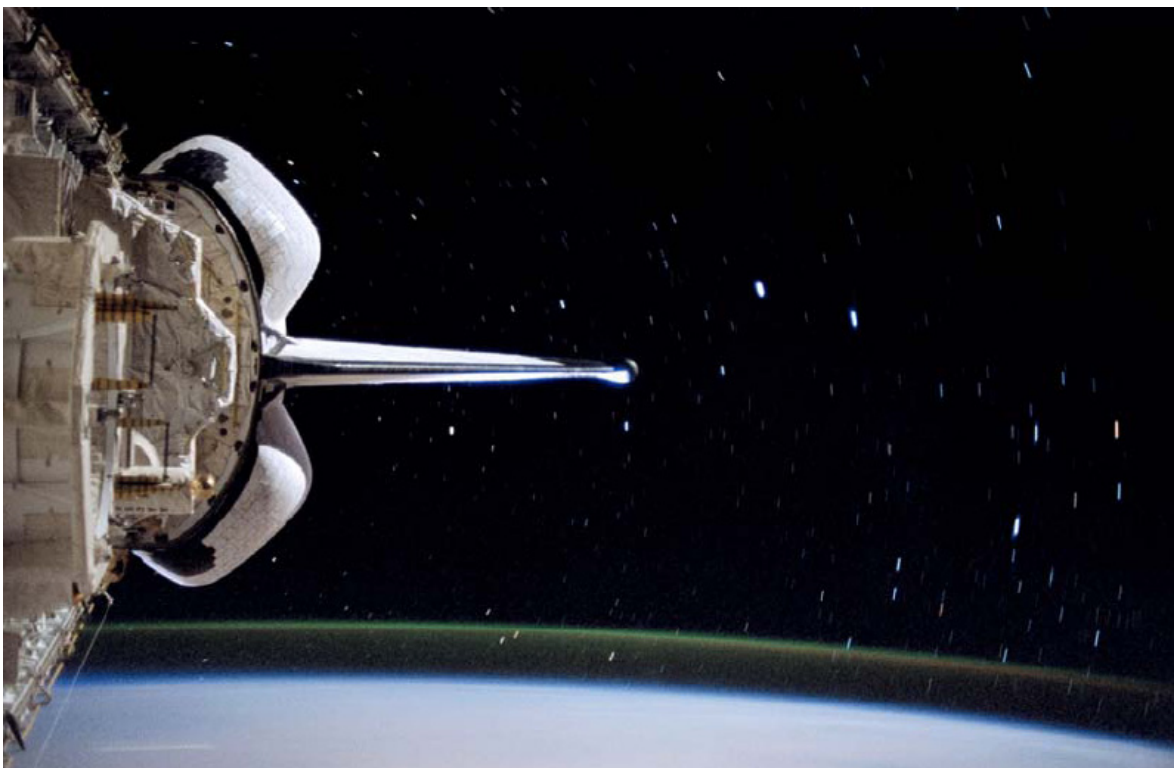


Figure 1-4 : Photo of nightglow (green glow in upper atmosphere) taken by ESA astronaut Claude Nicollier from the Space Shuttle.

Given the fact that the payload can take measurements of the Nightglow only during the eclipse SwissCube will have a sun-synchronous orbit. The eclipse period is about 30% of the complete orbital period.

1.1.5 Electrical Power System Role

The Electrical Power System supplies the satellite payload and the other subsystems. So, the primary role of the EPS is capturing solar energy and transmitting it to the subsystems. In orbit the solar cells generate power from solar radiations and also from albedo. This power is mainly produced during the daylight. During the eclipse, the solar cells are not exposed to radiations, except the IR radiations emitted by the earth which will be also exploited but with a bad efficiency. Anyway, a part of the energy must be stored in batteries in order to return it to deliver continuous power during eclipses, or peak demands.

In short, the primary functions of the EPS are:

- Power generation
- Power storage
- Power conditioning
- Power distribution
- Power protection

Actually, the three main electrical consumers are:

- EPS (protection diodes, DC/DC converters, protection switches...)
- ACDS (magnetotorquers, motors, ...)
- COM (RF transmitter, ...)

The payload will take photographs during the eclipse but this work doesn't consume a lot of energy.

The secondary function of the EPS is protecting the different subsystems against a phenomenon called "Single Event Latch-up" (SEL). This phenomenon happens when a high energy particle hits the device. If the impact on the device is of a serious nature, the high energy particle can directly cause damage to the device. This phenomenon happens very quickly and must be detected and corrected in hardware.

In case of the power not being turned off at a latch-up, a burn-out can occur and destroy the chip.

1.2 Project Objectives

1.2.1 Solar Cells

- Buy the solar cells selected during the phase A [Annexe 1].
- Build an electrical model as relevant as possible;
- Make a plastic support (for tests) to protect and connect two solar cells in parallel;
- Measure the Current-Voltage characteristic of the real GaAs triple junction solar cells;
- Determine extreme working points;
- Compare model with measurements;

1.2.2 Batteries

- Choose a type of batteries, justify the choice and buy them;
- Characterize this type of batteries;
- Test the batteries under the conditions of use during the mission in order to have a preliminary qualification;

1.2.3 Power management

- Study a strategy to manage the power from solar cells to users with a hot redundancy system;
- Study a strategy to provide and control two supply voltages of 3.3V and 5V;
- Study the boot strategy to guarantee a 15 minutes delay after jettisoning;

1.2.4 Design of electronics

- Design high reliability electronics able to support vacuum and thermal constraints.
- Design high efficiency electronics in order to spare as much energy as possible;
- Supervise the PCB routing of the engineering model;
- Test the engineering model under the conditions of use during the mission;

1.2.5 Kill-switches

- Study the kill-switches location and redundancy in order to guarantee the reliability.
- Test the kill-switches – selected by the “Structure and Configuration” designer – under the conditions of use during the mission.

1.3 Baseline Design

The EPS Baseline Design results from an adaptation of a power system for a micro-satellite designed at ESTEC [R2].

1.3.1 Architecture

The suggested architecture is simple and robust. It consists of the following main parts:

- 1) Solar Cells
- 2) Battery
- 3) Charge System
- 4) Discharge System
- 5) Dissipation System
- 6) Capacitor
- 7) Analog Control System

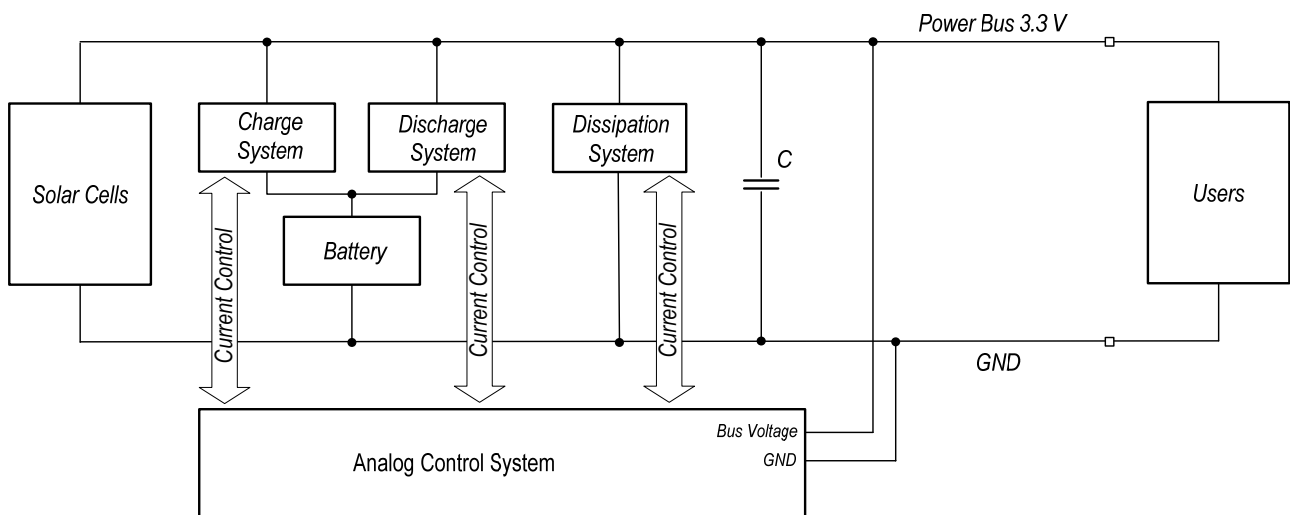


Figure 1-5 : Schematic Power System block diagram

1.3.2 Basic Principle

The solar cells behave like a variable current source (the current depends on the insolation). Users are a variable current consumer (the consumption depends on operation modes). The charge system and the dissipation system are controlled current consumers. The discharge system is a controlled current source. The algebraic sum of all these currents is equal to the capacitor current. The voltage of the capacitor is given by the integral of its current. So it is easy to control the capacitor voltage (i.e. the bus voltage) by controlling the current of charge, discharge and dissipation. This control is carried out by an analog system.

1.3.3 Voltage Control

When the bus voltage is exceeding 3.3 V, the charge system supplies the battery in order to reduce the bus voltage until 3.3V. When the bus voltage is going below 3.3 V the discharge system supplies the bus in order to increase its voltage until 3.3V. If the battery is completely charged, it is necessary to dissipate the energy generated by the solar cells in the dissipation system in order to maintain the bus voltage at 3.3V.

2 POWER SYSTEM REQUIREMENTS

Abstract

This chapter focuses on requirements' specifications for the SwissCube Electrical Power System. The satellite must withstand some critical constraints during launch (acceleration and vibrations) but it must mainly withstand the space environment which is very hostile regarding the vacuum, the temperature and the radiations. Therefore it is very important to design a robust electronics taking in account these requirements.

2.1 Summary of Power System requirements

- Orbit	SSO
- Altitude	400 - 1000 kilometers
- Launch acceleration	15 g
- Launch vibrations	1 g (sine amplitude)
- Maximum eclipse	36 min
- Minimum daytime	56.6 min
- Solar constant	1350 [W/m ²]
- Maximum cumulated radiation dose	37.4 krad[Si] for the electronics
- Temperature	-40 to 60 °C for the electronics (except for batteries) -55 to 75 °C for solar cells
- Vacuum	10 ⁻⁴ Pascal

In flight, the depressurization rate under the fairing does not exceed 5 kPa/s [R3]

- Life	1 year
- Mass	146 grams (batteries and solar cells included)
- Volume	85 x 85 x 20 (TBD more precisely)
- Bus regulation	3.3 Volt ± 9% (at the user interface)
- RF supply	5 Volt ± 5% (at user interface)
- Total power capability of the power bus (daylight)	3.30 Watt peak 1.85 Watt average
- Total power capability of the power bus (eclipse)	3.30 Watt peak 0.88 Watt average
- Total power to charge the battery	0.7 Watt average (to the battery) - TBC
- Charge and Discharge efficiency	> 90%

Some of these requirements are more critical than others. Most critical of them are certainly the temperature ranges (mainly for the batteries) and the vacuum.

2.2 Vacuum

At the altitude of 1000 kilometers the atmospheric density is very low.

- Average atmospheric density: $2.8 \cdot 10^{-15}$ [kg/m³] [R1]

At such altitude the atmospheric pressure can be considered as vacuum. Therefore all components used in the electrical power supply must be tested for their ability to withstand the vacuum in accordance with two criteria:

- Withstand mechanical constraints of vacuum tests
- Withstand out gassing tests (TBD)

The requirements given by ECSS [N1] about the vacuum out gassing test for the screening of space materials are:

- Pressure: 10^{-3} [Pa]
- Temperature: 125 [°C]
- Duration: 24 [h]

Reaching a vacuum of 10^{-3} Pa requires efficient vacuum pump (turbo-pump) and vacuum chamber. This specialised equipment will be available at EPFL during winter 06/07. High vacuum tests will be carried out in January (TBD).

For the moment, preliminary tests are performed at HEIG-VD with a simpler vacuum equipment for the engineering model.



Figure 2-1 : Vacuum System

Equipment characteristics:

- Guaranteed vacuum pressure : $5 \cdot 10^{-4}$ [mbar] => $5 \cdot 10^{-2}$ [Pa]

This present report contains only preliminary vacuum tests results. Of course the attention is especially turned on the battery because it is the most sensitive component of EPS.

2.3 Temperature

The satellite must be able to survive in very hostile thermal environment during launch but mainly in orbit.

VEGA LV will pass through the different atmospheric layers which has specific temperatures:

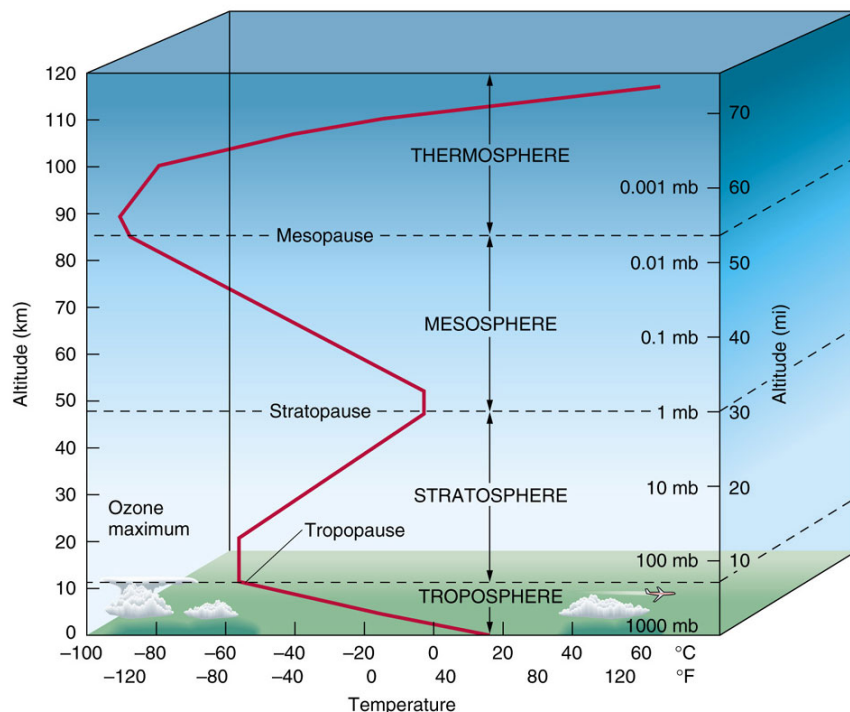


Figure 2-2 : Atmospheric temperature and pressure as a function of altitude.

During launch the satellite is in the P-POD and must be able to endure a temperature range of -40°C to 80°C [N2].

The temperature in orbit when the satellite is out of the P-POD depends mainly on the thermal design of the satellite. The preliminary thermal analysis gives a maximal temperature range of -55 to 75 °C outside the satellite and -40 to 60°C inside the satellite, but this last range depends on where the PCB is situated in the CubeSat. In fact the maximal range for the EPS electronics will probably be better (about -30 to 40°C, TBC).

So electronics must be able to operate at -40 to 60°C. The only exception is made for the battery because the temperature operating range of the selected batteries is more restrictive. It will be necessary to find a solution in order to guarantee the following range:

- Storage: -20 to 60°C
- Discharge: -20 to 60°C
- Charge: 0 to 45°C

2.4 Derating

In vacuum environment there is no air convection. Therefore all heat transportation will be either heat conduction or heat radiation. It is the reason why all components must be derated in the manner outlined in ECSS [N3] when it is possible.

Here is an example for a tantalum capacitor:

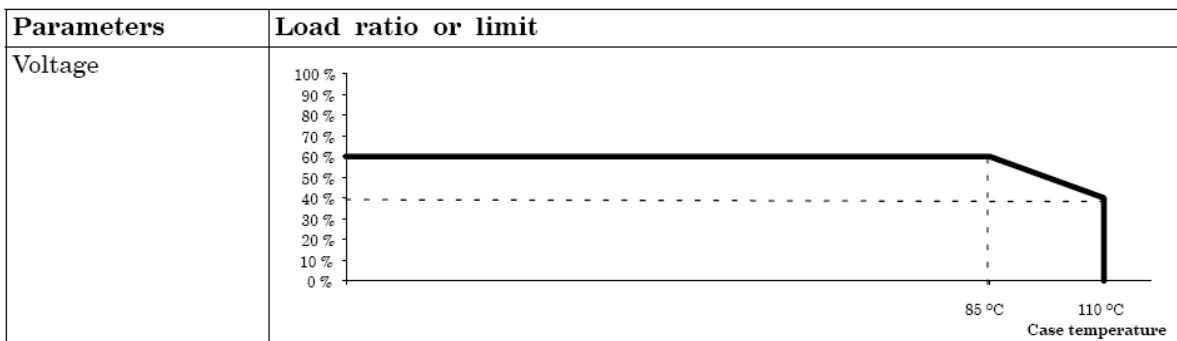


Figure 2-3 : Derating of solid tantalum capacitors

The temperature of the tantalum capacitor used on the 3.3V power bus can reach 80 °C. So the derating must not be more than 60%. It means that 3.3V is 60% of the manufacturer's specified voltage value at the most.

2.5 Radiation

The electro magnetic radiation and the particle radiation from sun and earth can affect electronics. Both kinds of radiation will wear down electronics over time. For that reason electronics have to be conscientiously chosen and tested (TBD) to be sure they withstand the radiation.

When a high energy particle hits a logic device it can change digitally stored data or cause a gate to open or close at the wrong time. This phenomenon is called a Single Event Upset (SEU). If the impact on the device is of a more serious nature, the high energy particle can directly cause damage to the device. This is called a Single Event Latch-up (SEL) [R4].

Software can be programmed to detect and correct SEU's, but SEL's must be detected and corrected in hardware.

The cumulative radiation effects have been evaluated in phase A [R5]. The analysis was done using the ESA Spenvis Tool.

The worst trapped radiation dose cumulated for 1 year behind 1mm of Al at 1000 km is 37.4 krad[Si].

2.6 Acceleration and Vibration

During the launch, the satellite will have a powerful acceleration. The on board power supply has to be able to withstand an acceleration of 15 g [N2]. But in the VEGA LV, the acceleration will probably be lower.

The figure below shows a typical longitudinal static acceleration-time history for the LV during its ascent flight. The peak longitudinal acceleration does not exceed 5.5 g for a payload above 300 kg:

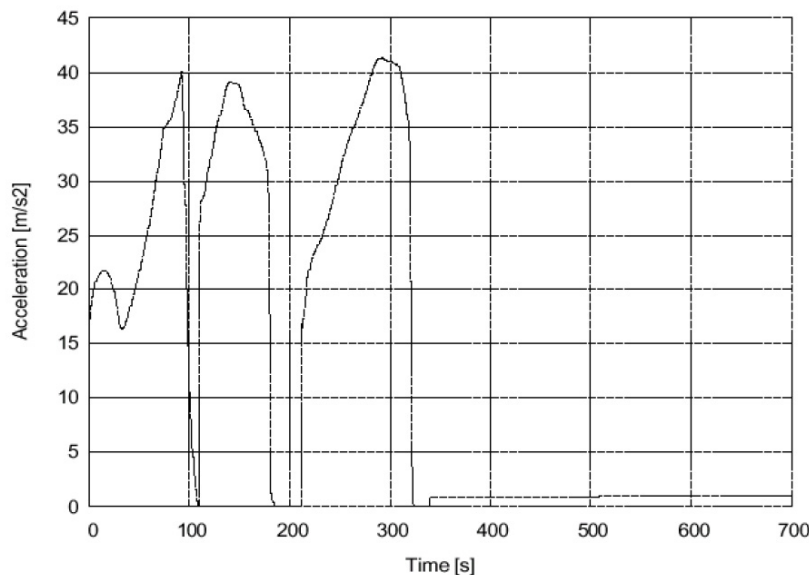


Figure 2-4 : Typical Longitudinal Steady-state Static Acceleration for the reference mission [R3]

There will be also strong vibrations during the ascent flight. Sinusoidal excitations derived from motors pressure oscillations and controlled POGO effect may affect the LV during its flight (mainly the atmospheric flight), as well as during some of the transient phases of the flight. The envelope of the sinusoidal (or sine-equivalent) vibration levels at the spacecraft base does not exceed the values given in this table:

DIRECTION	LONGITUDINAL		LATERAL	
Frequency Band (Hz)	5 - 45	45 - 100	5 - 25	25 - 100
Sine Amplitude (g)	≤ 0.8	≤ 1.0	≤ 0.8	≤ 0.5

Figure 2-5 : Sine Excitation at Spacecraft Base[R3]

Tall and heavy components could therefore break during the acceleration. The use of mechanical components, such as turn potentiometers or micro switches, should be avoided whenever possible. Vibrations tests will be carried out during next year (TBD).

3 SUMMARY OF ARCHITECTURE SELECTION

Abstract

Several architectures were analyzed since the beginning of the SwissCube project. At the beginning, the objective was to use the function of MPPT in order to obtain the maximum of power from the solar cells. However, for more reliability, it has been decided that the EPS will not depend on the use of a microcontroller. But it is difficult to track the MPP without a microcontroller. Build an analog MPPT system is possible [R12], but for that, it is necessary to work with discrete components which limit the working frequency. Thus it implies the use of bigger and heavier components (inductor, capacitor,...). Moreover that also requires using several solar cells as references (one per face). It is the reason why this alternative was abandoned. The chosen architecture for the Baseline Design is architecture without MPPT. The system works on a fixed working point on the I-V characteristic. This chapter briefly describes the different architectures considered.

The architectures are presented and discussed in order to fit within the three following requirements:

- High efficiency
- High reliability
- Redundancy

It should be noted that there is a perpetual compromise between reliability and redundancy. To increase redundancy it is necessary to use more components. On the other hand, if more components are required, reliability is reduced because the risk of breakdown is higher. So it is necessary to choose a good compromise which guarantees a high reliability with a sufficient redundancy. This sufficient redundancy is reached when all the sensitive components are redundant.

3.1 Architecture with MPPT

As mentioned before, it is possible to track the MPP with an analog system but it is not conceivable for SwissCube. At the beginning of the project the system analysis began with a numeric MPPT system (using a microcontroller to do the MPPT and the charge-discharge regulation).

First architectures were always built according to this schematic representation:

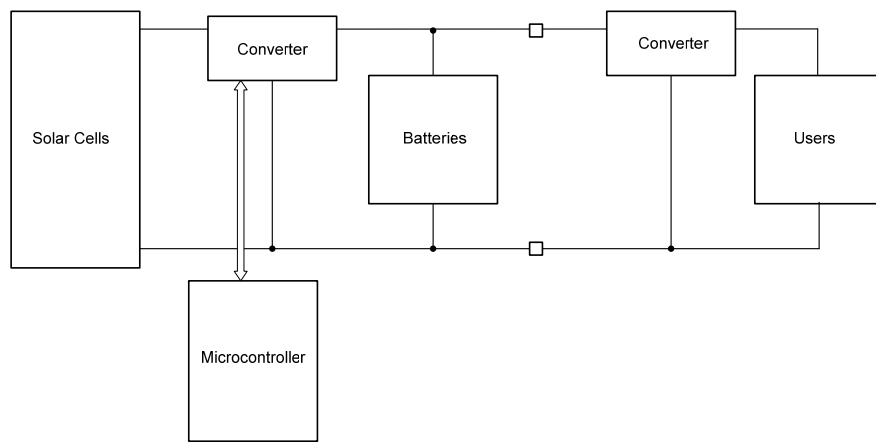


Figure 3-1 : Schematic representation

Energy is taken from solar cells and then injected into the batteries with a DC/DC converter controlled by the microcontroller. The users can take this energy through a second converter (or another system of regulation). The part which links the solar cells to the batteries is analyzed in detail below. The part which links the batteries to the users is very similar for each configuration.

Three configurations have been considered:

- 1) Solar cells in series – Batteries in series (abbreviated Ss-Bs)
- 2) Solar cells in series – Batteries in parallel (abbreviated Ss-Bp)
- 3) Solar cells in parallel – Batteries in parallel (abbreviated Sp-Bp)

3.1.1 Solar cells in series – Batteries in series

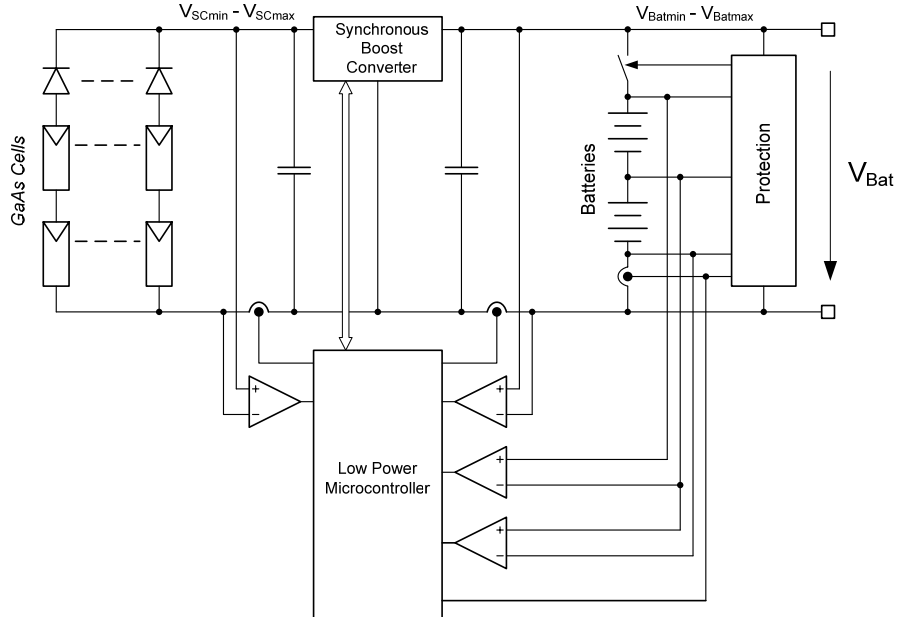


Figure 3-2 : Configuration 1)

3.1.2 Solar cells in series – Batteries in parallel

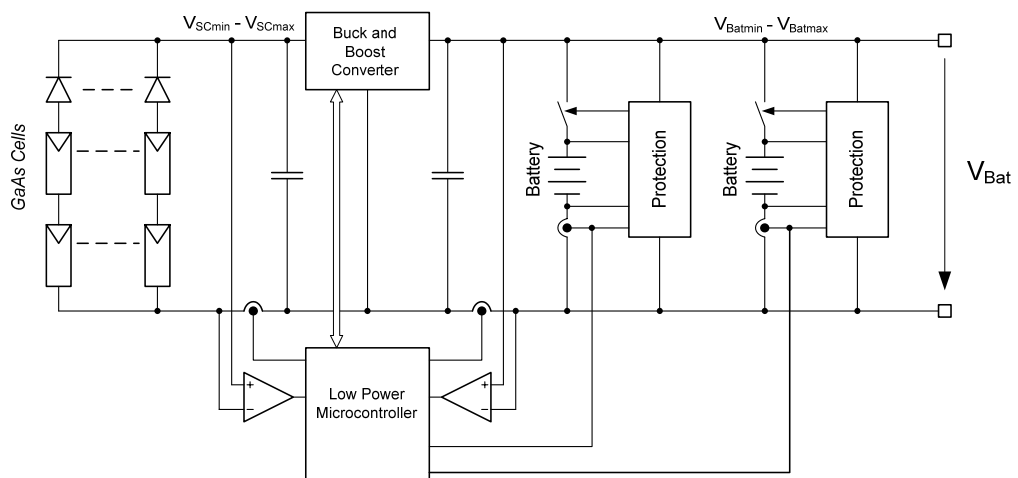


Figure 3-3 : Configuration 2)

3.1.3 Solar cells in parallel – Batteries in parallel

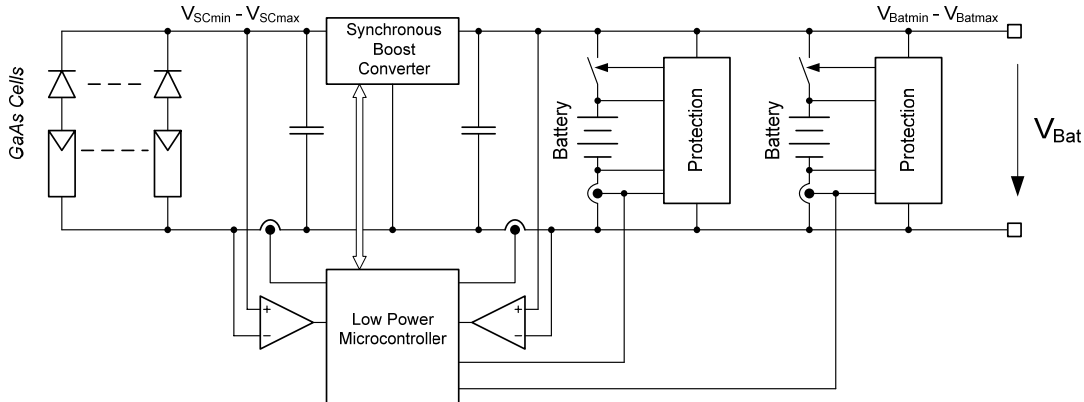


Figure 3-4 : Configuration 3)

3.1.4 Synthesized comparison

<i>Config.</i>	<i>Main advantages</i>	<i>Main drawbacks</i>	<i>Notes</i>
<i>Ss-Bs</i>	Boost converter; Total power losses on the diodes is low;	<u>Batteries in series:</u> - if one breaks down, both are deactivated; <u>Solar cells in series (by 2 on each side):</u> - if one breaks down, both are deactivated; - the internal resistance is higher;	
<i>Ss-Bp</i>	Total power losses on the diodes is low; Batteries in parallel;	Buck and Boost converter is required; <u>Solar cells in series (by 2 on each side):</u> - if one breaks down, both are deactivated; - the internal resistance is higher;	
<i>Sp-Bp</i>	Solar cells in parallel; Batteries in parallel; Boost converter;	Total power losses on the diodes is higher;	Best Config.

So, if it is necessary to use the MPPT to supply the satellite, the Sp-Bp architecture seems to be the best one. But even if this configuration is the best it has not enough redundancy. So other architectures have been studied using this Sp-Bp configuration. At this point of the analysis, it was

difficult to find a good compromise between reliability and redundancy. For example one of the best results was to have a full redundancy of the Sp-Bp configuration:

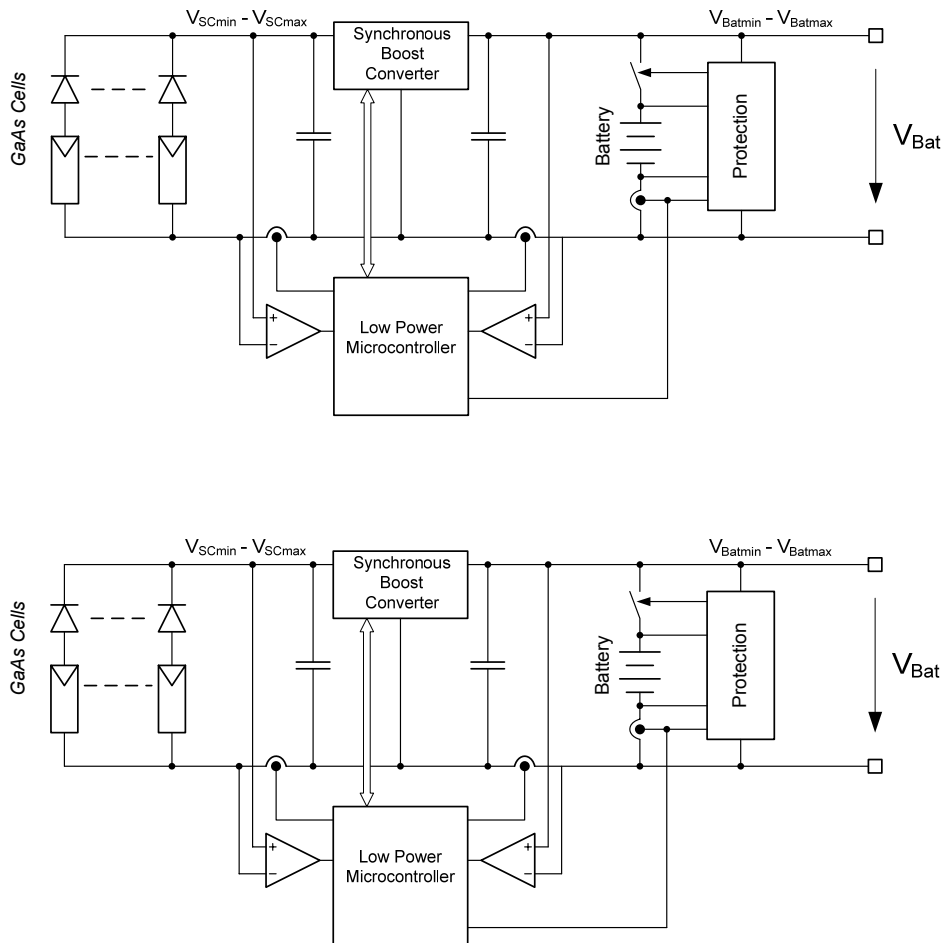


Figure 3-5 : Full redundancy

In this configuration the first system uses one solar cell of each side of the satellite and the second system uses the other solar cell of each side. So each system uses the half of the power from solar cells. Problems appear if one of the two systems is deactivated (due to a failure of the battery for example); the second system will provide only the half of the power generated by the solar cells.

The drawback is: redundancy is increased, but reliability is decreased.

It was very difficult to find a “hybrid solution” which fits with the requirements. So it has been decided to explore another way: the architecture without MPPT. It was a good decision.

3.2 Architecture without MPPT

As mentioned in the introduction, the Baseline Design results from an adaptation of a power system for a micro-satellite designed at ESTEC. The system works on a fixed working point of the solar cells characteristic.

This architecture has undoubtedly more advantages than last configurations.

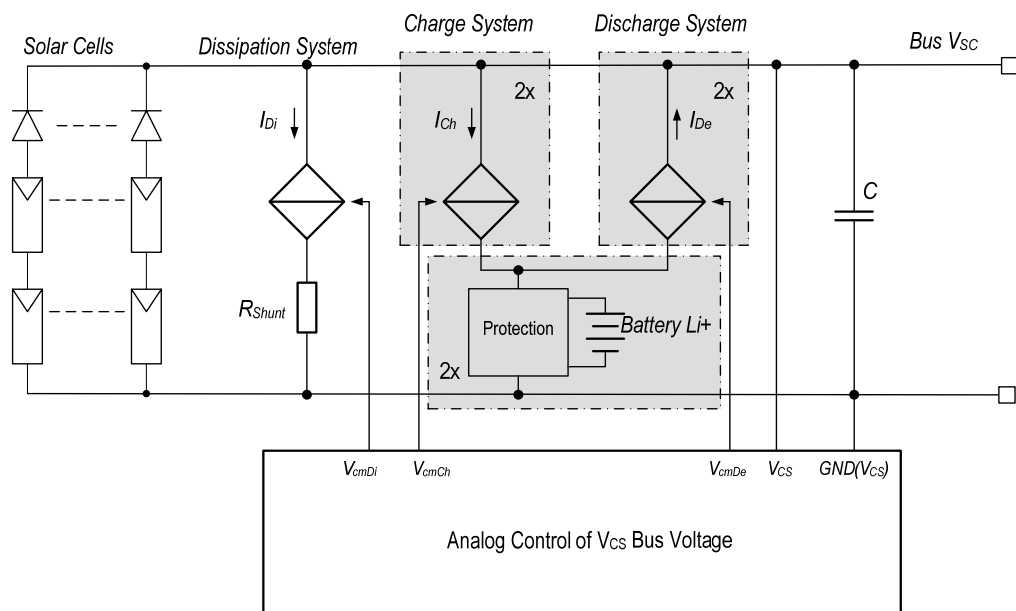


Figure 3-6 : Fixed working-point architecture

Main advantages	Main drawbacks
<ul style="list-style-type: none"> Total power losses on the diodes is low; Totally independent batteries; Hot redundancy of all sensitive's components; Very high efficiency ($\eta \approx 100\%$) when energy is directly transmitted from solar cells to users; High Charge efficiency ($\eta > 90\%$); High Discharge efficiency ($\eta > 90\%$); Robust analog system; 	<p><u>The MPP is not tracked:</u></p> <p>It means that the power taken from the cells will be of about 5% less than the power at the MPP.</p> <p><u>Solar cells in series (by 2 on each sides):</u></p> <ul style="list-style-type: none"> - if one breaks down, both are deactivated; - the internal resistance is higher;

In order to increase the reliability it has been decided to also have a redundancy of the solar cells connector and diodes. Here is another representation of the architecture.

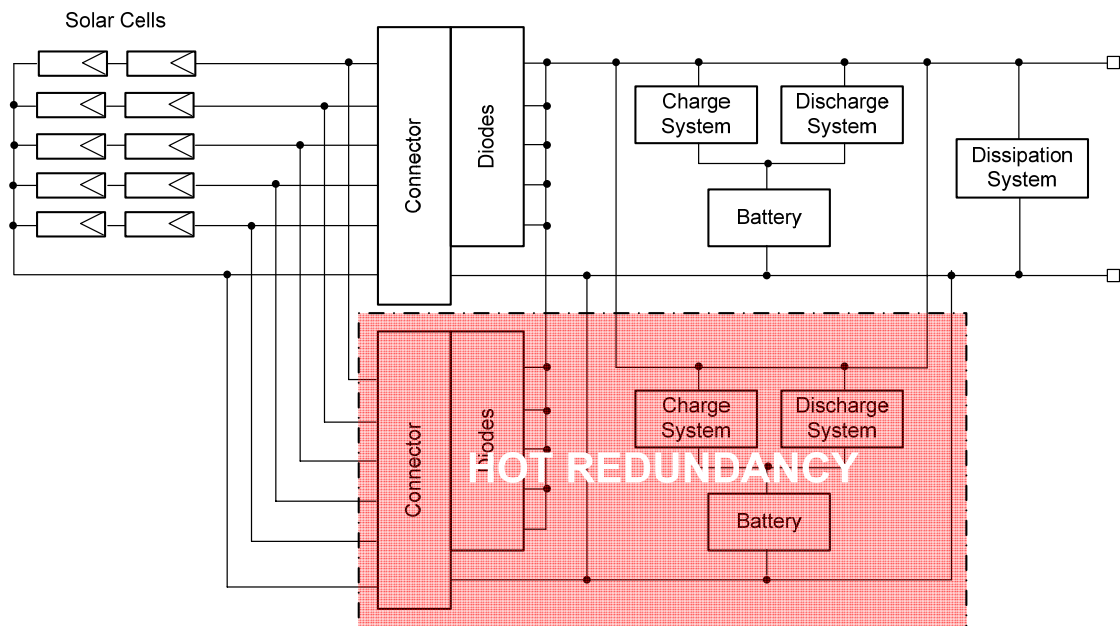


Figure 3-7 : Hot redundancy

This architecture is really reliable and fits within the requirements.

4 SOLAR CELL: MODELLING AND MEASUREMENTS

Abstract

To understand the electronic behaviour of a solar cell, it is useful to create a model which is electrically equivalent, and is based on discrete electrical components whose behaviour is well known. An ideal solar cell may be modelled by a current source in parallel with a diode. In practice no solar cell is ideal, so a shunt resistance and a series resistance component are added to the model.

This chapter will describe the classical model and then the simplified model which is generally used in most simulation studies.

In the second place, the simplified model will be fitted on the solar cell [Annexe 1] in order to compare it with the measurements and validate it.

4.1 General description

4.1.1 Electrical functioning

The following description is taken from a paper of Geoff Walker (University of Queensland, Australia) [R6].

“Solar cells consist of p-n junctions manufactured in a thin wafer of semiconductor. In the dark, the I-V output relation of a solar cell has an exponential characteristic similar to that of a diode.

When exposed to light, photons with energy greater than the band gap energy of the semiconductor are absorbed and create an electron-hole pair. These carriers are swept apart under the influence of the internal electric fields of the p-n junction and create a current proportional to the incident radiation. When the cell is short circuited, this current flows in the external circuit; when open circuited, this current is shunted internally by the intrinsic p-n junction diode. The characteristic of this diode therefore sets the open circuit voltage characteristics of the cell.”

4.1.2 Models

The following commentary about the solar cell models is taken from a paper of Engin Karatepe (Ege University, Bornova, Turkey) [R7].

“Different solar cell models have been developed to describe the electrical behaviours of solar cells, but the electrical equivalent circuit is a convenient and common way in most simulation studies. The five parameters of interest in the equivalent circuit are the photo-current (I_{ph}), series resistance (R_s), parallel resistance (R_{sh}), diode saturation current (I_s) and the ideal factor (n). The current-voltage characteristic of a solar cell is described by a mathematical equation that is both implicit and nonlinear. While some authors use numerical analysis methods to solve the implicit nonlinear equation of the I-V relation, others use analytical methods with a series of simplifications and approximations. In most studies, only the photo-current and the diode saturation current are changed with irradiation and temperature, respectively.”

In our case, a series of simplifications will be used to easily solve the equation. It is important to know that an assumption should be done carefully, especially under low irradiation conditions, because all of the circuit parameters depend on both irradiation and cell temperature. So, every assumption forces the model to fall into error. It is the reason why Engin Karatepe suggests using a neural network for improving the accuracy of the solar cell model.

However, the simplified electrical model is really enough accurate to do preliminary simulations. The neural network model might be useful for the continuation of the phase B.

4.1.3 Measurements

Preliminary measurements have been realised with an incandescent light on two solar cells in series with a diode. These measurements are not particularly representative because the spectrum of an incandescent light is not the same as the solar spectrum. They just give an idea of the I-V characteristic and where the MPP is located. More representative measurements will be carried out next year with a solar spectrum generator (probably at IMT Neuchatel, TBD).

4.2 Classical Model

It is possible to build a realistic model with a current source, two diodes and two resistors (series and parallel). The two diodes have different behaviours. In this manner it is possible to precisely adapt the characteristic of the model to the real behaviour of a solar cell.

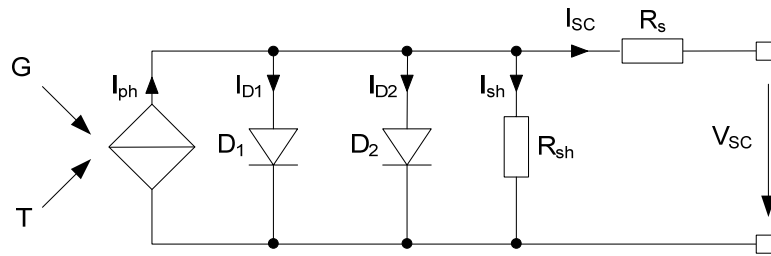


Figure 4-1 : Two diodes Model

Ohmic losses appear mainly in the connections of the cell. These losses are modelled with a resistor in series, R_s . Leakage currents of the cell are modelled with a parallel resistor R_{sh} (generally from 4 to 30Ω).

The output current I_{sc} is given by the following relation:

$$I_{sc} = I_{ph} - I_{D1} - I_{D2} - I_{sh} \quad 4.1$$

The photo-current depends on the insolation G and the working temperature T:

$$I_{ph} = I_{CC_{std}} \frac{G}{G_{nom}} (\Delta I_T (T - 298) + 1) \quad 4.2$$

With

I_{CCstd}	[A]	: short-circuit current of the solar cell in standard conditions: $G_{nom}=1.000 \text{ W/m}^2$ et $T=25^\circ\text{C}=298\text{K}$
G	[W/m ²]	: insolation
T	[K]	: temperature
ΔI_T	[K ⁻¹]	: short-circuit current variation as a function of the temperature

The current through the diode D₁ is given by the following relation:

$$I_{D1} = I_{S1} \left(e^{\frac{q(V_{SC} + R_S I_{SC})}{n_1 kT}} - 1 \right) \quad 4.3$$

The saturation current I_{S1} is:

$$I_{S1} = K_1 T^3 e^{\frac{-E_g}{kT}} \quad 4.4$$

Parameters used in relations 4.3 and 4.4 are described below:

q	[As]	: electric charge
k	[J/K]	: Stefan-Boltzmann constant: $k = 1.380 \cdot 10^{-23}$
n_1	[1]	: emission coefficient depending on the semiconductor material
T	[K]	: temperature
I_{S1}	[A]	: saturation current of D ₁ , depending on the temperature
K_1	[A/(cm ² K ³)]	: manufacturer's thermal constant
E_g	[J]	: forbidden band energy
V_{SC}	[V]	: voltage at cell's terminals
I_{D1}	[A]	: current through D ₁

For D₂ relations 4.3 and 4.4 become:

$$I_{D2} = I_{S2} \left(e^{\frac{q(V + R_S I_{SC})}{n_2 kT}} - 1 \right) \quad 4.5$$

$$I_{S2} = K_2 T^{\frac{5}{2}} e^{\frac{-E_g}{kT}} \quad 4.6$$

With

n_2	[1]	: emission coefficient depending on the semiconductor material
I_{S2}	[A]	: saturation current of D ₂ , depending on the temperature
K_2	[A/(cm ² K ^{5/2})]	: manufacturer's thermal constant
I_{D2}	[A]	: current through D ₂

Thus, the global model of the solar cell is described by the following equation:

$$I_{SC} = I_{CC_{std}} \frac{G}{1000} \left(\Delta I_T (T - T_{ref}) + 1 \right) - K_1 T^3 e^{-\frac{E_g}{kT}} \left(e^{\frac{q(V + R_s I_{SC})}{n_1 kT}} - 1 \right) - K_2 T^2 e^{-\frac{E_g}{kT}} \left(e^{\frac{q(V + R_s I_{SC})}{n_2 kT}} - 1 \right) - \frac{V_{SC} + R_s I_{SC}}{R_{sh}} \quad 4.7$$

In this equation, the current I_{SC} is a function of:

- the temperature,
- the voltage at cell's terminals,
- the insolation,
- itself

Therefore, this relation is implicit. It is possible to calculate I_{SC} using an iterative algorithm (calculus by continual approach). This algorithm gives a classical and efficient model of a photovoltaic cell.

It is possible to simplify this model in not taking into account the resistor R_s in the model but in using it in the simulation like a cables resistor.

In the literature there are also models with only one diode and they give satisfactory results too.

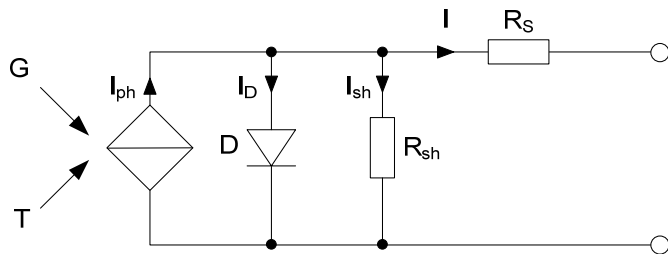


Figure 4-2 : One diode Model

4.3 Simplified Model

It is still possible to simplify the model in removing R_p :

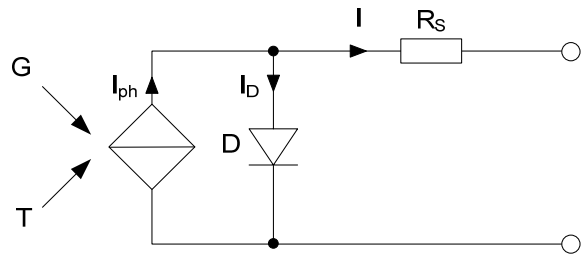


Figure 4-3 : Simplified Model

For this model the general relation is:

$$I_{CS} = I_{ph} - I_S \left(e^{\frac{q(V_{CS} + R_S I_{CS})}{nkT}} - 1 \right) \quad 4.8$$

When the cell is in the dark ($G=0 \Rightarrow I_{ph}=0$), the relation 4.8 is nothing else than the Shockley ideal diode equation.

The photo-current varies in a quasi linear manner with the temperature. Knowing this photo-current at a given temperature T_{ref} and for a given insolation, it is possible to estimate the same photo-current at another temperature T .

$$I_{ph(T)} = I_{ph(T_{ref})} (1 + K_0 (T - T_{ref})) \quad 4.9$$

The photo-current is a linear function of the insolation.

$$I_{ph(T_{ref})} = \frac{G}{G_{nom}} I_{CC(T_{ref})} \quad 4.10$$

Therefore, K_0 is determined by two measurements of the short-circuit current at two different temperatures but with the same insolation.

$$K_0 = \frac{1}{I_{CC(T_{ref})}} \frac{\partial I_{CC}}{\partial T} = \frac{I_{CC(T)} - I_{CC(T_{ref})}}{I_{CC(T_{ref})}} \frac{1}{T - T_{ref}} \quad 4.11$$

The diode saturation current I_S is a function of the operating temperature. In a first approximation, the relation is:

$$I_{S(T)} = I_{S(T_{ref})} \left(\frac{T}{T_{ref}} \right)^{\frac{3}{n}} e^{\frac{-E_g}{nk} \left(\frac{1}{T} - \frac{1}{T_{ref}} \right)} \quad 4.12$$

For a given temperature, the diode saturation current is determined by a measure of the voltage (open circuit) at the cell's terminals and a measure in short-circuit.

$$I_{S(T_{ref})} = \frac{I_{CC(T_{ref})}}{e^{\frac{qV_0(T_{ref})}{nkT_{ref}}} - 1} \quad 4.13$$

The series resistance R_s is determined by a measure of the voltage and the current with constant temperature and insolation on two working points which are near the open circuit functioning. In open circuit functioning, indeed, it is possible to measure the dynamic resistance of the diode.

$$r_D = \frac{\partial V_{0(T_{ref})}}{\partial I_{D(T_{ref})}} = \frac{1}{\frac{\partial I_{ph(T_{ref})}}{\partial V_{0(T_{ref})}}} = \frac{1}{\frac{\partial I_{S(T_i)}}{\partial V_{0(T_{ref})}} \left(e^{\frac{qV_{0(T_{ref})}}{nkT_{ref}}} - 1 \right)} = \frac{nkT_{ref}}{qI_{S(T_i)} e^{\frac{qV_{0(T_{ref})}}{nkT}}} \quad 4.14$$

Therefore the series resistance is:

$$R_s = -\frac{\partial V_{(T_{ref})}}{\partial I_{(V_{0(T_{ref})})}} - r_D = -\frac{\partial V_{(T_{ref})}}{\partial I_{(V_{0(T_{ref})})}} - \frac{nkT_{ref}}{qI_{S(T_{ref})} e^{\frac{qV_{0(T_{ref})}}{nkT_{ref}}}} \quad 4.15$$

Finally, the implicit relation between I_{SC} and V_{SC} is:

$$I = \left(\frac{G}{G_{nom}} \left(1 + K_0 (T - T_{ref}) \right) - \left(\frac{T}{T_{ref}} \right)^{\frac{3}{n}} \frac{e^{\frac{-E_g}{nk} \left(\frac{1}{T} - \frac{1}{T_{ref}} \right)}}{e^{\frac{qV_{0(T_{ref})}}{nkT_{ref}}} - 1} \left(e^{\frac{q(V_{SC} + R_s I_{SC})}{nkT}} - 1 \right) \right) I_{CC(T_{ref})} \quad 4.16$$

In order to precisely determine the K_0 coefficient, the current of saturation I_s and the series resistance R_s , it requires a solar spectrum generator as well as a very efficient measurement equipment.

These measurements (which are not carried out yet) will make it possible to precisely identify the parameters of the cell. They will be carried out next year (TBD).

For the moment the solar cells' datasheet give enough information to build the preliminary model.

4.3.1 Parameters definition

First, here are the parameters given by the solar cells' manufacturer [Annexe 1]:

1Cell of 30.18 cm², BOL, T_{ref} = 25°C, G=1350W/m²

Average open circuit voltage	:	V ₀	=	2.554	[V]
Average short circuit current	:	I _{SC}	=	0.498	[A]
Voltage at max. power	:	V _{SCPmax}	=	2.258	[V]
Current at max. power	:	I _{SCPmax}	=	0.480	[A]
Maximal power	:	P _{max}	=	1.083	[W]
Average efficiency	:	η	=	26.6	[%]
Temperature gradients	:	∂V ₀ /∂T	=	-6.0	[mV/°C]
	:	∂I _{SC} /∂T	=	0.272	[mA/°C]
	:	∂V _{SCPmax} /∂T	=	-6.4	[mV/°C]
	:	∂P _{max} /∂T	=	2.72	[mW/°C]

Assumptions:

Diode quality factor	:	n	=	1.5	[\cdot]
Band gap voltage	:	V _g	=	1.75	[V]

4.3.2 Iterative Algorithm I_{SC}=f(V_{SC})

With the help of the parameters given by the manufacturer it is possible to find a working point as a function of the insolation and the temperature. Given the fact that the relation 4.16 is implicit, it is necessary to do a calculus by continual approach with the Newton's method:

$$I_{CS} = I_{ph} - I_S \left(e^{\frac{q(V_{CS} + R_S I_{CS})}{nkT}} - 1 \right)$$

solve the following equation: $f(I_{CS[k]}) = I_{CS[k]} - I_{CS[k-1]} = 0$

$$\Rightarrow I_{CS[k]} = I_{CS[k-1]} - \frac{f(I_{CS[k-1]})}{\frac{\partial f(I_{CS[k-1]})}{\partial I_{CS[k-1]}}} \quad 4.17$$

With this method the convergence is very rapid. In order to limit the duration of calculation the number of iterations must be limited. In the present case, five iterations have been chosen.

Here is the Matlab code of the simplified model:

```

function Isc = Cell_GaAs(Vsc,G,TaC)

% Model of Ga RWE3G-ID2/150-8040 solar cell : I=f(V,T)
% Use of function : Isc = Cell_GaAs(Vsc,G,TaC)
% Vsc = Voltage on cell's terminals [V]
% G = relative insolation [-] (G=1 => 1350 W/m^2)
% TaC = temperature of the cell in operation [°C]

% Boltzman's constant
k = 1.38e-23;

% Electric charge
q = 1.60e-19;

% Quality factor of the diode (1<n<2)
n = 1.5;

% Band gap voltage (1.12eV < Vg < 1.757eV)
Vg = 1.75;

% Reference values
Tref = 273 + 25; % temperature
Vo_Tref = 2.554; % open circuit voltage (G=1 et T=Tref)
Icc_Tref = 0.498; % short circuit current (G=1 et T=Tref)

% Temperature of the cell in operation
TaK = 273 + TaC;

% Photo-current thermal coefficient
K0 = 2.72e-4/Icc_Tref;

% Photo-current (G=1 et T=Tref)
Iph = Icc_Tref * G * (1 + K0*(TaK - Tref));

% Diode saturation current (T=Tref)
Is_Tref = Icc_Tref / (exp(q*Vo_Tref/(n*k*Tref))-1);

% Diode saturation current (T=Tak)
Is = Is_Tref * (TaK/Tref).^(3/n) .* exp(-(Vg * q/(n*k)).*(1./TaK - 1/Tref));

% Calculation of series resistance
X2v = q*Is_Tref/(n*k*Tref) * exp(q*Vo_Tref/(n*k*Tref));
dVdI_Vo = - 0.3833; % mesurement of the I-V characteristic's slope for V=Vo
Rs = - dVdI_Vo - 1/X2v; % series resistance

```

```
% Iterative calculation of Isc
Isc = zeros(size(Vsc));

for j=1:5;
Isc = Isc - (Iph - Is.*exp(q*(Vsc+Isc.*Rs)./(n*k*Tref))-1)/...
(-1 - (Is.*exp(q*(Vsc+Isc.*Rs)./(n*k*Tref))-1).*q*Rs./(n*k*Tref));
end
```

Figure 4-1 : Matlab function of the simplified model

Now, it is possible to trace the I-V characteristic as a function of the insolation and the temperature.

4.3.3 Variations of the Insolation

Here is the I-V characteristic as a function of the insolation for a constant temperature for one cell:

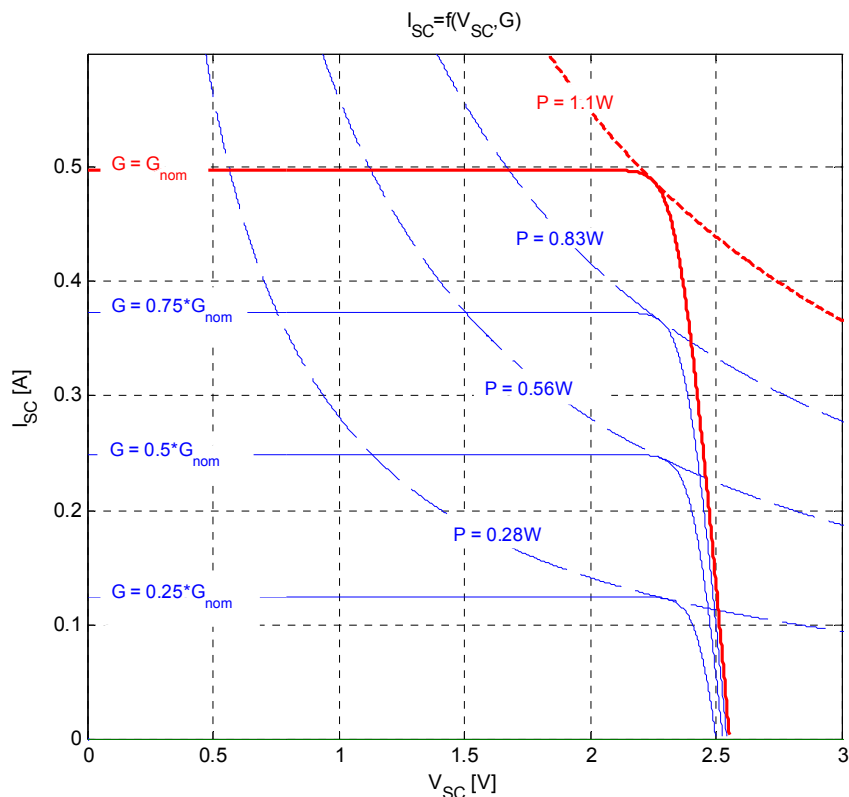


Figure 4-4 : I-V characteristics as a function of the insolation ($G_{nom} = 1350\text{W/m}^2$, $T = 25^\circ\text{C}$)

For each insolation case there is a working point where the power is maximal. This working point is called MPP (Maximal Power Point). So it is important to know exactly where the MPP is located on the characteristic of the cell because it is necessary to take as much power from the cell as possible. The model shows that MPP's are approximately at the same voltage, if the temperature is constant.

Here is plotted the power as a function of the voltage at the cell's terminals for several values of insolation:

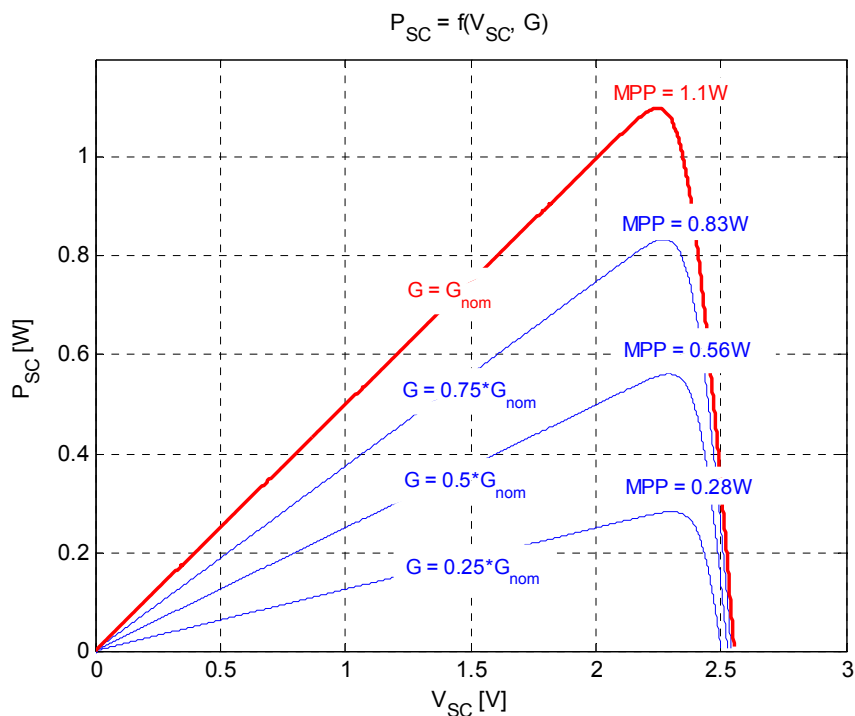


Figure 4-5 : Power characteristics as a function of the insolation ($G_{nom}=1350\text{W/m}^2$, $T=25^\circ\text{C}$)

Whichever insolation there is, the MPP is at a higher voltage than 2V.

These different MPPs can move on the right or on the left if the temperature varies, so it is very important to know the voltage of the MPP in the worst case.

4.3.4 Variations of the Temperature

As shown below, the open circuit voltage decreases and the short circuit current increases (in lower proportions) when the temperature increases. Of course, the worst case appears when the temperature reaches 75°C.

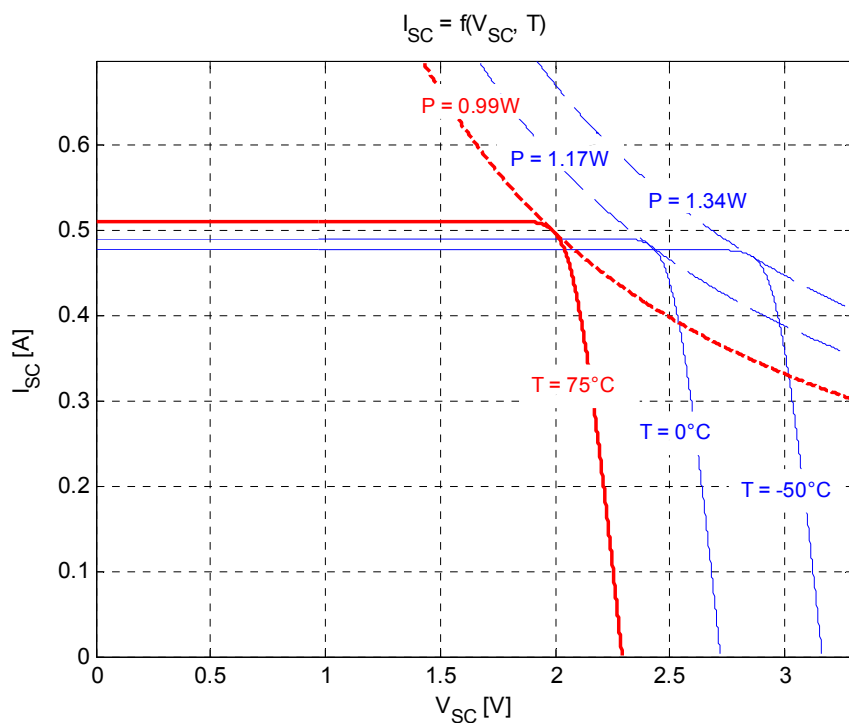


Figure 4-6 : I-V characteristics as a function of the temperature ($G=1350\text{W/m}^2$)

When the temperature is less than 75°C, the voltage of MPPs is more than 2V.

4.3.5 Series connection

Connect two solar cells in series does not pose any problem. The current will be the same than for one cell but the voltage will be doubled. So, to model the I-V characteristic of two cells in series, the open circuit voltage is just doubled in the model.

4.3.6 Protection Diode

If a voltage higher than the open circuit voltage is imposed on the cell's terminal, a negative current will appear. In this case, the cell becomes a consumer. This phenomenon can be avoided with a Schottky protection diode. This diode is placed on each parallel branch of the solar network.

The voltage on the diode must be as low as possible. The using of a Schottky diode is the best choice because the voltage at its terminals is no more than 0.5V. This value can be easily introduced in the model.

The power losses on the diode are not trifling and they must be taken in account in the power budget.

4.3.7 I-V characteristic of two cells in series with a protection diode

On one face of the satellite there will be two cells in series with one protection diode as shown below:

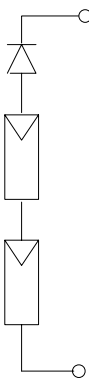


Figure 4-7 : Two solar cells in series with a protection diode

The model of the side is easily done by adding the characteristic of two cells and then by subtracting 0.5 V for the protection diode.

Here is plotted the I-V characteristic of the system with a temperature of 75°C (worst case) and an insolation of 1350 W/m².

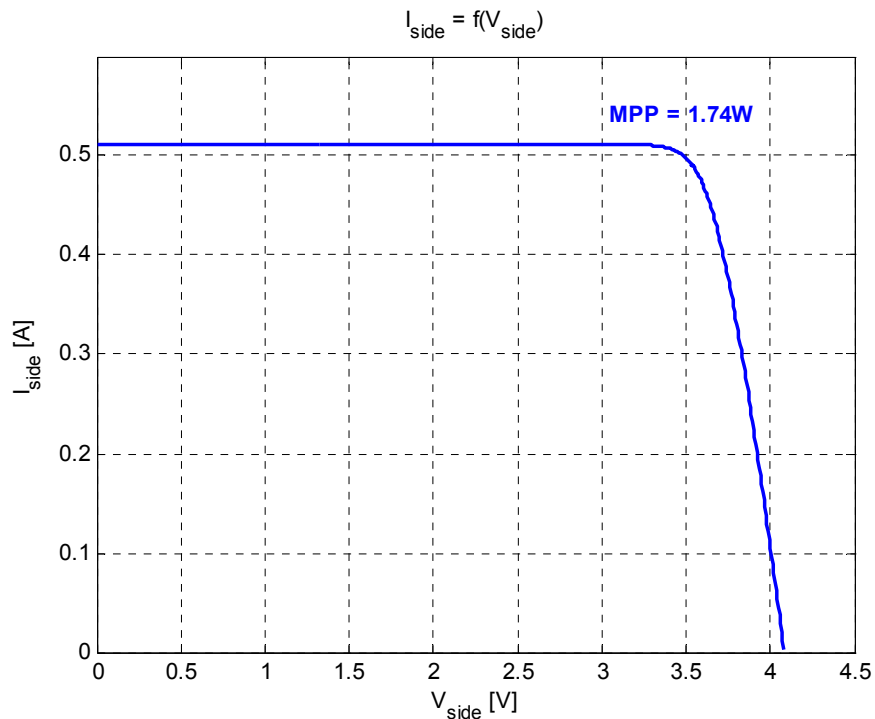


Figure 4-8 : I-V characteristic of one side of the satellite (G=1350W/m², T=75°C)

4.3.8 Comparison with measurements

Preliminary measurements have been realised with an incandescent light of 2000 W placed just 50cm over the cells. Cells are exposed to the light and they heat in the same time. The absorptivity of the cells is very high (≤ 0.91) and the thermal time constant is very low. So, the temperature of the cell grows very rapidly.

As said before, these measurements are not particularly representative because the spectrum of an incandescent light is not the same as the solar spectrum. However they give an idea of the I-V characteristic and where the MPP is located. These measurements have been done at a temperature of about 60°C.

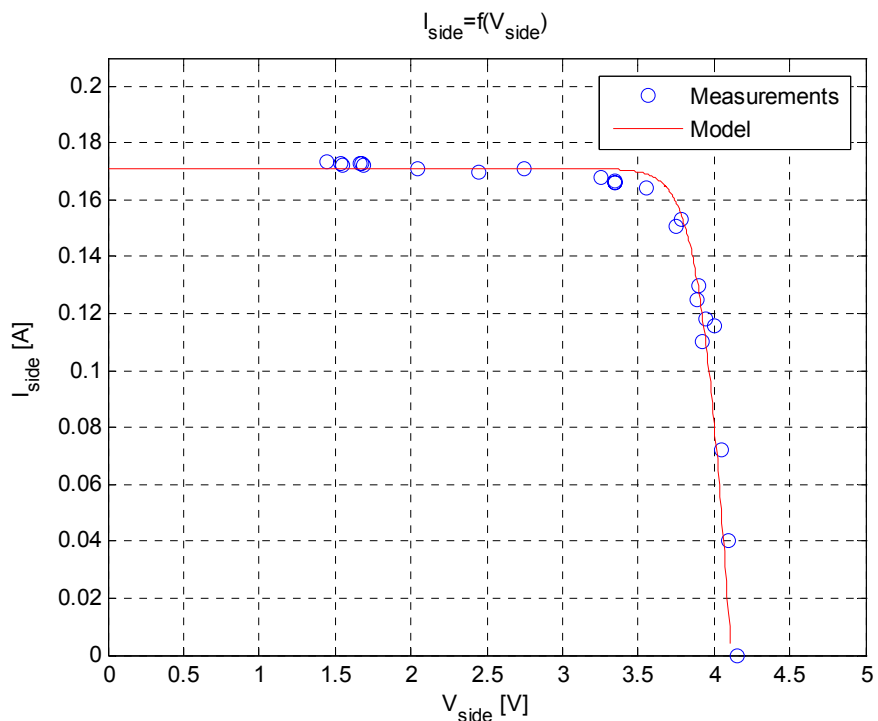


Figure 4-9 : Measurements ($T \approx 60^{\circ}\text{C}$) and model ($G=450 \text{ W/m}^2$, $T = 60^{\circ}\text{C}$, Quality fact. = 2)

4.3.9 Experimental Installation

As shown below the cells had no wire on their connector and the conductive surfaces where it is possible to solder wires are very small. So it was difficult to find a simple solution to build a small installation for test. The best solution was to lightly press on the conductive surfaces with a piece of copper coated with tin. A small spring presses the connection in order to guarantee a good contact with the solar cell.

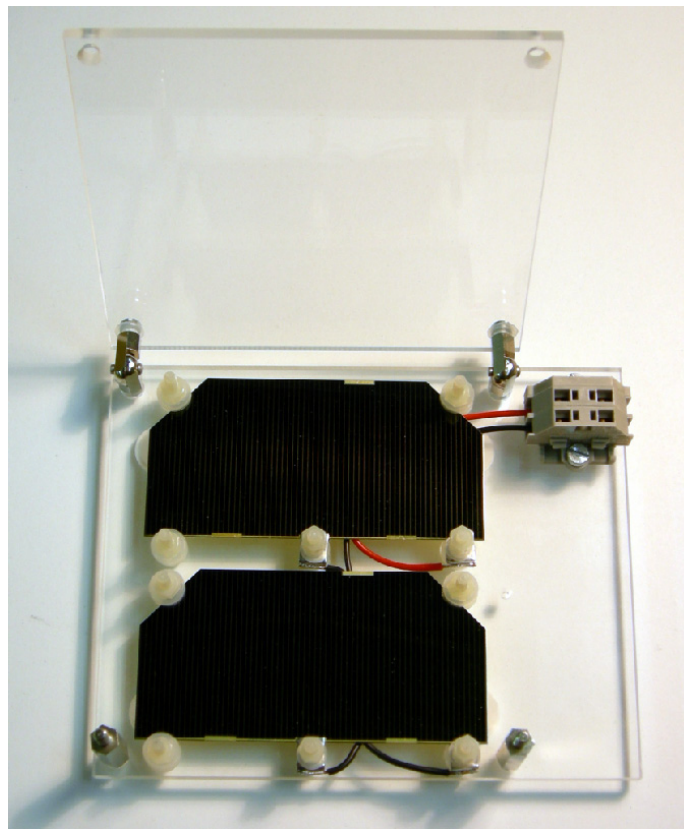


Figure 4-10 : Experimental installation with two cells in series



Figure 4-11 : Detail of one connection

5 BATTERY CONSIDERATION

Abstract

Undoubtedly, batteries are the most critical components of EPS at all points of view: their sensitivity, their life-time, their mass and volume, and their important role for the mission. It is absolutely necessary to test them under the conditions of use during the mission because the satellite is absolutely incapable of doing something during the eclipse without batteries. This chapter will present mainly the Lithium-Ion Polymer technology which has very high volumetric and gravimetric density. One type of Li-Poly batteries has been selected and tested in a vacuum chamber. The results are very positive.

5.1 Lithium-Ion Polymer Technology

Lithium-Ion Polymer batteries, or more commonly Lithium Polymer batteries (abbreviated Li-Poly) are rechargeable batteries which have technologically evolved from lithium-ion batteries. Ultimately, the lithium salt electrolyte is not held in an organic solvent like in the proven Lithium-Ion design, but in a solid polymer composite such as polyacrylonitrile. There are many advantages of this design over the classic Lithium-Ion design, including the fact that the solid polymer electrolyte is not flammable (unlike the organic solvent that the Li-Ion cell uses). Thus, these batteries are less hazardous if mistreated.

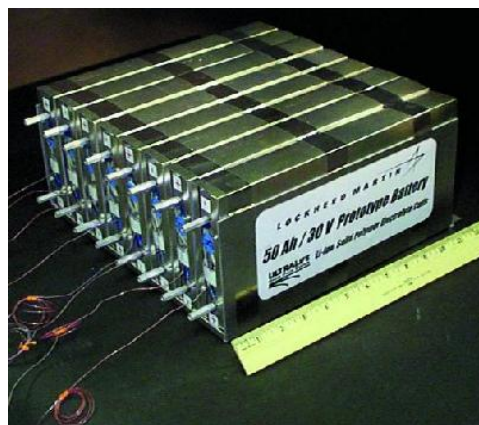


Figure 5-1 : A prototype Lithium-Ion Polymer Battery at NASA Glenn Research Center

The main difference between Li-Poly and Li-Ion cells is that in the latter cells, the rigid case presses the electrodes and the separator onto each other, whereas in polymer cells this external pressure is not required because the electrode sheets and the separator sheets are laminated onto each other.

Since no metal battery cell casing is needed, the battery can be lighter. Because of the denser packaging without intercell spacing between cylindrical cells and the lack of metal casing, the energy density of Li-Poly batteries is over 20% higher than that of a classical Li-Ion battery and approximately three times better than NiCd and NiMH batteries [R9].

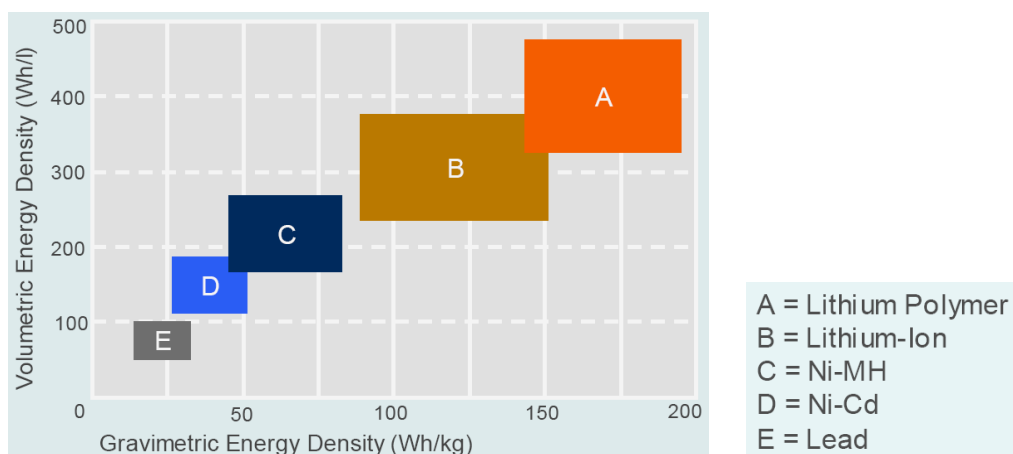


Figure 5-2 : Comparison of different rechargeable battery systems [R8]

5.2 Battery Selection

5.2.1 Importance of Thermal Design

First here is an example of batteries used in a functional Japanese CubeSat, [R10]:

<i>CubeSat</i>	<i>Battery type</i>	<i>Life expectancy [Cycles]</i>	<i>Charge operating temperature [°C]</i>	<i>Discharge operating temperature [°C]</i>
CUTE-I	Li-Ion	500	0 to 45	-20 to 60

CUTE-I CubeSat proves conclusively that it is conceivable to use batteries with standard temperature ranges. This is possible only if the thermal design works well, because the temperature inside the satellite depends mainly on this design.

The batteries' technology which has been selected for SwissCube is the VARTA Lithium Polymer technology (called PoLiFlex). The thermal requirements to use the PoLiFlex technology are very similar to the standard thermal requirements of Li-Ion batteries:

<i>Parameters</i>	<i>Unit</i>	<i>Critical</i>	<i>Satisfactory</i>	<i>Notes</i>
Gravimetric energy density	[Wh/l]		370	High
Volumetric energy density	[Wh/kg]		200	Very high
Charge operating temperature	[°C]	0 to 45		The appreciation depends on the thermal design
Discharge operating temperature	[°C]	-20 to 60		The appreciation depends on the thermal design
Life expectancy ≥70% of Capacity	[Cycles]		500	Standard
Charge retention 1 year at -20 to 20°C 3 month at -20 to 45°C 1 month at -20 to 60°C	[%] of Capacity	>70		The appreciation depends on the thermal design

5.2.2 VARTA PoLiFlex

There are several reasons to opt for the PoLiFlex technology:

- It has a solid reputation for quality, safety and reliability (PoLiFlex batteries are used for: safe gas monitoring, biomedical, mining and petrochemical applications).
- It does not exhibit the memory effect seen in NiCd batteries. This allows the battery to be charged from any state of charge, without degradation of performance.
- It is recommended by Clyde-Space [R11] (manufacturer of electrical power systems for small satellites).
- It has been recently tested with hard requirements at ESA [no source available for the moment]

ESA has recently study the possibility to use Lithium Polymer technologies for space applications. During these tests, PoLiFlex technology performed very well under the conditions that it was subjected to. PoLiFlex cells were found to not have any problems with bulging whereas all of the other cells did. Here is a summary of these tests:

- Capacity at C/10 under vacuum: unaffected.
- Radiation up to 500krad: unaffected.
- DPA
- Capacity at -10C, 0C, 20C and 40C
- Resistance
- Self Discharge
- Missions Scenario Tests:
 - o Discharge C/4; Charge C/2 (5 cycles)
 - o Discharge C/2; Charge C/10 (5 cycles)
 - o Discharge C/15; Charge C/10 (5 cycles)
- EMF vs SOC
- Cycling Tests at reduced pressure (15-20 mbar) - 30% DOD, C/3
- Discharge >1500 cycles (still on going)

Besides, the PoLiFlex technology doesn't need a clamp to prevent bulging. The reason for this is the cell internal construction. It is different to most other lithium polymer cells. As known, most will suffer from bulging.

The vacuum tests carried out at HEIG-VD revealed that 'bag' of the cell swells from a certain value of vacuum. The advantage with the PoLiFlex cell is that the 'bag' doesn't hold the electrodes and separator together. This is achieved using ultrasonic welds between the plates. Therefore, the swelling of the 'bag' doesn't affect the performance.

It is also interesting to consider the safety tests requirements of PoLiFlex carried out by VARTA:

Test	Description	required results
Overcharging Test	<ul style="list-style-type: none"> - Charging Current I: 3 times max. allowed charging current - Charging Voltage U: PoLiFlex cells: 4.8 V; purchased cells: according to manufacturer specification - max. 12 V - Charging Time t = $t = 2.5C / I$, (Current in CA) – at open voltage - $t = 12h$ – at limited charging voltage (manufacturer specification) - If necessary additional safety elements according to UL file <u>Testing Conditions:</u> <ul style="list-style-type: none"> - Test at RT - Cell in discharged state (3.0 V after 1.0 C discharge) - An integrated overcurrent or overtemperature safety element is not allowed to be activated. (the maximum load has to be chosen) - The cell will be connected in series with a direct current source and a charging current is applied. 	no bursting, no fire
Short Circuit Test	<u>Testing Conditions:</u> <ul style="list-style-type: none"> - Test at RT - Cell used in charged state (3h with 1.0 CA to 4.2 V, $I_{min} 0.02C$) - Cell is shortened in the test with a maximum resistance of $100m\Omega$ (to be documented) 	no bursting, no fire Maximum temperature 150°C
Voltage Reversal Charge Test	<u>Testing Conditions:</u> <ul style="list-style-type: none"> - Test at RT - Cell in discharged state (3.0 V after 1.0 C discharge) - 1C; 12V until cell temperature is back at RT ($t_{max} = 1h$) 	no bursting, no fire Maximum temperature 75°C
Nailing Test	<u>Testing Conditions:</u> <ul style="list-style-type: none"> - Cell in charged state (4.25 V) 	No fire, no rupture Maximum temperature = 125°C
Oventest	<u>Testing Conditions:</u> <ul style="list-style-type: none"> - Charge conditions: cell fully charged (according to UL1642) 3h/ 4.25 V (1C) - Heating of the cell in the temperature box to 130°C (D $5^{\circ}\text{C}/\text{min} \pm 2^{\circ}\text{C}$) - 10 minutes holding time at 130°C 	No fire, no rupture

Figure 5-3 : Safety tests of PoLiFlex [R8]

Two different types of PoLiFlex – which are very similar – have been chosen to do some tests:

- PLF423566 (with wires and protection circuit) : 24 pieces, received in November
- PLF503759 (with wires and protection circuit) : 12 pieces, will arrive in January

PLF503759 is the favourite type for the moment. A description of this latter type is given below.

5.2.3 PLF503759

The PLF503759 cell has a nominal capacity of 1210 mAh. This capacity has been chosen because it is recommended to take a DOD of 30% for this type of application [R1]. So the capacity available to supply the satellite during the eclipse is 360 mAh. This amount of energy is sufficient (TBC).

Here is an illustration of this cell:



Figure 5-4 : PLF503759 (scale 1:1)

Here is the typical charge profile of a PoLiFlex battery and the voltage range for a DOD of 30%:

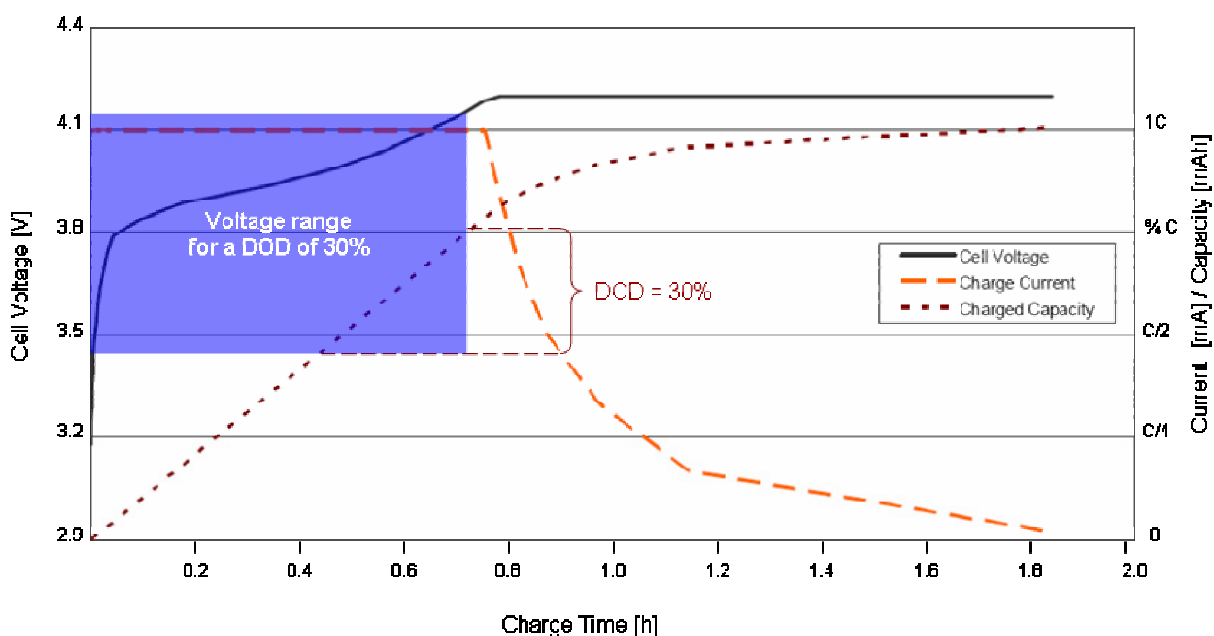


Figure 5-5 : Typical charge profile (1C, 20°C) with the defined voltage range for the application

It has been decided to work in the constant charge current part of the profile. The battery is considered charged at $\frac{3}{4}$ C. The authorized voltage range is about from 3.35 to 4.15V (this range will vary a little bit due to the temperature variations, as described in the “Baseline Design” chapter).

The DOD is 30% of the capacity if only one battery is used. But the power system will have a hot redundancy. So it will work with two batteries in the same time. Therefore, the DOD will be only 15%. This low DOD will increase the life expectancy. Then, if one battery breaks down, the system can survive with the other battery without problem (the DOD will be 30% again).

It is also important to consider the discharge profile. This profile varies as a function of the charging current:

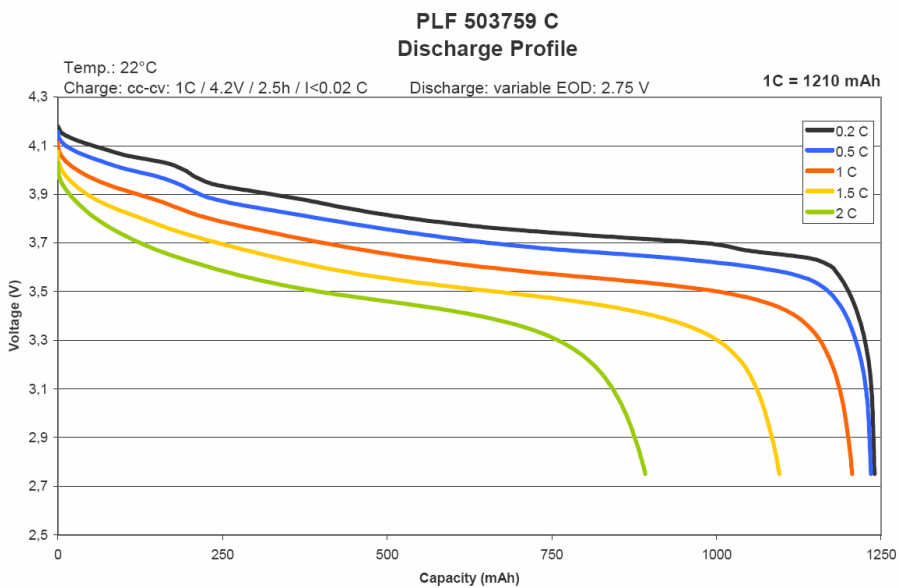


Figure 5-6 : Discharge Profile vs Charge Current (@ 20°C)

And it varies with the temperature variations too:

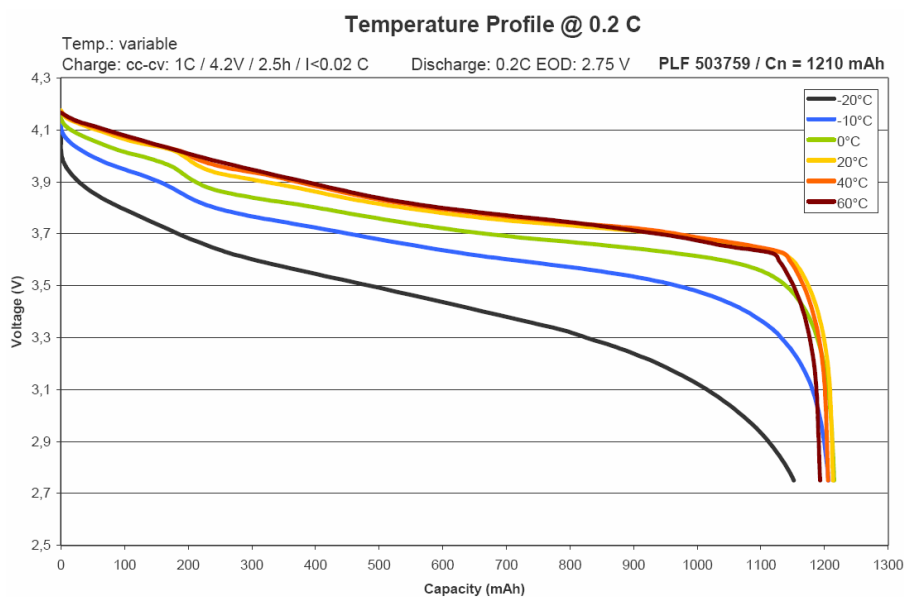


Figure 5-7 : Discharge Profile vs Temperature (@ 0.2C)

If the charging current is low the difference between discharge profiles is not significant but in the case of high charging current (1C, for example) the difference becomes critical:

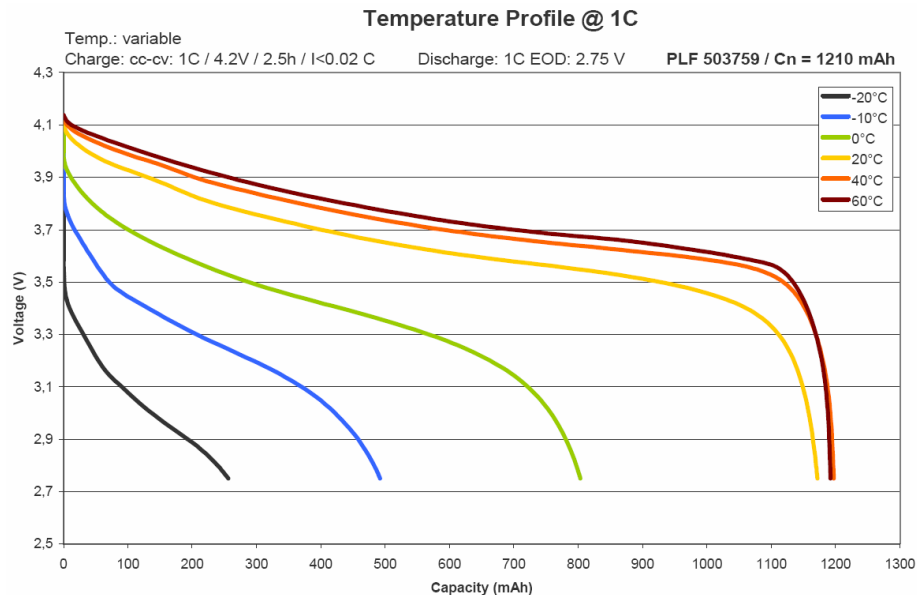


Figure 5-8 : Discharge Profile vs Temperature (@ 1C)

If one battery breaks down the second battery will work alone. So its discharging current will be doubled (at about 0.7C). In this case with a temperature of -20°C, the capacity of the battery is critically reduced.

It is the reason why the thermal design must be thought up to have a sufficient temperature during the discharge. It will probably necessary to use a heat link between the batteries and the electrical devices which are hot during the eclipse (TDB by thermal subsystem).

If it is possible to guarantee at least -10°C during the discharge the problem is resolved but the safety margin is very low. If it is possible to guarantee 0°C, the situation is still better.

If it is not possible to guarantee -10°C during the discharge, it will be necessary to think about another solution. Here are several ways:

- Use three batteries (with a triple redundancy system) => the discharging current will be lower even if one battery breaks down.
- Use batteries with a higher capacity => the discharging current will be lower even if one battery breaks down
- Heat the batteries with a part of their own energy (with a small heater resistor)
- Build an insulated box for the batteries.

Here is the life expectancy profile:

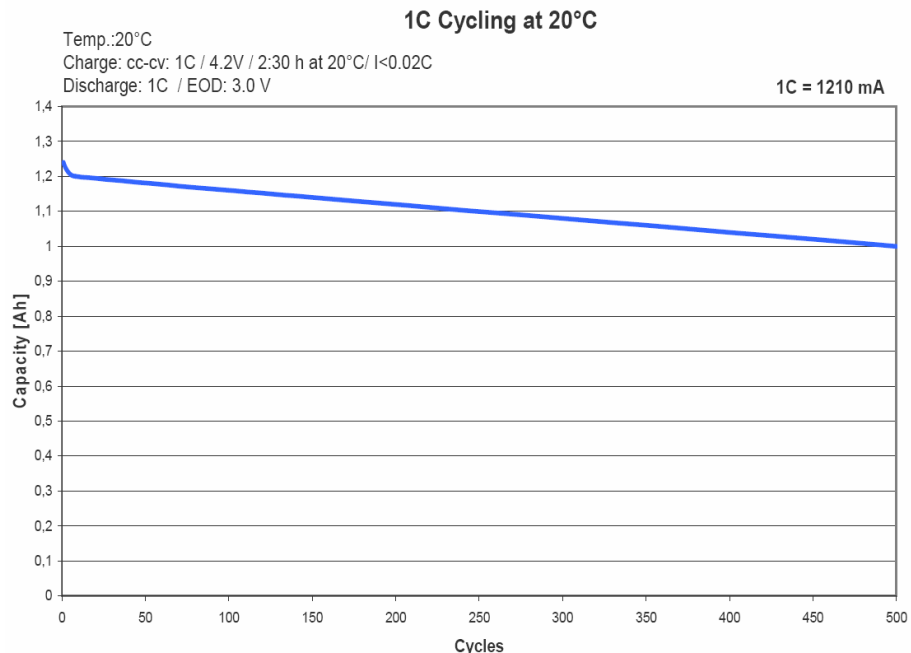


Figure 5-9 : Life expectancy (1C, @20°C)

This profile is valid if the battery is completely charged and then completely discharged with a current of 1C. As said before, the life can be appreciably increased with a DOD of 30%.

The satellite will do approximately 15 orbits in one day. The mission lasts one year. So it easy to determine the number of cycles:

$$15 \text{ cycles/day} \cdot 365 \text{ days/year} = 5475 \text{ cycles/year}$$

However the DOD is 30%. Knowing that probably 1/3 of the eclipses will not consume a lot of energy the number of cycles will certainly be higher than 2000 (TDC). But with this technology it is not possible to absolutely guarantee 5475 cycles with only one battery.

If the both batteries work correctly the DOD is 15 % and they will probably be able to supply the satellite during one year (TBC).

5.2.4 Protection Circuit Module (PCM)

Each cell is intrinsically protected by an overcharge, overdischarge and overcurrent detection system. This electronic system is integrated on the battery by the manufacturer. The specifications of this protection module are:

- Overcharge detection: $4.325 \text{ V} \pm 25 \text{ mV}$ (0.5 to 2 s delay)
- Overdischarge detection: $2.50 \text{ V} \pm 80 \text{ mV}$ (62.5 to 250 ms delay)
- Overcurrent detection : 3.0 to 5.5 A (4 to 16 ms delay)

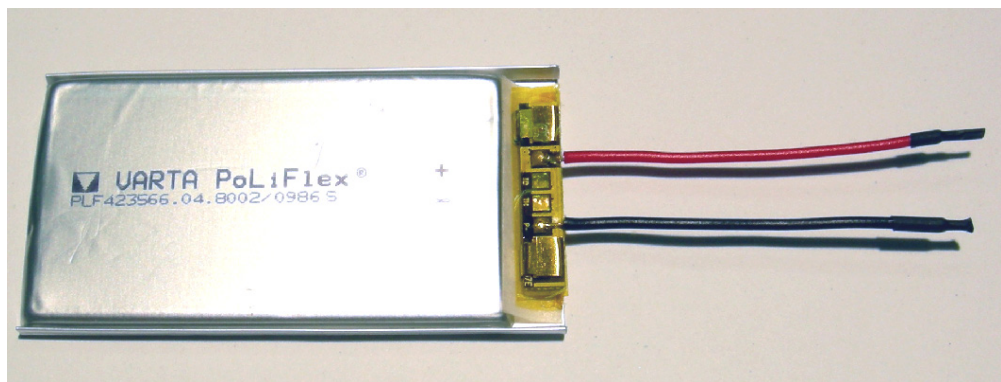


Figure 5-10 : PCM is integrated on the cell and can be easily removed.

The PCM is designed in such a way that it is easy to make a measure of the battery temperature. The second picture below shows two empty places where it is possible to weld temperature variable resistors. This possibility will not be used because the temperature of the battery will be measured by another component (TMP35, 36 or 37).

The big component on the right is the protection power switch of the PCM

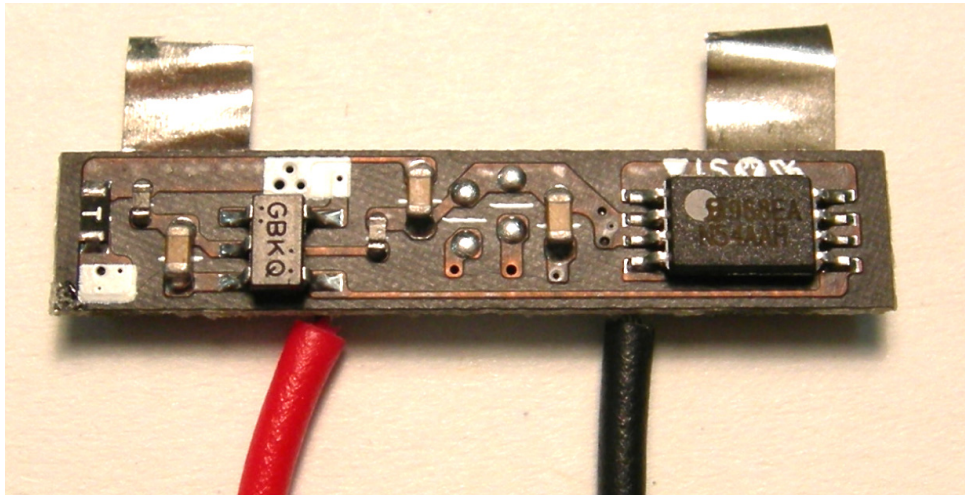
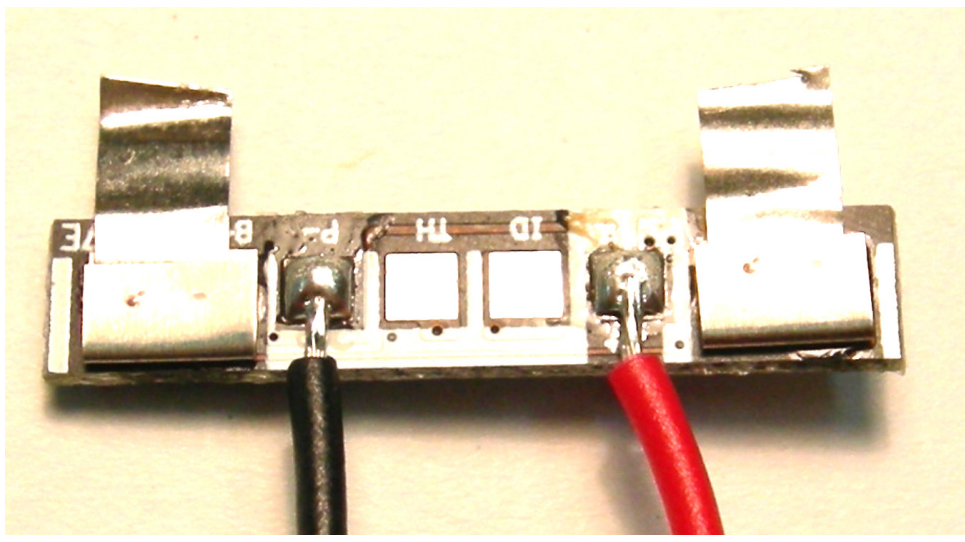


Figure 5-11 : Details of the PCM

When one of the protections is activated the battery is disconnected from the rest of the circuit. But it is not definitively disconnected. The PCM has been tested and here are the results:

Nominal mode:

The voltage at terminals of the PCM is the same that the battery voltage (without load).

Overcharge detection:

When the battery voltage goes over 4.3V the protection is activated and the voltage at terminals of the PCM is forced to 4.0V. When the battery voltage goes back under 4.3V the protection is automatically deactivated and the voltage at terminals of the PCM is the same again.

Overdischarge detection:

When the battery voltage goes under 2.5V the protection is activated and the voltage at terminals of the PCM is forced to 0V. To deactivate the protection, the voltage at terminals of the PCM must be higher than 3.2V.

The measurements are plotted below. First, the battery voltage has been simulated with a power supply voltage from 3.5 to 4.4V and then from 3.5 to 0V. The red characteristic is the voltage at terminals of the PCM.

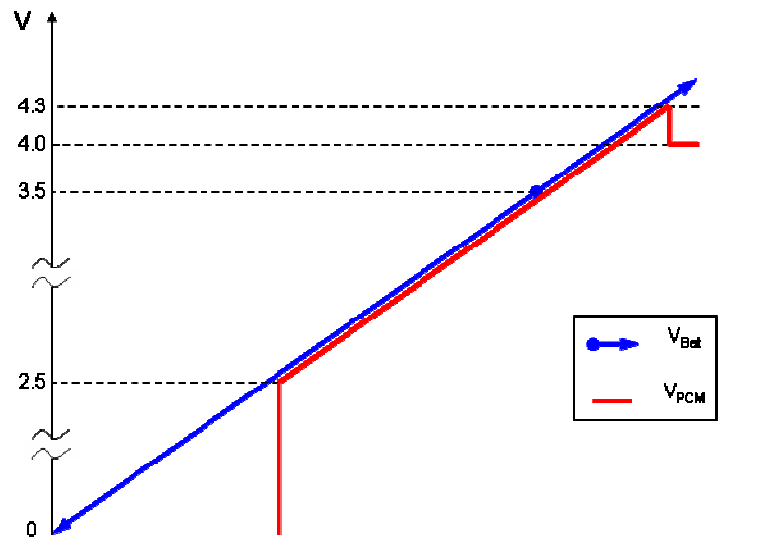


Figure 5-12 : Test of PCM

Overcurrent detection: (tested only for discharge)

When the discharging current grows, the voltage at terminals of the PCM decreases until 2.5V. In fact, it seems that the overcurrent protection uses the overdischarge detection to cut off the battery. To deactivate the protection, the voltage at terminals of the PCM must be higher than 3.2V.

The overcurrent detection works well but it could be problematical when discharging the batteries during eclipse. The discharge is already a critical point due to the temperature but if the current needed is high the discharge will stop too quickly due to the overcurrent detection. This difficulty must be studied (TDB).

5.3 Synthesized Power Budget

Here is described a simplified power budget which takes into consideration the average power consumption during the daylight and during the eclipse. The consumption of EPS is included in the user's consumption.

Assumptions: (from the power budget (v9) made by "System Engineering")

- Av. energy produced with the solar cells during the daylight: 1740 mWh
- Av. energy produced with the solar cells during the eclipse: 0 mWh
- Av. energy consumed by the users during the daylight with 30% margin: 1040 mWh
- Av. energy consumed by the users during the eclipse with 30% margin: 525 mWh
- Efficiency of charge: >90%
- Efficiency of discharge: >90%

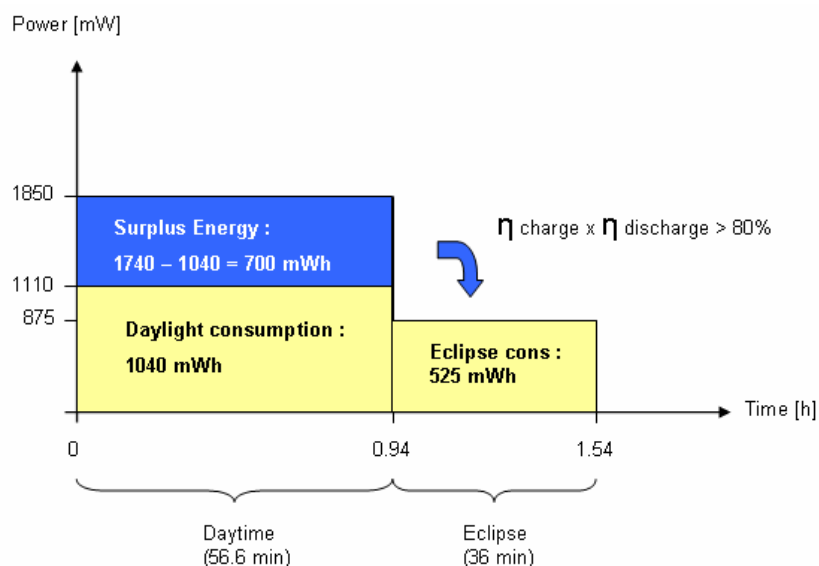


Figure 5-13 : Synthesized Power budget

So the energy stocked in the battery is:

$$E_{\text{Bat}} = 700 \text{ mWh} \cdot 90\% = 630 \text{ mWh.}$$

This amount of energy represents a Capacity of:

$$C = 630 \text{ mWh}/3.3 \text{ V} = 190 \text{ mAh.}$$

The capacity available on the battery is 360 mAh, so there is no problem.

6 BASELINE DESIGN

Abstract

This chapter explains the electronic design of EPS step by step. The table of content well summarizes its content:

6.1 General Description

The use of a microcontroller to do function of MPPT has not been kept. The radiation hardening is not sufficient whichever the microcontroller used (PIC of Microchip or MSP430 of Texas Instrument).

The solution consists in using the solar cells like current sources. The solar cells are connected in series by two and then in parallel. This configuration allows to directly connecting the solar cells to the power bus of 3.3V (V_{SC}). The DC/DC converters for the charge and the discharge of the battery are also used like current sources (I_{Ch} and I_{De}). In the case of the power generated by the solar cells is higher than the power consumed by the charge and the users another controlled current source dissipates the surplus of power through a power resistor. All current sources are in parallel in order to have a constant voltage at the terminals of the capacitor C. This capacitor transforms all the currents sources into a voltage source which is the power bus of the satellite. The figure below shows the general structure:

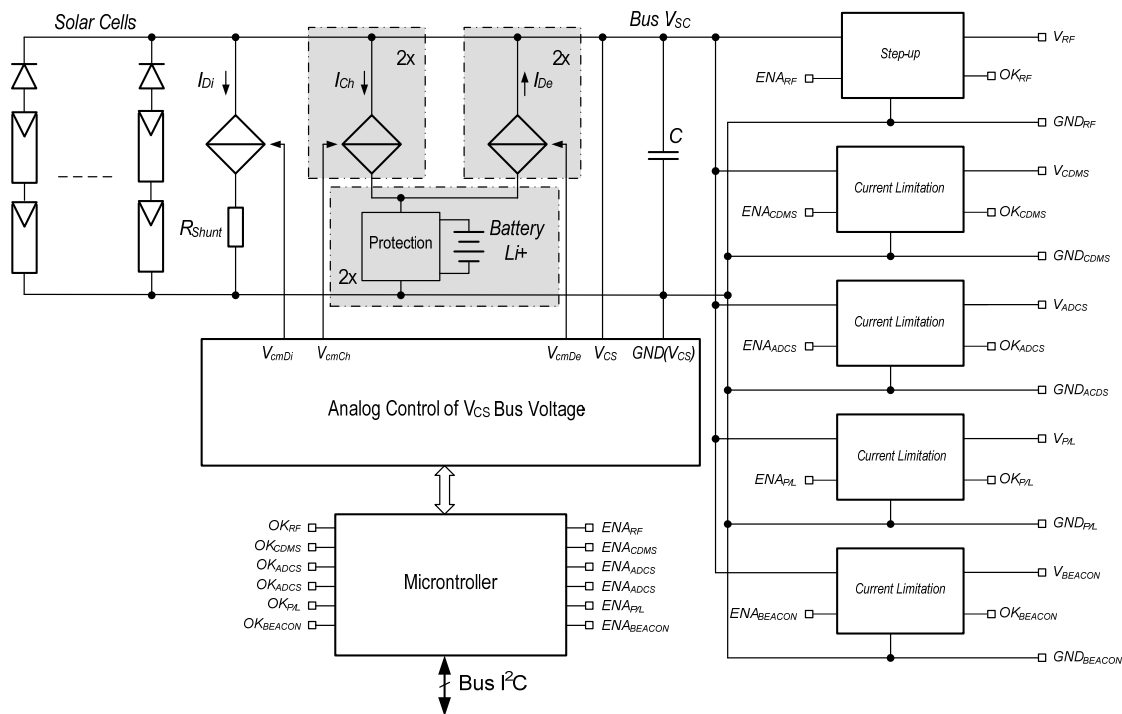


Figure 6-1 : General Structure

A hot redundancy has been chosen: the batteries are independently controlled with two separate circuits. The power bus V_{CS} is distributed to each users through a current limitation circuit. There is an exception for the telecommunication system (RF) which needs a higher voltage of 5V. This voltage is provided by a step-up converter.

6.2 Specifications

The voltage of the power bus is controlled with the charge and discharge systems and the dissipation system too.

Here is a flow chart of the Bus voltage control:

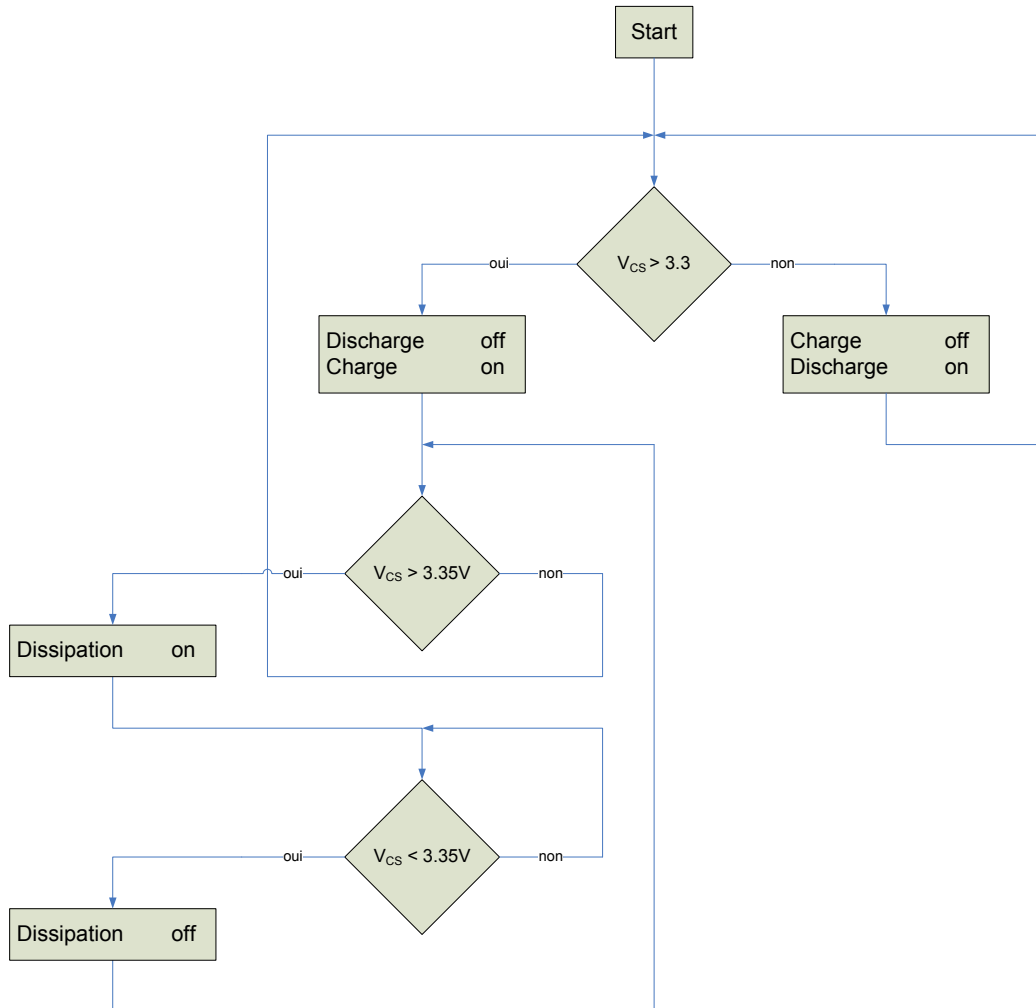


Figure 6-2 : Flow chart of the Power Bus voltage control

The nominal voltage of the power bus is 3.3V. Between the power bus and the users a maximum drop voltage of 0.1V is envisaged on the protection switches (current limitations). Thus, the nominal voltage at users interface will be ideally between 3.2 and 3.3V. However, knowing the constraints (temperatures variations, the dynamic of the converters, ...), the voltage at users interface can vary between 3.0V and 3.6V (maximal range), for in a nominal operation mode.

The regulation of the power bus is carried out by controlling the current sources. When the bus exceeds 3.3V, the charge system is activated with a maximum command when the bus reaches 3.35 V. When the power bus goes down under 3.3V the discharge system is activated with a maximum

command when the bus reaches 3.23 V. If the voltage of the bus exceeds 3.35V, the dissipation system is activated, with a maximum command when the bus reaches 3.4 V.

In the case of failure of the EPS the power bus can reach a maximum value of 4.2V.

6.3 Battery Charge Circuit

6.3.1 Step-up converter

Considering the critical mass budget requirement for EPS it is important to make a good converter selection because of the significant weight of the inductor.

In a DC/DC step-up converter the required inductance is inversely proportional to the frequency (for a constant current ripple). In order to have a small size inductor it is necessary to work with a very high frequency. This requirement imposes the use of a converter including the switching component.

The high frequency operation (up to 3 MHz) of the LTC3421 allows the use of small surface mount inductors.

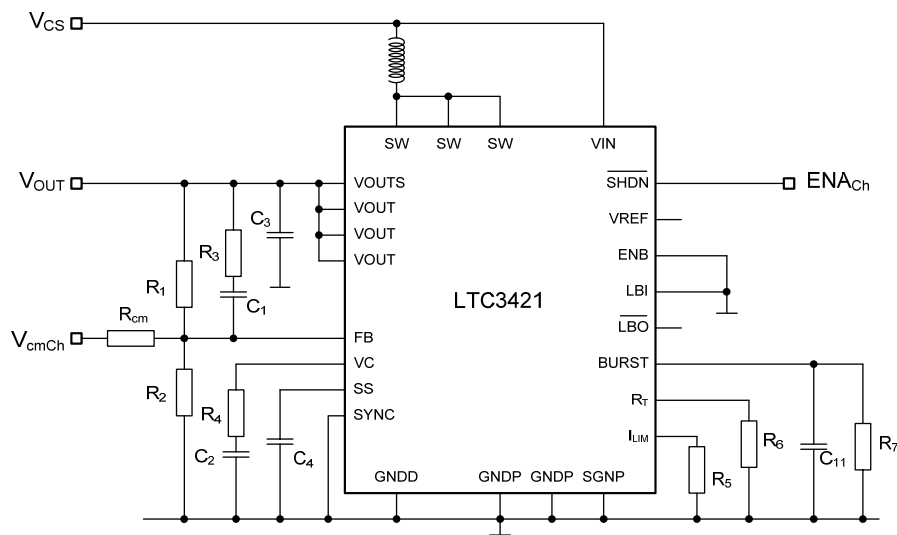


Figure 6-3 : LTC3421 with his external passive components

6.3.2 Voltage Control

The input voltage of this step-up converter is the solar cells voltage. The output voltage is directly the voltage at terminals of batteries.

The voltage divider (R_1/R_2) measures the output voltage (feedback). This voltage divider is modified with the command voltage V_{cmCh} and the resistor R_{cm} , so as to be able to control the output voltage.

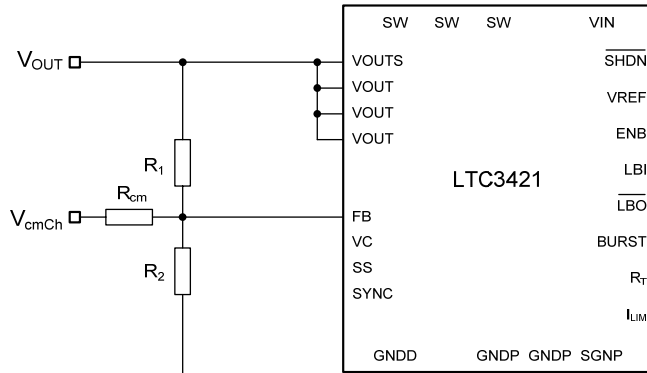


Figure 6-4 : Voltage Control

$$v_{FB} = \frac{R_2 R_{cm}}{R_1 R_2 + R_1 R_{cm} + R_2 R_{cm}} v_{OUT} + \frac{R_1 R_2}{R_1 R_2 + R_1 R_{cm} + R_2 R_{cm}} v_{cmCh} \quad 6.1$$

In steady state, the v_{FB} voltage corresponds to the internal reference voltage of the LTC3421 ($V_{REF}=1.220V$).

For $v_{cmCh}=V_{cmChMin}$, v_{OUT} is maximum (4.15V).

$$V_{REF} = \frac{R_2 R_{cm}}{R_1 R_2 + R_1 R_{cm} + R_2 R_{cm}} V_{OUT\max} + \frac{R_1 R_2}{R_1 R_2 + R_1 R_{cm} + R_2 R_{cm}} V_{cmChMin} \quad 6.2$$

For $v_{cmCh}=V_{cmChMax}$, v_{OUT} is minimum (3.3V)

$$V_{REF} = \frac{R_2 R_{cm}}{R_1 R_2 + R_1 R_{cm} + R_2 R_{cm}} V_{OUT\min} + \frac{R_1 R_2}{R_1 R_2 + R_1 R_{cm} + R_2 R_{cm}} V_{cmChMax} \quad 6.3$$

So it is possible to choose and calculate the values of R_{cm} , R_1 , and R_2 .

$$R_1 = \frac{V_{OUT\max} - V_{OUT\min}}{V_{cmChMax} - V_{cmChMin}} R_{cm} \quad 6.4$$

$$R_2 = \frac{V_{REF}}{\frac{1}{R_1} V_{OUT\max} + \frac{1}{R_{cm}} V_{cmChMin} - \frac{R_1 + R_{cm}}{R_1 R_{cm}} V_{REF}}$$

6.3.2.1 Choice of components

In order to determine R_{cm} , R_1 , and R_2 it is important to know that the variation of the reference voltage is not negligible.

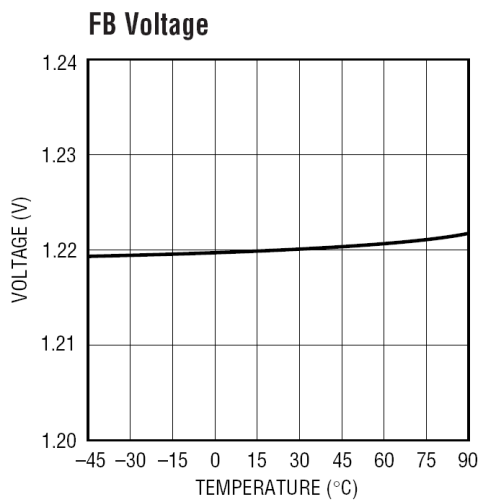


Figure 6-5 : LTC3421, Typical V_{FB} Voltage vs Temperature

This reference voltage of the feedback V_{FB} is the same that the reference voltage V_{REF} of the converter. However, V_{FB} varies less than V_{REF} when the temperature varies. The extreme values given by the datasheet are:

$$V_{FBmax} = 1.244 \text{ V}$$

$$V_{FBnom} = 1.220 \text{ V}$$

$$V_{FBmin} = 1.196 \text{ V}$$

The output voltage range desired is:

$$V_{OUTmax} = 4.15 \text{ V}$$

$$V_{OUTmin} = 3.3 \text{ V}$$

So with the help of a short Matlab routine the following results are obtained:

$$R_1 = 29.4 \text{ k} \pm 0.1\%$$

$$R_2 = 13.7 \text{ k} \pm 0.1\%$$

$$R_{cm} = 150 \text{ k} \pm 0.1\%$$

It is important to have a good precision on these resistances in order to guarantee that V_{OUT} don't come out of the maximal range of 3.3 V to 4.15 V. Therefore it is necessary to use a 0.1% tolerance.

Here is plotted $V_{OUT\min}$ and $V_{OUT\max}$ as a function of V_{FB} :

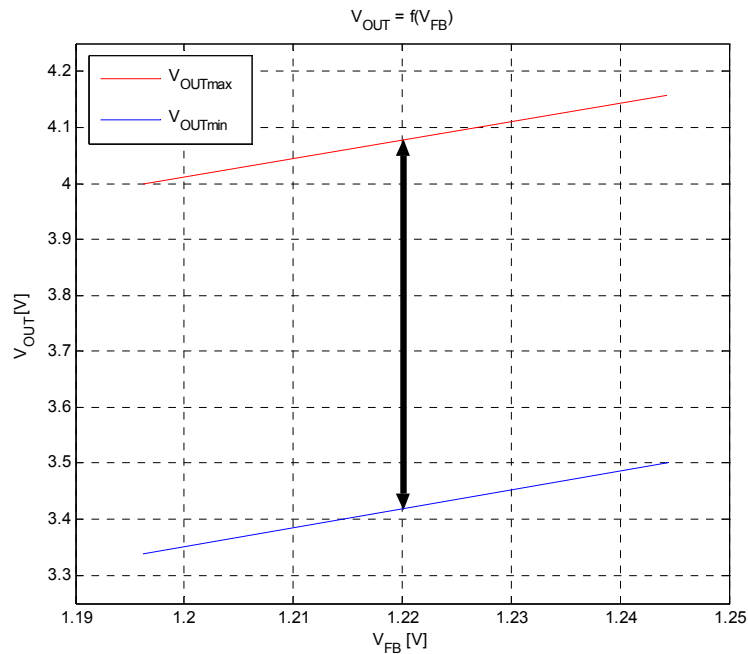


Figure 6-6 : V_{OUT} vs V_{FB}

Extreme and nominal points:

When $v_{FB} = V_{FB\max}$: $V_{OUT\max} = \mathbf{4.16 \text{ V}}$
 $V_{OUT\min} = \mathbf{3.50 \text{ V}}$

When $v_{FB} = V_{FB\text{nom}}$: $V_{OUT\max} = \mathbf{4.08 \text{ V}}$
 $V_{OUT\min} = \mathbf{3.42 \text{ V}}$

When $v_{FB} = V_{FB\min}$: $V_{OUT\max} = \mathbf{4.00 \text{ V}}$
 $V_{OUT\min} = \mathbf{3.33 \text{ V.}}$

6.3.2.2 Transfer Function

By separating the working point and the variation around it, it is possible to write:

$$\begin{aligned} v_{cmCh} &= \Delta V_{cmCh} + V_{REF} \\ v_{OUT} &= \Delta V_{OUT} + V_{OUTNom} \end{aligned} \quad 6.5$$

Where

$$V_{OUTNom} = \left(\frac{R_1}{R_2} + 1 \right) V_{REF} = 3.82 \text{ V} \quad 6.6$$

So, for the nominal working point the variation is:

$$\Delta V_{OUT} = -\frac{R_1}{R_{cm}} \Delta V_{cmCh} \quad 6.7$$

In dynamic state, it is assumed that the step-up converter is a system of 2nd order. With the help of Laplace it becomes:

$$V_{OUT}(s) = -\frac{R_1}{R_{cm}} \frac{\omega_n^2}{s^2 + 2\xi\omega_n s + \omega_n^2} V_{cmCh}(s) \quad 6.8$$

Where ω_n and ξ must be defined by measurements.

The transfer function between the output voltage and the command voltage is described by the following relation:

$$G_{Step-up}(s) = \frac{V_{OUT}(s)}{V_{cmCh}(s)} = -\frac{R_1}{R_{cm}} \frac{\omega_n^2}{s^2 + 2\xi\omega_n s + \omega_n^2} \quad 6.9$$

6.3.3 Burst Mode Control

The battery charge current can take any value in the range of 0 to 1 Ampere. In order to have a high efficiency even if the charge current is low it is needed to use the Burst Mode operation.

Burst Mode operation can be automatic controlled. The IC will automatically enter Burst Mode operation at light load and return to fixed frequency PWM mode for heavier loads. The user can program the average load current at which the mode transition occurs using a RC network connected from BURST pin to ground.

For example, here is the efficiency of a typical application with very similar characteristics in comparison to our system. The Burst Mode is activated when the output current is between 0 and $I_{BURST} = 100 \text{ mA}$

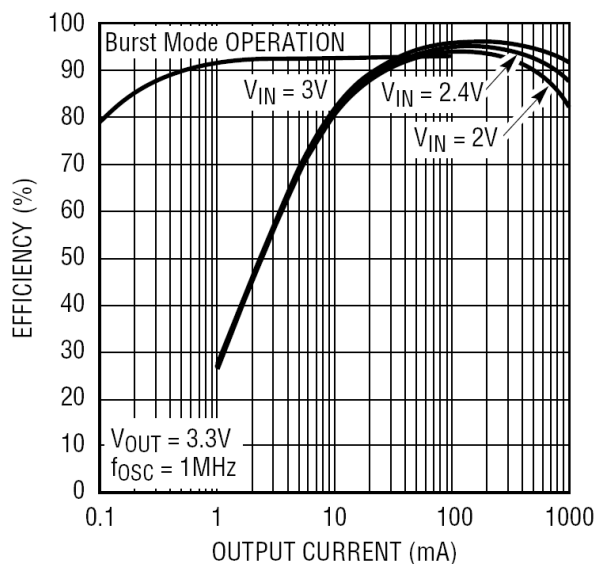


Figure 6-7 : Typical Application @ 1 MHz

6.3.3.1 Choice of components

The value of the resistor will control the average load current (I_{BURST}) at which Burst Mode operation will be entered and exited (there is hysteresis to prevent oscillation between modes), according to the formula:

$$R_7 = R_{BURST} = \frac{2}{I_{BURST}} \quad 6.10$$

Where R_{BURST} is in $\text{k}\Omega$ and I_{BURST} is in A

In order to precisely know the value of I_{BURST} it is necessary to make some tests but for the first design we can consider that $I_{BURST} \approx 100$ mA. Therefore the resistance required is 20 k.

The equation given for the capacitor on BURST is for the minimum value to prevent ripple on BURST from causing the part to oscillate in and out of Burst Mode operation at the current where the mode transition occurs:

$$C_5 = C_{BURST} \geq \frac{C_{OUT} \cdot V_{OUT}}{10000} \quad 6.11$$

Where C_{BURST} and C_{OUT} are in μF

For C_{OUT} , the datasheet recommends a ceramic capacitor of 22 μF . So C_{BURST} must be at least 7.5 nF but the datasheet recommends a capacitor of 0.1 μF .

Here is the RC network:

$$R_7 = 20 \text{ k} \pm 1\%$$

$$C_5 = 0.1 \mu\text{F}$$

$$C_7 = 22 \mu\text{F}$$

6.3.4 Oscillator frequency

There are several considerations in selecting the operating frequency of the converter. The first is the physical size of the converter. As the operating frequency goes up, the inductor and filter capacitors go down in value and size. The second is the efficiency of the converter because the switching losses due to gate charge are going up proportional with frequency.

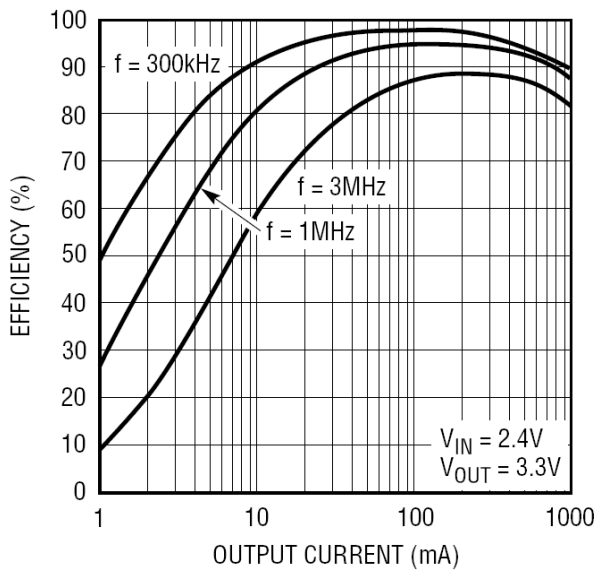


Figure 6-8 : Efficiency vs Frequency

The good compromise for the charge circuit is an oscillator frequency of 1 MHz.

6.3.4.1 Component Choice

The frequency of operation is set through a resistor from the RT pin to ground according to the formula:

$$f_{osc} = \frac{28100}{R_6} \quad 6.12$$

Where f_{osc} is in kHz and R_6 is in kΩ.

So the choice for R_6 is $28 \text{ k} \pm 1\%$

6.3.5 Inductor selection

For high efficiency, it is important to choose an inductor with high frequency core material, such as ferrite, to reduce core losses. The inductor should have low ESR (equivalent series resistance) to reduce the RI^2 losses and must be able to handle the peak inductor current without saturating.

The minimum inductance value is proportional to the operating frequency and is limited by the following constraints:

$$L > \frac{3}{f} \quad \text{and} \quad L > \frac{V_{SC\min} \cdot (V_{OUT\max} - V_{SC\min})}{f \cdot I_{Ripple} \cdot V_{OUT\max}} \quad 6.13$$

Where

L = inductance in μH

I_{Ripple} = allowable inductor current ripple (Amps Peak-Peak)

f = operating frequency in MHz

The datasheet recommends an inductor of $4.7 \mu\text{H}$. With this inductance $I_{Ripple_max} \approx 150 \text{ mA}$. This ripple is acceptable.

6.3.5.1 Component Choice

The RLF7030T SMD inductor from TDK is ideal for this application.

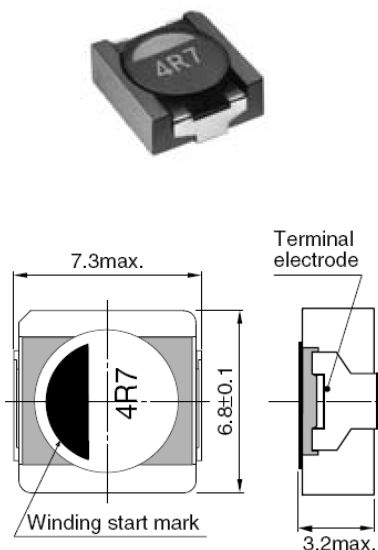


Figure 6-9 : RLF7030T-4R7M3R4 Shapes and Dimensions

6.3.6 Internal Current Limitation

The programmable current limit circuit sets the maximum peak current. This clamp level is programmed with a resistor from ILIM to ground. In Burst Mode operation, the current limit is automatically set to a nominal value of 0.6A peak for optimal efficiency.

$$I_{LIM} = \frac{150}{R_5} \quad 6.14$$

Where: I_{LIM} is in A and R_5 is in kΩ.

6.3.6.1 Component Choice

As it will be describe in the “Charge Current Control” chapter, the current is controlled with a regulation loop. This automatic current control fixes the limit charging current at 1A. The internal current limit of the LTC3421 must not be activated if the control loop is working well. In order to guarantee this requirement the internal current limit is fixed at 2A. Therefore, $R_5 = 75$ kΩ.

6.3.7 Shut-Down the converter

The LTC3421 is shut down by pulling the SHDN pin below 0.3V, and activated by pulling the pin initially above 1V and maintaining a high state down to 0.5V.

6.3.8 Other passive components

As recommended in the datasheet:

- **SS Pin:** 0.1 μ F capacitor is used to program a Soft-Start time of 32ms.
- **VC Pin:** A frequency compensation network (100 k Ω and 470 pF) is connected from this pin to ground to compensate the loop.

Between VIN Pin and FB Pin, a RC network can be added in order to filter the ripple

6.4

Charge Current Control

It is important to control the battery charge current in order to be sure that the I_{Bat_max} is not too high. Therefore, it is necessary to add a current control loop on the step-up converter.

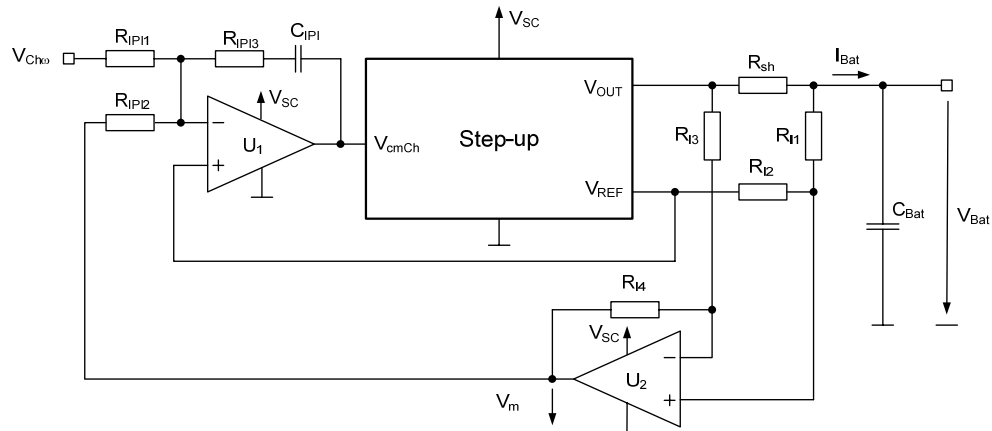


Figure 6-10 : Schema de la mesure de du courant I_{Bat} et regulator de courant

6.4.1 Charging current measure

The current measurement is carried out with a shunt resistor (R_{sh}) and a differential amplifier. This amplifier gives a voltage (v_m) proportional to the current:

$$v_m = \frac{R_{I3} + R_{I4}}{R_{I1} + R_{I2}} \frac{R_{I2}}{R_{I3}} v_{Bat} - \frac{R_{I4}}{R_{I3}} (v_{Bat} + R_{sh} i_{Bat}) + \frac{R_{I3} + R_{I4}}{R_{I1} + R_{I2}} \frac{R_{I1}}{R_{I3}} V_{REF} \quad 6.15$$

If $R_{I1} = R_{I3}$ and $R_{I2} = R_{I4}$

$$v_m = -\frac{R_{I2}}{R_{I1}} R_{sh} i_{Bat} + V_{REF} \quad 6.16$$

In small signals state ($v_m = \Delta V_m + V_{REF}$), the relation 6.16 becomes:

$$\Delta V_m = -\frac{R_{I2}}{R_{I1}} R_{sh} \Delta I_{Bat} \quad 6.17$$

From the relation 6.17, it is possible to determine the transfer function of the charge current measure system:

$$G_{mICh}(s) = \frac{V_m(s)}{I_{Bat}(s)} = -\frac{R_{I2}}{R_{I1}} R_{sh} \quad 6.18$$

6.4.1.1 Component Choice

The battery withstands currents higher than 1A. However, the maximal current is fixed at 1 A in order to increase the life-time of the battery:

$$I_{\text{Bat_max}} = 1 \text{ A} \pm 10\%$$

The power losses on the shunt resistor must be as lower as possible. So it has been decided to use a shunt with a low ohmic value:

$$R_{\text{sh}} = 0.05 \Omega \pm 1\%$$

$$\text{Maximal losses on the shunt: } R_{\text{sh}} \cdot (I_{\text{Bat_max}})^2 = 0.05 \cdot 1^2 = 50 \text{ mW}$$

When the charging current is maximal, V_m is minimal:

$$V_{m_{\text{min}}} = 0 \text{ V}$$

When the charging current is null:

$$V_{m_{\text{max}}} = V_{\text{REF}} = 1.22 \text{ V}$$

In this control loop, the variation of the reference and the tolerance on the resistors is not prominent given the fact that the tolerance of the charging current is not accurate.

In order to avoid the saturation of the current measurement, the gain between I_{Bat} and V_m is modified. $V_m = 0$ when $i_{\text{Bat}} = 2 \cdot I_{\text{Bat_max}} = 2 \text{ A}$

Then, gains will be adjusted on the PI regulator in order to guarantee that the current exceeds $I_{\text{BAT_max}}$.

With the relation 6.16, it is now possible to determine the resistors:

$$V_{m_{\text{min}}} = -\frac{R_{I2}}{R_{I1}} R_{\text{sh}} \cdot I_{\text{Bat_max}} + V_{\text{REF}} \quad 6.19$$

So, the resistive divider is:

$$\frac{R_{I2}}{R_{I1}} = 12.2 \quad 6.20$$

The chosen resistors are:

$$R_{I2} = R_{I4} = 270 \text{ k} \pm 1\%$$

$$R_{I1} = R_{I3} = 22 \text{ k} \pm 1\%$$

6.4.2 Voltage at terminals of the battery

The charging current of the battery depends on the output voltage of the step-up converter and the voltage of the battery. The battery is modelled by a high value capacitor. Its capacitance can be calculated like this:

$$C_{Bat} = \frac{Q_{Bat}}{V_{Bat_max} - V_{Bat_min}} \quad 6.21$$

Where

$$\begin{aligned} V_{Bat_max} &= 4.2 \text{ V} \\ V_{Bat_min} &= 2.7 \text{ V} \\ Q_{Bat} &= 1200 \text{ mAh} = 4320 \text{ C} \end{aligned}$$

$$\Rightarrow C_{Bat} = \frac{4320}{4.2 - 2.7} = 2880 \text{ F} \quad 6.22$$

And then,

$$\left. \begin{aligned} v_{OUT} &= v_{Bat} + (R_{sh} + R_s) i_{Bat} \\ i_{Bat} &= C_{Bat} \frac{\partial v_{Bat}}{\partial t} \end{aligned} \right\} \quad v_{OUT} = \frac{1}{C_{Bat}} \int i_{Bat} dt + V_{BatNom} + (R_{sh} + R_s) i_{Bat} \quad 6.23$$

R_s is the internal resistance of the battery.

In small signal state ($v_{OUT} = V_{BatNom} + \Delta V_{OUT}$), it is possible to determine the transfer function between the output voltage of the step-up converter and the charging current of the battery, from the relation 6.23:

$$G_{Bat} = \frac{I_{bat}(s)}{V_{OUT}(s)} = \frac{sC_{Bat}}{1 + s(R_{sh} + R_s)C_{Bat}} \quad 6.24$$

6.4.3 Current regulator

By examining the transfer function of the system to control, it is easy to see that the current regulator could be Proportional-Integrator.

$$\begin{aligned} v_{cmCh} &= -\frac{R_{IP3}}{R_{IP1}} \left(v_{Ch\omega} - V_{REF} + \frac{1}{R_{IP3}C_{IP1}} \int (v_{Ch\omega} - V_{REF}) dt \right) \\ &\quad - \frac{R_{IP3}}{R_{IP2}} \left(v_m - V_{REF} + \frac{1}{R_{IP3}C_{IP1}} \int (v_m - V_{REF}) dt \right) + V_{REF} \end{aligned} \quad 6.25$$

By separating the working point and the variation around it, it is possible to write:

$$\begin{aligned} \Delta V_{cmCh} &= v_{cmCh} - V_{REF} \\ \Delta V_{Ch\omega} &= v_{Ch\omega} - V_{REF} \\ \Delta V_m &= v_m - V_{REF} \end{aligned} \quad 6.26$$

And we obtain:

$$\Delta V_{cmCh} = -\frac{R_{IPI3}}{R_{IPI1}} \left(\Delta V_{Ch\omega} + \frac{R_{IPI1}}{R_{IPI2}} \Delta V_{Chm} + \frac{1}{R_{IPI3} C_{IPI1}} \int \left(\Delta V_{Ch\omega} + \frac{R_{IPI1}}{R_{IPI2}} \Delta V_{Chm} \right) dt \right) \quad 6.27$$

With the help of Laplace, the last relation becomes:

$$V_{cmCh}(s) = - \underbrace{\left(V_{Ch\omega}(s) + \frac{R_{IPI1}}{R_{IPI2}} V_{Chm}(s) \right)}_{e_I(s)} \frac{R_{IPI3}}{R_{IPI1}} \frac{1 + s R_{IPI3} C_{IPI1}}{s R_{IPI3} C_{IPI1}} \quad 6.28$$

From the relation 6.28 it is possible to determine the transfer function of the current regulator:

$$G_{PlCh} = \frac{V_{cmCh}(s)}{e_I(s)} = -\frac{R_{IPI3}}{R_{IPI1}} \frac{1 + s R_{IPI3} C_{IPI1}}{s R_{IPI3} C_{IPI1}} \quad 6.29$$

6.5 Battery Discharge Circuit

6.5.1 Step-down converter

In order to have a small size inductor a high frequency converter has been selected. The high frequency operation (up to 4 MHz) of the LTC3414 allows the use of small surface mount inductors.

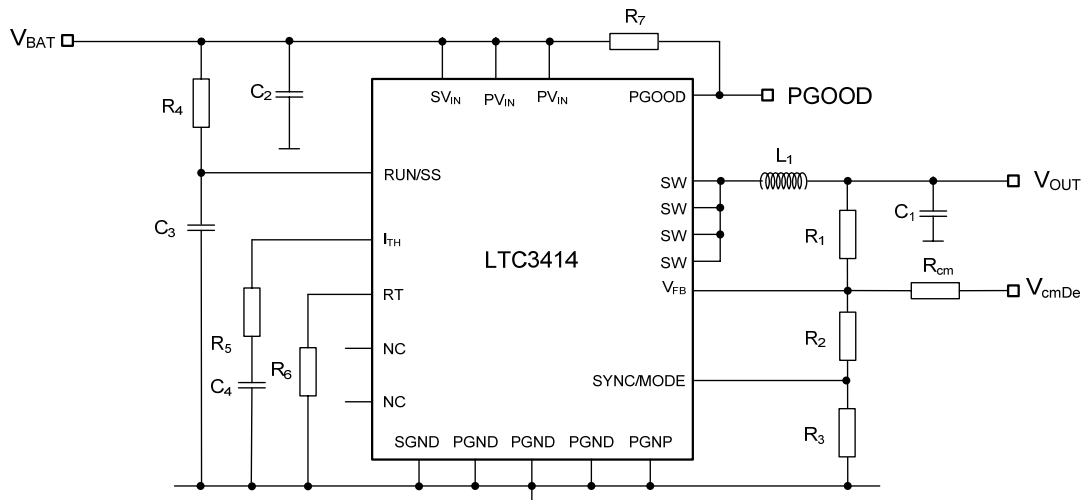


Figure 6-11 : LTC3414 with his external passive components

6.5.2 Voltage Control

The input voltage of the step-down converter is the battery voltage. The output voltage is directly the voltage at terminals of the solar cells.

The voltage divider (R_1 and R_2+R_3) measures the output voltage (feedback). This voltage divider is modified with the command voltage V_{cmDe} and the resistor R_{cm} , so as to be able to control the output voltage.

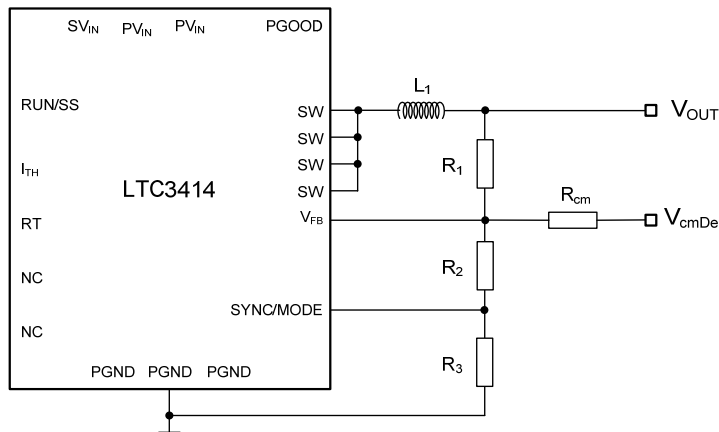


Figure 6-12 : Voltage Control

When the bus voltage is minimal (3.23 V), the output voltage $V_{OUT} = V_{OUT_{max}} = 3.5$ V. This voltage value is intentionally chosen enough high so as to guarantee the activation of the discharge. The current control loop will work to modify V_{OUT} in order to guarantee that the discharging current don't exceed $1\text{ A} \pm 10\%$

When the bus voltage is nominal (3.3V), the error is null $\Rightarrow V_{OUT} = V_{OUT_{min}} = 3.1$ V. This voltage value is intentionally chosen enough low so as to guarantee the deactivation of the discharge. This voltage value will not appear on the output of the converter because the current cannot circulate on the other way. The output voltage should be stabilized at 3.3V

The following equations are defined by the Figure 6-12:

$$v_{FB} = \frac{R_{cm}(R_2 + R_3)}{R_l(R_2 + R_3) + R_l R_{cm} + R_{cm}(R_2 + R_3)} v_{OUT} + \frac{R_l(R_2 + R_3)}{R_l(R_2 + R_3) + R_l R_{cm} + R_{cm}(R_2 + R_3)} v_{cmDe} \quad 6.30$$

In steady state, the v_{FB} voltage corresponds to the internal reference voltage of the LTC3414 ($V_{REF}=0.8V$).

For $v_{cm}=V_{cmDeMin}$, v_{OUT} is maximal (3.5 V):

$$V_{REF} = \frac{R_{cm}(R_2 + R_3)}{R_l(R_2 + R_3) + R_l R_{cm} + R_{cm}(R_2 + R_3)} V_{OUT_{max}} + \frac{R_l(R_2 + R_3)}{R_l(R_2 + R_3) + R_l R_{cm} + R_{cm}(R_2 + R_3)} V_{cmDeMin} \quad 6.31$$

For $v_{cm}=V_{cmDeMax}$, v_{OUT} is minimal (3.1V):

$$V_{REF} = \frac{R_{cm}(R_2 + R_3)}{R_1(R_2 + R_3) + R_1R_{cm} + R_{cm}(R_2 + R_3)} V_{OUT\min} \\ + \frac{R_1(R_2 + R_3)}{R_1(R_2 + R_3) + R_1R_{cm} + R_{cm}(R_2 + R_3)} V_{cmDeMax} \quad 6.32$$

So it is possible to choose and calculate the values of R_{cm} , R_1 , R_2 and R_3 , knowing that R_3 defines the transition from Burst mode to Continue mode (see Burst Mode Control).

$$R_1 = \frac{V_{OUT\max} - V_{OUT\min}}{V_{cmDeMax} - V_{cmDeMin}} R_{cm} \\ R_2 + R_3 = \frac{V_{REF}}{\frac{1}{R_1}V_{OUT\max} + \frac{1}{R_{cm}}V_{cmDeMin} - \frac{R_1 + R_{cm}}{R_1R_{cm}}V_{REF}} \quad 6.33 \\ \frac{R_3}{(R_1 + R_2 + R_3)} = \frac{V_{BURST}}{V_{OUT}}$$

6.5.2.1 Choice of components

The output voltage range desired is:

$$V_{OUTmax} = 3.5 \text{ V}$$

$$V_{OUTmin} = 3.1 \text{ V}$$

With the help of a short Matlab routine the following results are obtained (with E24 resistor category)

$$R_1 = 270 \text{ k} \pm 1\%$$

$$R_2 = 36 \text{ k} \pm 1\%$$

$$R_3 = 47 \text{ k} \pm 1\%$$

$$R_{cm} = 2 \text{ M} \pm 1\%$$

The resistor precision is not critical in this case so using 1% tolerance is possible.

6.5.2.2 Transfer Function

By separating the working point and the variation around it, it is possible to write:

$$v_{cmDe} = \Delta V_{cmDe} + V_{REF}$$

$$v_{OUT} = \Delta V_{OUT} + V_{OUTNom} \quad 6.34$$

Where

$$V_{OUTNom} = \left(\frac{R_1}{(R_2 + R_3)} + 1 \right) V_{REF} = 3.40 \text{ V} \quad 6.35$$

So, for the nominal working point the variation is:

$$\Delta V_{OUT} = -\frac{R_1}{R_{cm}} \Delta V_{cmDe} \quad 6.36$$

In dynamic state, it is assumed that the step-down converter is a system of 2nd order. With the help of Laplace it becomes:

$$V_{OUT}(s) = -\frac{R_1}{R_{cm}} \frac{\omega_n^2}{s^2 + 2\xi\omega_n s + \omega_n^2} V_{cmDe}(s) \quad 6.37$$

Where ω_n and ξ must be defined by measurements.

The transfer function between the output voltage and the command voltage is described by the following relation:

$$G_{Step_Down}(s) = \frac{V_{OUT}(s)}{V_{cmDe}(s)} = -\frac{R_1}{R_{cm}} \frac{\omega_n^2}{s^2 + 2\xi\omega_n s + \omega_n^2} \quad 6.38$$

6.5.3 Burst Mode Control

The battery discharge current can take any value in the range of 0 to 1 Ampere. In order to have a high efficiency even if the charge current is low we need to use the Burst Mode operation.

Connecting the SYNC/MODE pin to a voltage in the range of 0 to 1V enables Burst Mode operation. In Burst Mode operation, the internal power MOSFETs operate intermittently at light loads. This increases efficiency by minimizing switching losses.

For example, here is the efficiency of a typical application. The Burst Mode is activated at a light current of about 0.6 A.

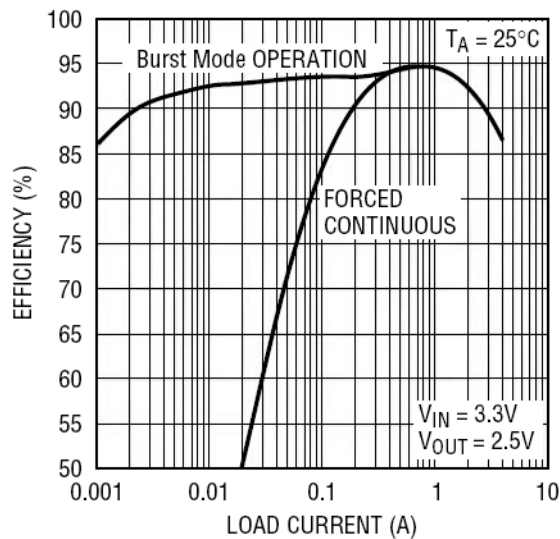


Figure 6-13 : Efficiency vs Load Current

6.5.3.1 Choice of components

During Burst Mode Operation, the voltage on the SYNC/MODE pin determines the burst clamp level, which sets the minimum peak inductor current, I_{BURST} , for each switching cycle according to the following equation:

$$I_{BURST} = 11.5 \cdot (V_{BURST} - 0.383) \quad 6.39$$

V_{BURST} is the voltage on the SYNC/MODE pin. I_{BURST} can only be programmed in the range of 0A to 7A. For values of V_{BURST} greater than 1V, I_{BURST} is set at 7A. For values of V_{BURST} less than 0.4V, I_{BURST} is set at 0A.

In order to precisely know the value of I_{BURST} it is necessary to make some tests but for the first design we can consider that $I_{BURST} \approx 0.7$ A $\Rightarrow V_{BURST} \approx 0.44$ V.

Therefore R_3 is defined by the following equation:

$$\frac{R_3}{(R_1 + R_2 + R_3)} = \frac{V_{BURST}}{V_{OUT}} \quad 6.40$$

6.5.4 Oscillator frequency

Although frequencies as high as 4MHz are possible, the efficiency of the converter is going down with frequency.

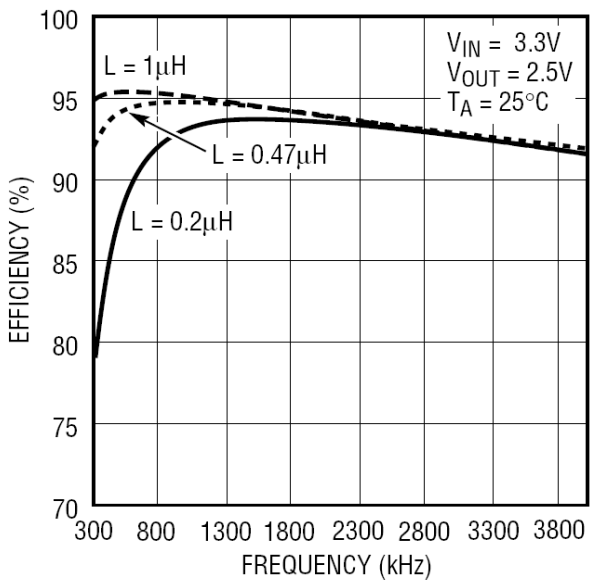


Figure 6-14 : Efficiency vs Frequency

So with a 47 μ H inductance and a frequency of 1 MHz the efficiency will be very high.

6.5.4.1 Component Choice

The operating frequency of the LTC3414 is determined by an external resistor that is connected between pin RT and ground. The value of the resistor sets the ramp current that is used to charge and discharge an internal timing capacitor within the oscillator and can be calculated by using the following equation:

$$R_6 = \frac{3.08 \cdot 10^{11}}{f} - 10 \cdot 10^3 \quad 6.41$$

Where f is in Hz and R₆ is in Ω .

So the choice for R₆ is 300 k \pm 1%

6.5.5 Inductor selection

For a given input and output voltage, the inductor value and operating frequency determine the ripple current. The ripple current increases with higher V_{IN} ($= V_{BAT}$) or V_{OUT} and decreases with higher inductance:

$$I_{Ripple} = \frac{V_{OUT}}{f \cdot L} \cdot \left(1 - \frac{V_{OUT}}{V_{BAT}}\right) \quad 6.42$$

Where

L = inductance in μH

I_{Ripple} = inductor current ripple (Amps Peak-Peak)

f = operating frequency in MHz

The datasheet recommends using an inductor of $0.47 \mu H$. But with this value the current ripple will be too much high when $V_{BAT} = V_{BAT_{max}}$:

$$I_{Ripple} = \frac{3.3}{1 \cdot 0.47} \cdot \left(1 - \frac{3.3}{4.15}\right) = 1.44 A \quad 6.43$$

To guarantee that the ripple current stays below a specified maximum, the inductor value should be chosen according to the following equation:

$$L = \frac{V_{OUT}}{f \cdot I_{Ripple}} \cdot \left(1 - \frac{V_{OUT}}{V_{BAT_{max}}}\right) \quad 6.44$$

The current ripple of the inductor of the step-up converter was 150 mA. The same value is chosen for the inductor of the step-down converter:

$$L = \frac{3.3}{1 \cdot 0.150} \cdot \left(1 - \frac{3.3}{4.15}\right) = 4.5 \mu H \quad 6.45$$

6.5.5.1 Component Choice

The RLF7030T SMD inductor from TDK ($4.7 \mu H$) is also ideal for this application.

6.5.6 Output Capacitor

The output voltage ripple mainly depends on the ESR of the output capacitor:

$$\Delta V_{OUT} \leq I_{Ripple} \cdot \left(ESR + \frac{1}{8 \cdot f \cdot C_{OUT}} \right) \quad 6.46$$

Where

- ΔV_{OUT} = output voltage ripple in V
- I_{Ripple} = inductor current ripple (Amps Peak-Peak)
- ESR = effective series resistance in Ω
- f = operating frequency in MHz
- C_{OUT} = output capacitor in μF

Here is the output voltage ripple with an output capacity of 440 μF and an ESR of 0.5 Ω :

$$\Delta V_{OUT\max} = 0.15 \cdot \left(0.5 + \frac{1}{8 \cdot 1 \cdot 440} \right) = 75 mV \quad 6.47$$

6.5.6.1 Component Choice

It is important to know that the output voltage ripple will not change a lot if C_{OUT} varies. The output ripple is directly dependant on the ESR. So it is important to find capacitors with very low ESR. Special polymer capacitors offer very low ESR but have lower capacitance density than other types. This way has been explored with 2 different manufacturers of capacitors:

Eurofarad: PM90SR2 (for space application)

- Dielectric: Metallised polyester (P.E.T)
- Technology: Self-healing; non-inductive; thermoplastic case; epoxy resin sealed

This type of capacitors is very efficient, but too much heavy (~ 50 grams for 150 μF), too much expansive (~ 500 Euros without qualification tests...) and too much big (~ 30 mm 3).

AVX: FFB54D0117K

- Dielectric: non-impregnated metallised polypropylene or polyester dielectric
- Technology: Self-healing; very high dielectric strength in operating conditions up to 105°C.

For this type of capacitors, the price was not a problem but it is also too much heavy (~ 35 grams for 110 μF) and too much big (~ 30 mm 3).

It has been necessary to search in others technologies:

Tantalum capacitors have the highest capacitance density but it is important to only use types that have been surge tested for use in switching power supplies. Aluminium electrolytic capacitors have significantly higher ESR. Ceramic capacitors have excellent low ESR characteristics but they are not available for high capacitances. So the second way was the tantalum capacitors.

The EPPL has made a selection of tantalum solid electrolyte capacitors [N4]. In the TAJ series of AVX the final choice has been made:

AVX: TAJY227K010R (space qualified):

- Dielectric: Standard Tantalum
- Technology: very high capacitance density; temperature range from -55 to +125°C

For this type of capacitors, the price, the mass, the size and the ESR are not a problem:

Mass: ~ 3 grams for 220 μ F

Size: ~ 5 mm³

Price: ~1.4 Euro

ESR: 0.5 Ω at 100 kHz

These characteristics fit very well with the requirements.

By placing multiple capacitors in parallel the equivalent ESR is reduced. Three TAJY227K010R will be used in parallel (the third is for redundancy). So the equivalent ESR will certainly be lower than 0.5 Ω .

It is also important to know what happens when tantalum capacitor breaks down. Some tests (TBD) must be done to define if the capacitor becomes an open circuit or a closed circuit. If the capacitor becomes an open circuit there is no problem because the redundancy can prevent this failure. But if the capacitor becomes a closed circuit the voltage of the power bus will fall down and the mission is lost as long as the short circuit is active. It should be possible to use a matrix of capacitor like this one to prevent both types of failure:

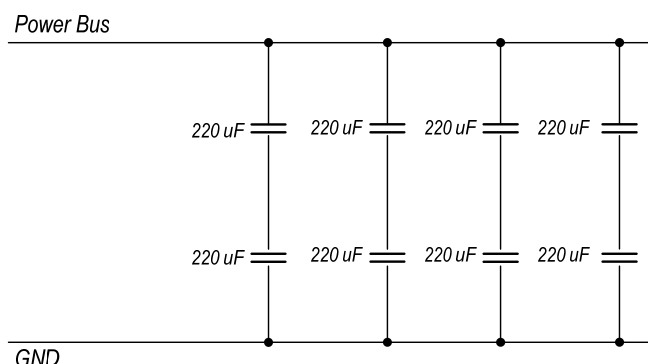


Figure 6-15 : Matrix of capacitors, $C_{eq} = 440 \mu F$

The equivalent capacity is:

$$C_{eq} = 4 \cdot \frac{1}{\frac{1}{220\mu F} + \frac{1}{220\mu F}} = 440\mu F \quad 6.48$$

So if one of the capacitors becomes an open circuit the equivalent capacity becomes $330\mu F$. If one of the capacitors becomes a closed circuit the equivalent capacity stays at $440\mu F$.

However, some destructive tests have already revealed that tantalum capacitors become neither an open circuit nor a closed circuit. After tests capacitors became a resistance of about 300k to 500k. In this case the matrix of capacitor has no more interest. These results must be confirmed with other tests.

6.5.7 Shut-Down the converter

It is possible to shut down the converter with the RUN/SS pin. This pin is the Run Control and Soft-Start Input. Forcing this pin below 0.5V shuts down the LTC3414. In shutdown all functions are disabled. Less than $1\mu A$ of supply current is consumed.

But in order to be sure that the battery is completely disconnected of the converter, a switch is used as a protection between the battery and the converter (see the “Charge and discharge security” chapter). An analysis still must be done (TBD) to know if this component is really necessary, because it is big and it adds a resistance of $30\text{ m}\Omega$ on the power line between the battery and the converter.

6.5.8 Other passive components

As recommended in the datasheet:

- **I_{TH} Pin:** A RC network ($20\text{ k}\Omega$ and 470 pF) is connected from this pin to ground.
- **PGOOD:** A $100\text{k}\Omega$ resistor is connected from this pin to V_{IN}

6.6 Discharge Current Control

It is important to control the battery charge current in order be sure that the $I_{\text{Bat_max}}$ is not too high. Therefore, it is necessary to add a current control loop on the step-up converter.

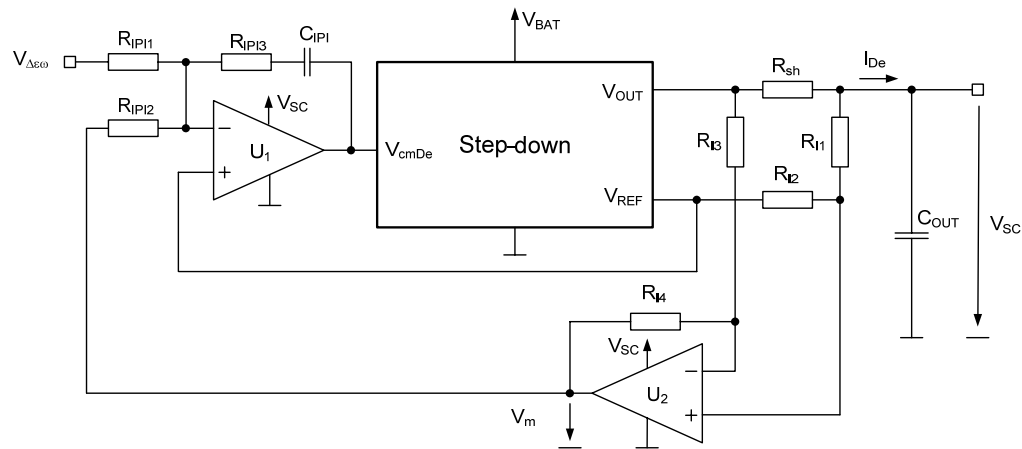


Figure 6-16 : Measure system of the discharge current

6.6.1 Discharging current measure

The current measurement is carried out with a shunt resistor (R_{sh}) and a differential amplifier. This amplifier gives a voltage (v_m) proportional to the current.

If $R_{I1} = R_{I3}$ and $R_{I2} = R_{I4}$ the relation is:

$$v_m = -\frac{R_{I2}}{R_{I1}} R_{sh} i_{De} + V_{REF} \quad 6.49$$

In small signals state ($v_m = \Delta V_m + V_{REF}$), the relation 6.16 becomes:

$$\Delta V_m = -\frac{R_{I2}}{R_{I1}} R_{sh} \Delta I_{De} \quad 6.50$$

From the relation 6.17, it is possible to determine the transfer function of the discharge current measure system:

$$G_{mICh}(s) = \frac{V_m(s)}{I_{De}(s)} = -\frac{R_{I2}}{R_{I1}} R_{sh} \quad 6.51$$

6.6.1.1 Component Choice

The discharge current must be controlled. In order to improve quality of the measure, the discharge current measure is carried out on the output of the step-down converter (the current ripple is lower). Therefore, the ratio between input and output currents must be known. Considering an efficiency of 100% the power budget is:

$$\frac{I_{OUT}}{I_{BAT}} \approx \frac{V_{BAT}}{V_{OUT}} \quad 6.52$$

The ratio between input and output currents depends on the state of charge of the battery. If the battery is fully charged the ratio I_{OUT}/I_{BAT} will reach 1.3. If the battery is almost empty the ratio will reach 1. So, in order to guarantee that I_{BAT} is always lower than 1A, it is assumed that:

$$I_{BAT\max} \approx I_{OUT\max} \quad 6.53$$

The measure system of the discharging current is exactly the same as the measure system of the charging current.

6.6.2 Current regulator

By examining the transfer function of the system to control, it is easy to see that the current regulator could be Proportional-Integrator.

$$v_{cmDe} = -\frac{R_{IP3}}{R_{IP1}} \left(v_{De\omega} - V_{REF} + \frac{1}{R_{IP3}C_{IP1}} \int (v_{De\omega} - V_{REF}) dt \right) \\ - \frac{R_{IP3}}{R_{IP2}} \left(v_m - V_{REF} + \frac{1}{R_{IP3}C_{IP1}} \int (v_m - V_{REF}) dt \right) + V_{REF} \quad 6.54$$

By separating the working point and the variation around it, it is possible to write:

$$\Delta V_{cmDe} = v_{cmDe} - V_{REF} \\ \Delta V_{De\omega} = v_{De\omega} - V_{REF} \\ \Delta V_m = v_m - V_{REF} \quad 6.55$$

And then we obtain:

$$\Delta V_{cmDe} = -\frac{R_{IP13}}{R_{IP11}} \left(\Delta V_{De\omega} + \frac{R_{IP11}}{R_{IP12}} \Delta V_m + \frac{1}{R_{IP3}C_{IP1}} \int \left(\Delta V_{De\omega} + \frac{R_{IP11}}{R_{IP12}} \Delta V_m \right) dt \right) \quad 6.56$$

With the help of Laplace, the last relation becomes:

$$V_{cmDe}(s) = - \underbrace{\left(V_{De\omega}(s) + \frac{R_{IPI1}}{R_{IPI2}} V_m(s) \right)}_{e_I(s)} \frac{R_{IPI3}}{R_{IPI1}} \frac{1 + sR_{IPI3}C_{IP1}}{sR_{IPI3}C_{IP1}} \quad 6.57$$

From the relation 6.28 it is possible to determine the transfer function of the current regulator:

$$G_{PIDe} = \frac{V_{cmDe}(s)}{e_I(s)} = - \frac{R_{IPI3}}{R_{IPI1}} \frac{1 + sR_{IPI3}C_{IP1}}{sR_{IPI3}C_{IP1}} \quad 6.58$$

6.7 Power bus voltage control

6.7.1 Sum of currents

From the Figure 6-17 it is possible to define the relation between the different currents.

$$i_{CS} = i_{Ch} + i_C + i_{Util} + i_{sh} \quad 6.59$$

6.7.2 Relationship between the current and the voltage of the bus capacitor

The bus voltage is equal to the voltage at terminals of the bus capacitor C_{CS}

$$i_C = C_{CS} \frac{\partial V_{CS}}{\partial t} \quad 6.60$$

From 6.60 :

$$v_{CS} = \frac{1}{C_{CS}} \int i_C dt + V_{CSNom} = \Delta V_{CS} + V_{CSNom} \quad 6.61$$

With the help of Laplace the last relation becomes:

$$G_C(s) = \frac{V_{CS}(s)}{I_C(s)} = \frac{1}{sC_{CS}} \quad 6.62$$

6.7.3 Voltage Regulator

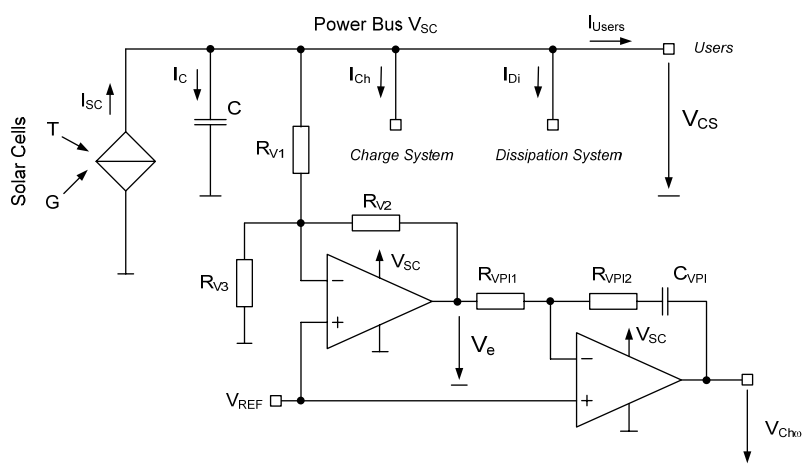


Figure 6-17 : Voltage measure and regulator

The difference between the bus voltage and the reference voltage is made by a differential amplifier.

$$v_e = -\frac{R_{V2}}{R_{V1}} \left(v_{CS} - \left(\frac{R_{V1}}{R_{V3}} + 1 \right) V_{REF} \right) + V_{REF} \quad 6.63$$

The working point is:

$$V_{CSNom} = \left(\frac{R_{V1}}{R_{V3}} + 1 \right) V_{REF} \quad 6.64$$

The regulator follows this relation:

$$v_{Ch\omega} = -\frac{R_{VPI2}}{R_{VPI1}} \left(v_e - V_{REF} + \frac{1}{R_{VPI2} C_{VPI1}} \int (v_e - V_{REF}) dt \right) + V_{REF} \quad 6.65$$

By setting:

$$\begin{aligned} v_e &= \Delta V_e + V_e = \Delta V_e + V_{REF} \\ v_{Ch\omega} &= \Delta V_{Ch\omega} + V_{Ch\omega} = \Delta V_{Ch\omega} + V_{REF} \\ v_{CS} &= \Delta V_{CS} + V_{CS} = \Delta V_{CS} + V_{CSNom} \end{aligned} \quad 6.66$$

The relation 6.65 becomes:

$$\Delta V_{Ch\omega} = -\frac{R_{VPI2}}{R_{VPI1}} \left(\Delta V_e + \frac{1}{R_{VPI2} C_{VPI1}} \int \Delta V_e dt \right) \quad 6.67$$

The transfer function of the voltage regulator is defined by this relation:

$$G_{PVCh}(s) = \frac{V_{Ch\omega}(s)}{V_e(s)} = -\frac{R_{VPI2}}{R_{VPI1}} \frac{1 + s R_{VPI2} C_{VPI1}}{s R_{VPI2} C_{VPI1}} \quad 6.68$$

R_{V1} and R_{V3} can be determined with the relation 6.64 but for that it is necessary to know the maximal variations of the voltage reference.

For this part of the charge system, a very accurate reference is used in order to guarantee a good precision. This is a 1.25V reference of ANALOG DEVICES (ADR127, A Grade). Here are its main characteristics:

Parameter	Symbol	Condition	Min	Typ	Max	Unit
OUTPUT VOLTAGE B Grade	V _O	@ 25°C	1.2485	1.25	1.2515	V
A Grade			1.2470	1.25	1.2530	V
INITIAL ACCURACY ERROR B Grade	V _{OERR}	@ 25°C	-0.12	+0.12	%	%
A Grade			-0.24	+0.24		%
TEMPERATURE COEFFICIENT B Grade	TCV _O	-40°C < T _A < +125°C		3	9	ppm/°C
A Grade				15	25	ppm/°C
DROPOUT (V _{OUT} - V _{IN})	V _{DO}	I _{OUT} = 0 mA	1.45			V
LOAD REGULATION		-40°C < T _A < +125°C; V _{IN} = 3.0 V, 0 mA < I _{OUT} < 5 mA -40°C < T _A < +125°C; V _{IN} = 3.0 V, -2 mA < I _{OUT} < 0 mA		85	400	ppm/mA
				65	400	ppm/mA
LINE REGULATION		2.7 V to 18 V I _{OUT} = 0 mA		30	90	ppm/V
PSRR		F = 60 Hz		-90		dB
RIPPLE REJECTION	ΔV _{OUT} /ΔV _{IN}	f = 60 Hz		60		dB
QUIESCENT CURRENT	I _Q	-40°C < T _A < +125°C, no load V _{IN} = 18 V V _{IN} = 2.7 V		95	125	µA
				80	95	µA
SHORT-CIRCUIT CURRENT TO GROUND		V _{IN} = 2.7 V V _{IN} = 18 V		15		mA
				30		mA
VOLTAGE NOISE Noise Density		@ 25°C f = 10 kHz 0.1 Hz to 10 Hz		300		nV/√Hz
				5		µV p-p
TURN-ON SETTLING TIME		To 0.1%, C _L = 0.2 µF		80		µs
LONG-TERM STABILITY		1000 hours @ 25°C		150		ppm/1000 hrs
OUTPUT VOLTAGE HYSTERESIS		See the Terminology section		300		ppm

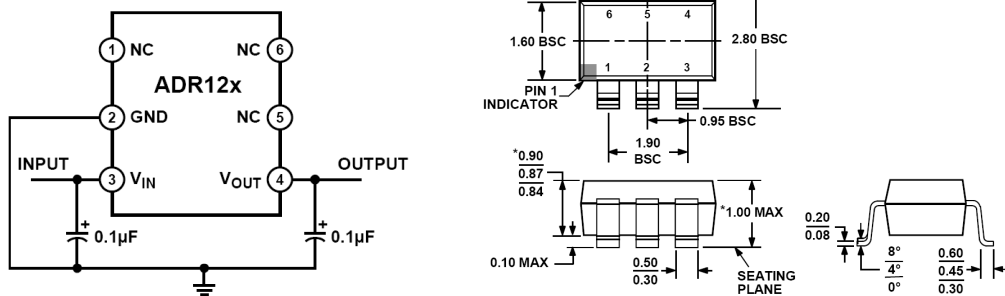


Figure 6-18 : ARD127

ARD127 is a new component (July 2006). Its performances are very interesting especially in B Grade. Unfortunately, the B Grade is not available before April 2007. For the engineering model the A Grade will be used. If the B Grade is available sufficiently soon it could be used.

At 25°C the reference voltage can be vary from 1.2470 to 1.2530. However the variations due to the temperature still must be taken into consideration. The extreme temperature range used for these calculation is -40 to 85°C (the requirement of -40 to 60°C was not defined when these calculations have been done) To define extreme variations of the reference the temperature coefficient of 25 ppm/°C must be used:

$$V_{REF_Min} = 1.2470 - 25 \text{ ppm} \cdot (25 + 40) = 1.2454 \quad [V]$$

$$V_{REF_Max} = 1.2530 + 25 \text{ ppm} \cdot (85 - 25) = 1.2545 \quad [V]$$

6.69

So the tolerance of the reference is about 0.7%.

Now it is possible to calculate R_{V1} and R_{v3} with the relation 6.64.

$$V_{SCNom} = 3.3 \text{ V}$$

Here are best values for R_{V1} and R_{v3} :

$$R_{V1} = 38.3 \text{ k} \pm 0.1\%$$

$$R_{v3} = 23.2 \text{ k} \pm 0.1\%$$

These values guarantee that the charge system is not activated before that the bus voltage reaches 3.3V (taking in account the reference variations).

So here is plotted the variation of the V_{SCNom} as a function of the reference voltage :

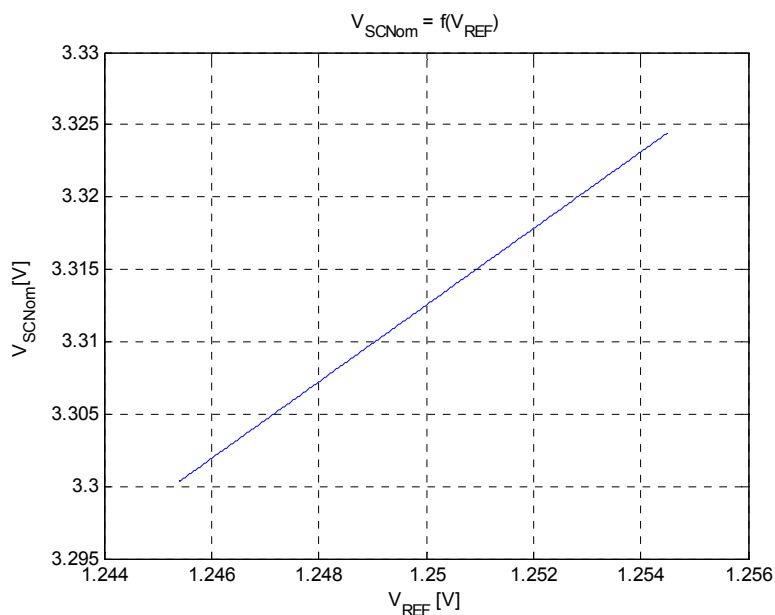


Figure 6-19 :

- With $V_{REF_Min} = 1.2454 \text{ V}$: $\mathbf{V_{SCNom} = 3.300 \text{ V}}$

- With $V_{REF_Nom} = 1.2500 \text{ V}$: $\mathbf{V_{SCNom} = 3.313 \text{ V}}$

- With $V_{REF_Max} = 1.2545 \text{ V}$: $\mathbf{V_{SCNom} = 3.324 \text{ V}}$

According to the relation 6.63 :

When $V_{SC} = V_{SCNom}$	the error is null	$\Rightarrow V_e = V_{REF}$
When $V_{SC} > V_{SCNom}$	the error is positive	$\Rightarrow V_e < V_{REF}$ (negative gain)
When $V_{SC} < V_{SCNom}$	the error is negative	$\Rightarrow V_e > V_{REF}$ (negative gain)

The starting of the dissipation system happens when $V_{SC} = V_{SC_di} = 3.35V$.

When $V_{SC} = V_{SC_di}$ the error is positive and maximal and it is equal to 0.05 V. For this maximal positive error $V_e = 0$ V.

The relation 6.70 defined the required resistor R_{V2} in order to guarantee that the charge doesn't overlaps with the dissipation:

$$R_{V2} = R_{V1} \cdot \frac{V_{REF}}{0.05} \quad 6.70$$

Best choice:

$$R_{V2} = 1 \text{ M} \pm 0.1\%$$

Here is plotted the working zone of the charge system. The starting of the charge is plotted in blue (command is minimal). When the bus voltage reaches the values plotted in green the set-point of charge is maximal.

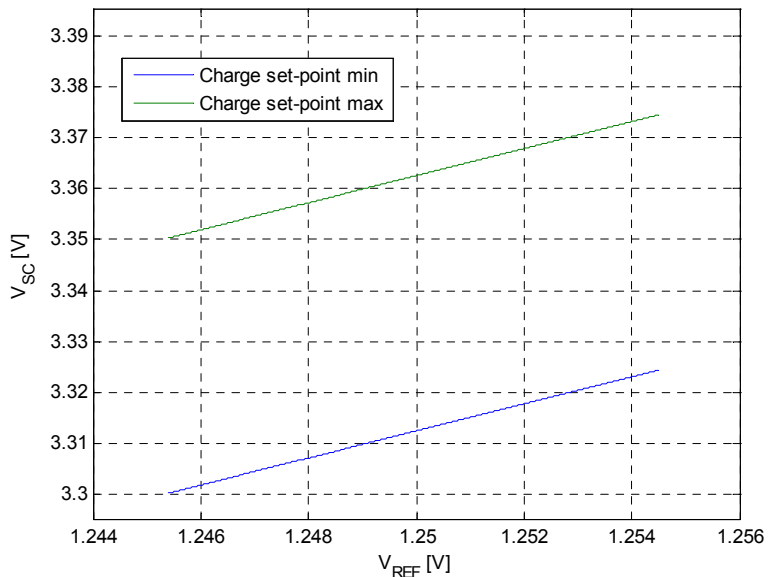


Figure 6-20 :

6.8 Control Block Diagram

From the transfer function defined in the last section, it is possible to edit a block diagram of the bus voltage control.

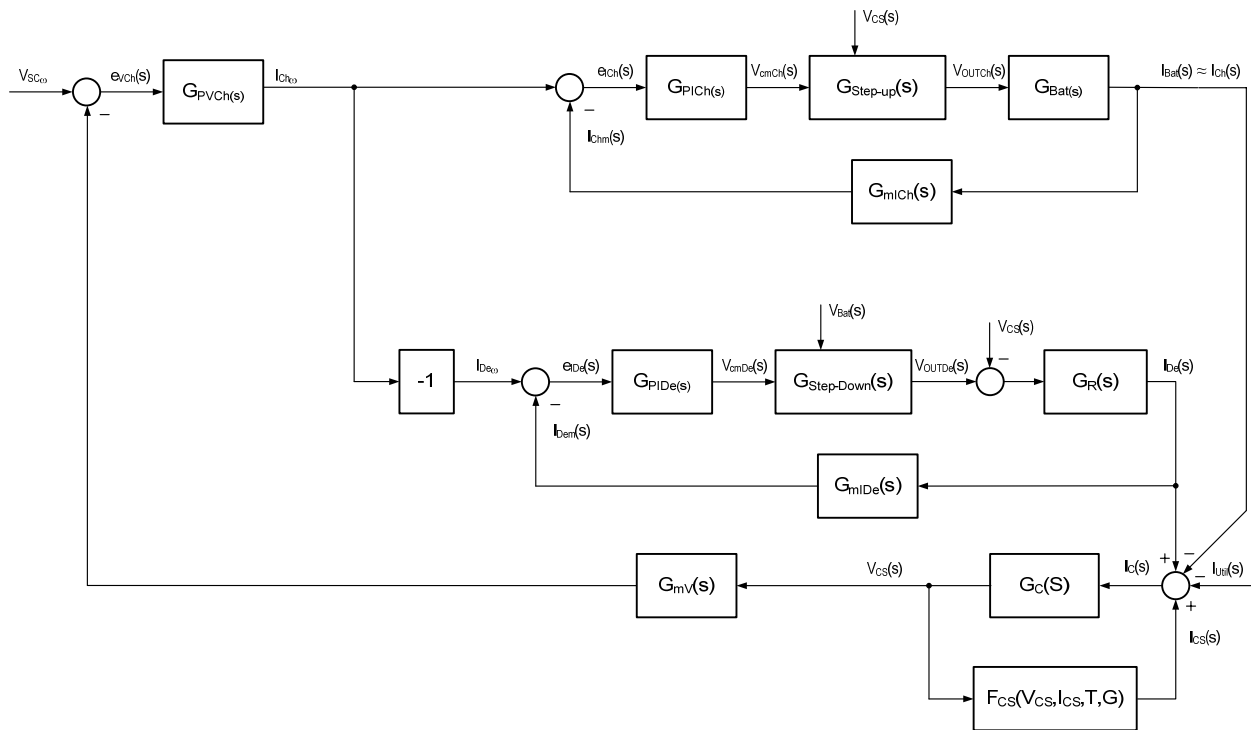


Figure 6-21 : Control Block Diagram

Both current control loops are controlled by the same PI voltage regulator.

The block $F_{SC}(V_{SC}, I_{SC}, T, G)$ models the non linear function of the solar cells.

$G_R(s)$ is the transfer function between the current and the voltage of the resistance of measure.

$$\text{So } G_R(s) = 1/R.$$

$G_{mV}(s)$ is the transfer function of the voltage measure system.

6.9 Charge and Discharge Securities

6.9.1 Introduction

The charge will stop itself when the battery reaches 4.15V (by the resistive divider of the feedback). But it is not the case for the discharge.

A security is used to stop the charge and the discharge when the battery voltage reaches $4.2\text{ V} \pm 1\%$ (for the discharge) or $3.19\text{ V} \pm 1\%$ (for the charge). This protection is carried out with the LTC1442. This component is an ultra low power dual comparator with reference and adjustable hysteresis.

Of course if this security has a failure during the mission the internal battery security (PCM) will be activated when the battery will reach $4.325\text{ V} \pm 25\text{mV}$ (for the charge) and $2.5\text{ V} \pm 80\text{mV}$ (for the discharge).

So there are three securities for the charge:

- Resistive divider stop the charge at 4.15 V
- LTC1442 shut down the LTC3421 at 4.2 V
- Internal security of the battery at 4.325 V

But for the discharge there are only two securities:

- LTC1442 shut down the LTC3414 at 3.19 V
- Internal security of the battery at 2.5 V

Given the fact that the discharge is more sensitive, it has been decided to use a protection switch (MIC2045) between the battery and the step-down converter. This switch (MIC2045) is opened by the LTC1442 when the battery voltage reaches 3.2V. An analysis must be done to decide if this switch is really necessary (TBD).

6.9.2 Design of protections with the LTC1442

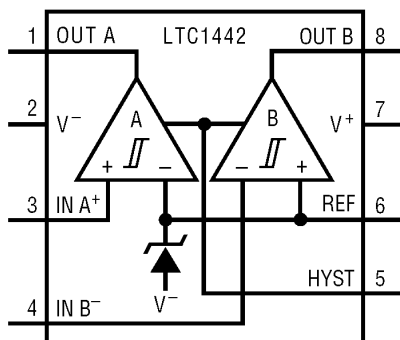


Figure 6-22 : LTC1442

The LTC1442 is an ultra low power dual comparator with built-in reference ($1.182V \pm 1\%$) and programmable hysteresis.

The comparator A is used for the charge security and the comparator B is used for the discharge security of the same battery. It is indeed important to use both converter of the part for the same battery (charge and discharge) in order to maintain the redundancy. If the part breaks down only one battery is in danger.

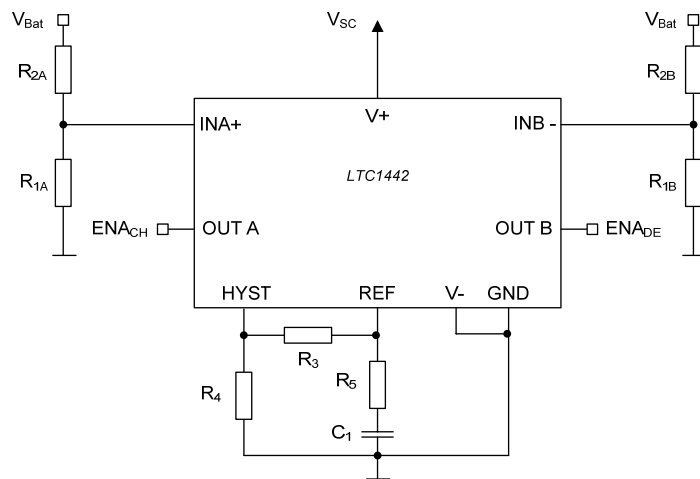


Figure 6-23 : Design of the LTC1442

Functioning: When the thresholds are reached the outputs are high.

Choice of the thresholds:

$$V_{BAT_{max}} \cdot \frac{R_{1A}}{R_{1A} + R_{2A}} = V_{REF} \quad 6.71$$

$$V_{BAT_{min}} \cdot \frac{R_{1B}}{R_{1B} + R_{2B}} = V_{REF} \quad 6.72$$

$$R_{1A} = 200 \text{ k} \pm 0.1\%$$

$$R_{2A} = 511 \text{ k} \pm 0.1\%$$

$$R_{1B} = 130 \text{ k} \pm 0.1\%$$

$$R_{2B} = 221 \text{ k} \pm 0.1\%$$

With these resistances $V_{BAT_{max}}$ is $4.20 \text{ V} \pm 1\%$ and $V_{BAT_{min}}$ is $3.19 \text{ V} \pm 1\%$

Design of the hysteresis (as recommended in the datasheet):

Charge comparator:

The required resistive divider ratio is:

$$\text{Ratio} = V_{\text{REF}}/V_{\text{IN}} = 1.182/4.2 = 0.281$$

The required hysteresis voltage band at the input is called V_{HBIN}

$$V_{\text{HBIN}} = 20 \text{ mV}$$

The hysteresis voltage band referred to the comparator input is called V_{HB}

$$V_{\text{HB}} = 20 \text{ mV} * 0.281 = 5.6 \text{ mV} \quad \Rightarrow \quad R_3 = 5.6 \text{ k}$$

Discharge comparator:

The required resistive divider ratio is:

$$\text{Ratio} = V_{\text{REF}}/V_{\text{IN}} = 1.182/3.19 = 0.371$$

The required hysteresis voltage band at the input is called V_{HBIN}

$$V_{\text{HBIN}} = 20 \text{ mV}$$

The hysteresis voltage band referred to the comparator input is called V_{HB}

$$V_{\text{HB}} = 20 \text{ mV} * 0.371 = 7.4 \text{ mV} \quad \Rightarrow \quad R_3 = 7.4 \text{ k}$$

So R_3 must be chosen between 5.6 k and 7.4k:

Choice:

$$R_3 = 6.8 \text{ k} \pm 1\%$$

As recommended in the datasheet:

$$R_4 = 2.4 \text{ M} \pm 1\%$$

$$R_5 = 430 \Omega \pm 1\%$$

$$C_1 = 1 \mu\text{F}$$

6.9.3 Discharge protection switch

The discharge is stopped at 3.2V by the MIC2045 protection switch. The detail of the design is given in the schematic [Annexe 2]. The switch is simply enabled by the LTC1442 when the battery voltage reaches 3.2V.

6.10 Dissipation system

When batteries are fully charged and subsystems use less energy than the energy produced by the solar cells, the bus voltage increases.

This situation is remedied with a dissipation system. It is used to draw off the surplus energy produced by the cells and converted it into heat through a dissipation resistance. So it is possible to maintain the voltage specifications of the bus by controlling the dissipation current.

It is favourable to use such a system for the following reasons:

- The surplus energy is not dissipated in the solar cells (it will avoid their overheating).
- It is not necessary to modify the working point of the cells.

The dissipation system is started when the bus voltage V_{SC} exceeds a threshold of 3.35 V, as the diagram shows it below:

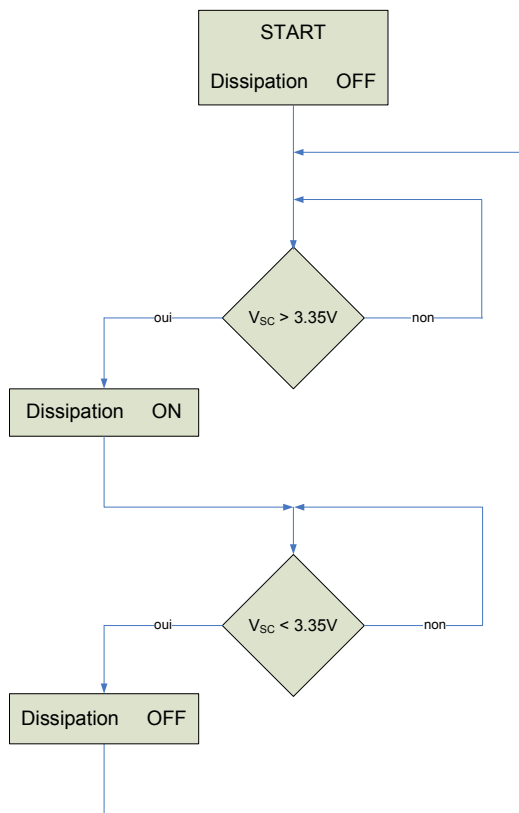


Figure 6-24 : Flow chart of the dissipation system

Note: It is really probable that the dissipation system will be shortly activated when a brutal stop of a consumer happens (voltage step on the bus).

6.10.1 Electronic design

A controlled current source is used in order to dissipate the heat in the dissipation shunt R_{sh} :

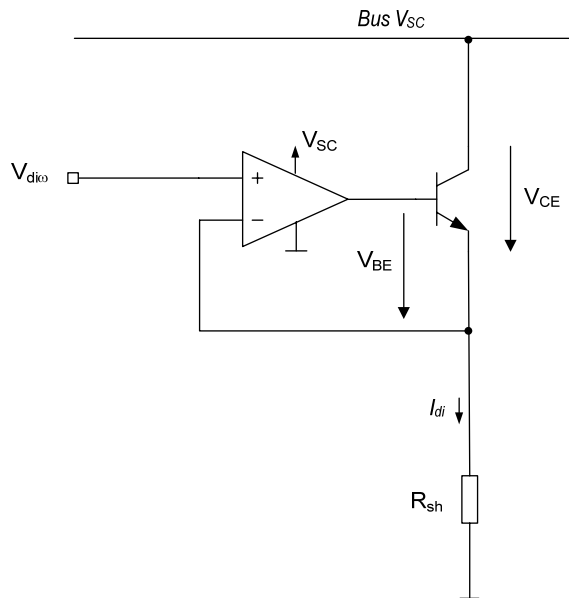


Figure 6-25 : Dissipation circuit

The intensity of the current is directly fixed by $V_{di\omega}$ (command voltage). Given the fact that the voltage is null between the input + and - of the amplifier, $V_{di\omega}$ is also on terminals of the shunt.

This system is a current control loop. Its gain is defined by the value of resistance.

$$G_{Linear}(s) = \frac{I_{di}(s)}{V_{di\omega}(s)} = \frac{1}{R_{sh_di}} \quad 6.73$$

The current control is carried out with an amplifier which orders a NPN power transistor. This transistor is in conduction as soon as $V_{di\omega}$ is higher than 0 V. The amplifier is a "rail to rail" type. It can provide a voltage equal to V_{SC} on the transistor base (in fact, there is a small voltage difference of a few tens of mV).

In order to guarantee the transistor saturation, V_{CEsat} and V_{BEsat} must be sufficient. These voltages depend on the I_{di} current. For I_{di_max} , the command voltage $V_{di\omega}$ must fit within the following inequation:

$$\begin{aligned} V_{di\omega} &< V_{SC} - V_{BEsat} \\ V_{di\omega} &< V_{SC} - V_{CEsat} \end{aligned} \quad 6.74$$

6.10.2 Calculation of the power dissipation

The dimensioning of the dissipation circuit is particularly important. The components must be dimensioned and laid out so as to dissipate all the power generated by the solar cells under conditions of an optimal insolation. The fact that the air convection is not present in space should be absolutely taken into consideration because it will really increase the heating.

If the whole power cannot be dissipated, the heating would produce the rupture of components with the considerable risk to definitively put the solar cells in short-circuit. It is the reason why it will be necessary to design a good a thermal link between the elements of dissipation and the structure of the satellite.

The energy is partly dissipated by the power transistor and partly by the dissipation resistance. The power dissipated by a bipolar transistor is made of two terms:

- 1) losses generated by the current of base
- 2) losses generated by the current of collector.

Losses generated by the current of base are generally not taken in account [R13]. In our application the losses generated by the current of base are negligible.

V_{CE} depends on the supply voltage V_{SC} and the command voltage V_{dio} :

$$V_{CE} = V_{SC} - V_{dio} \quad 6.75$$

V_{dio} is directly applied on terminals of the dissipation resistance. So the current is:

$$I_{di} = \frac{V_{dio}}{R_{sh_di}} \quad 6.76$$

The power dissipated by the transistor is:

$$P_{di_tr} = (V_{SC} - V_{dio}) \cdot \frac{V_{dio}}{R_{sh_di}} \quad 6.77$$

The power dissipated by the resistor is:

$$P_{di_sh} = \frac{V_{dio}^2}{R_{sh_di}} \quad 6.78$$

So, the total power dissipated is:

$$P_{di_tot} = (V_{SC} - V_{di\omega}) \cdot \frac{V_{di\omega}}{R_{sh_di}} + \frac{V_{di\omega}^2}{R_{sh_di}}$$
6.79

6.10.3 Choice of components

When all conditions are optimal ($G = 1350 \text{ [W/m}^2]$, albedo = 60% G, optimal attitude), solar cells could produce a maximal power of about 4.6 W. The worst case appears when the batteries are fully charged and when all the users are deactivated. Therefore, the dissipation system must be able to dissipate 4.6 W. So, it is possible to determine the maximal current:

$$I_{di_max} = \frac{P_{di_max}}{V_{SC}} = \frac{4.6}{3.35} = 1.37 \text{ [A]}$$
6.80

Knowing the maximal current and power it is now possible to choose a bipolar transistor. The transistor selected is the NPN: MJD44H11 in D-Pak:

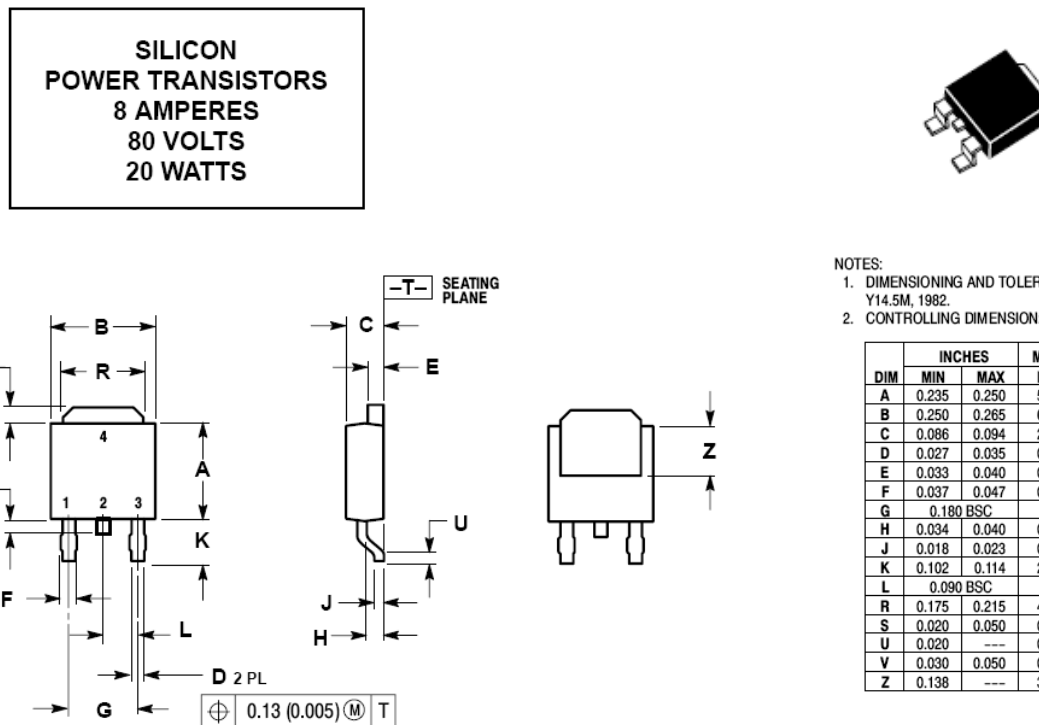


Figure 6-26 : NPN transistor : MJD44H11

The operating temperature of this component is: -55 to 150 °C

With the relation 6.81 and the characteristics given by the manufacturer, it is possible to determine V_{diode_max} which is firstly limited by V_{BEsat} as shown below:

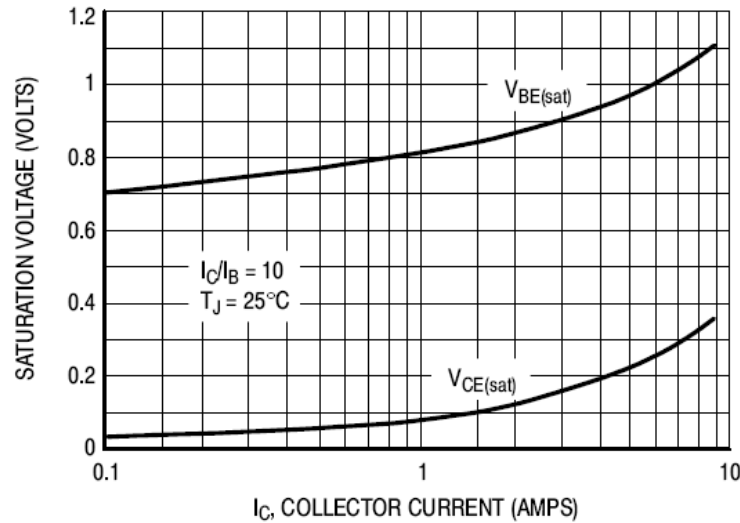


Figure 6-27 : MJD44H11 On-Voltages

For a maximal current of 1.37 A, V_{BEsat} must be at least 0.85 V in order to guarantee the saturation. Given the fact that this curves might change a little bit with the temperature, it is necessary to take a margin: $V_{BEsat} = 1$ V.

So the maximal command voltage is:

$$V_{diode_max} = V_{SC_di} - V_{BEsat} = 3.35 - 1 = 2.35 \text{ [V]} \quad 6.82$$

At this step, it is possible to determine the value of the dissipation resistance by plotting the power dissipated in the system when $V_{\text{diss}} = V_{\text{diss_max}}$ for different values of resistance:

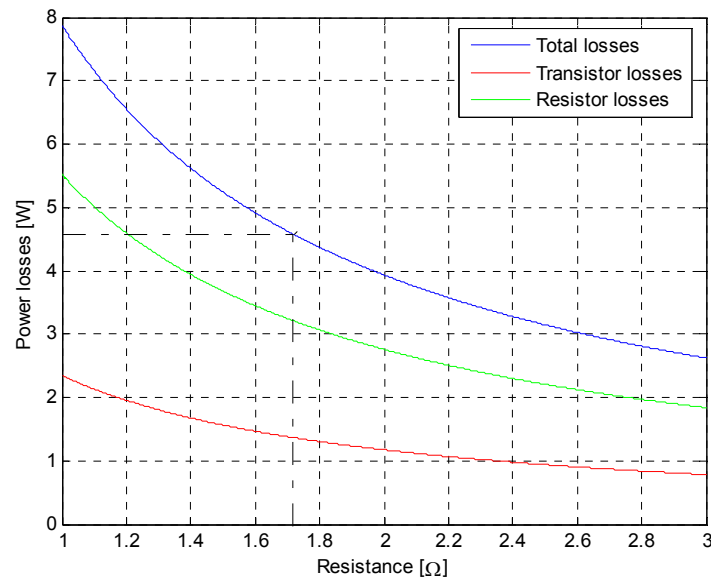
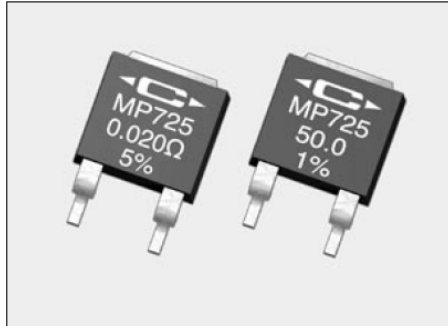


Figure 6-28 : Power losses vs Resistance

To dissipate 4.6 W, the graph shows a resistance of 1.71 Ω .

A D-Pack power resistor MP725 is used. Standard closest values are either $1.5\ \Omega$ or $2\ \Omega$.



Standard Resistance Values:

$0.020\ \Omega$	$0.25\ \Omega$	$3.00\ \Omega$	$25.0\ \Omega$	$150\ \Omega$
$0.025\ \Omega$	$0.30\ \Omega$	$3.30\ \Omega$	$27.0\ \Omega$	$200\ \Omega$
$0.030\ \Omega$	$0.33\ \Omega$	$4.00\ \Omega$	$30.0\ \Omega$	$250\ \Omega$
$0.033\ \Omega$	$0.40\ \Omega$	$5.00\ \Omega$	$33.0\ \Omega$	$300\ \Omega$
$0.040\ \Omega$	$0.50\ \Omega$	$7.50\ \Omega$	$40.0\ \Omega$	$330\ \Omega$
$0.050\ \Omega$	$0.75\ \Omega$	$8.00\ \Omega$	$47.0\ \Omega$	$400\ \Omega$
$0.075\ \Omega$	$1.00\ \Omega$	$10.0\ \Omega$	$50.0\ \Omega$	$470\ \Omega$
$0.10\ \Omega$	$1.50\ \Omega$	$12.0\ \Omega$	$56.0\ \Omega$	$500\ \Omega$
$0.15\ \Omega$	$2.00\ \Omega$	$15.0\ \Omega$	$75.0\ \Omega$	$560\ \Omega$
$0.20\ \Omega$	$2.50\ \Omega$	$20.0\ \Omega$	$100\ \Omega$	$750\ \Omega$
			$120\ \Omega$	$1.00\ K$

Model No.	Power Rating	Dielect. Strength V _{RMSAC}	Max. Voltage	Resistance		Terminal
				Min.	Max.	
MP725	25 Watts *	1,500	200	$0.020\ \Omega$	$1.00K$	Solderable

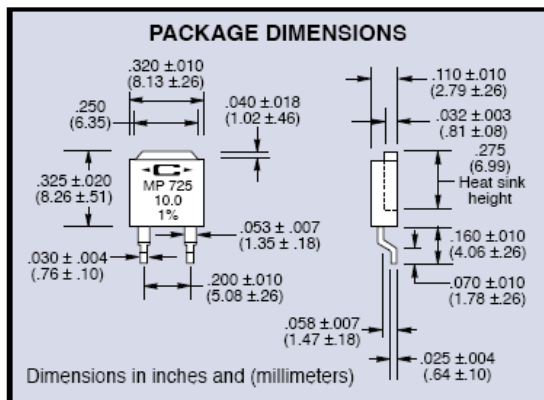


Figure 6-29 : MP725 Surface Mount Power Film Resistors

Here is plotted the total dissipated power as a function of the command voltage V_{dio} which varies from 0 to 2.35 V. First the power resistor is 1.5Ω and then of 2Ω :

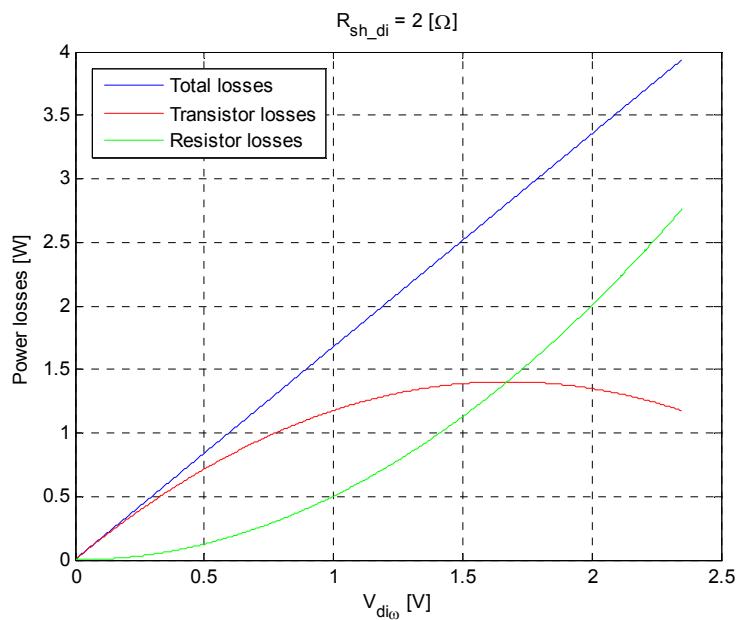
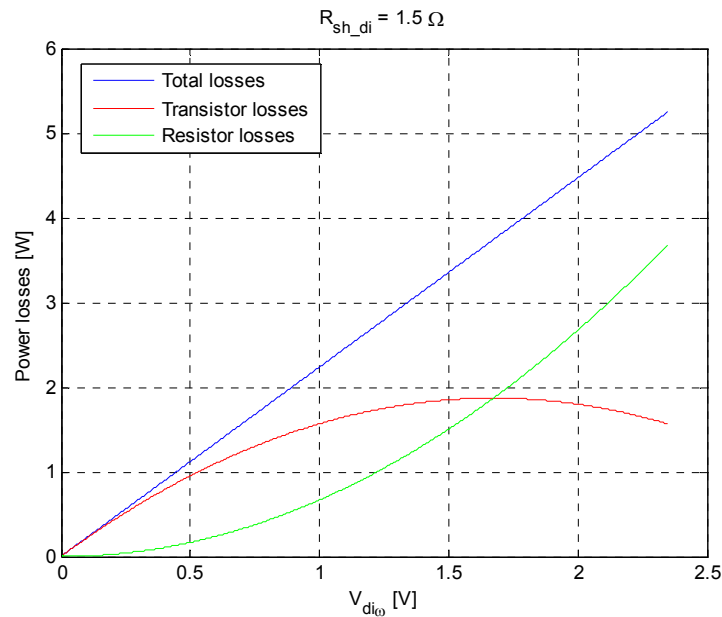


Figure 6-30 : Power losses vs V_{dio} with 1.5 and 2Ω

The dissipated power increases in a perfectly linear way.

To dissipate 4.6 W without exceeding V_{dio_max} , it is necessary to use a resistance of 1.5Ω .

It should be noted that when V_{dio} is low, the dissipation on the transistor is higher. When V_{dio} reaches the threshold of 1.68 V, the dissipation on the transistor is maximum (1.88 W) and precisely equal to the dissipation on the resistance. Then, when $V_{dio} = V_{dio_max}$ total dissipation is definitely higher than 4.6 W.

6.10.4 Control of the bus voltage with the dissipation system

The regulation of the bus voltage is carried out with a simple proportional regulator. When the bus voltage exceeds the starting threshold of the dissipation system ($V_{SC_di} = 3.35$ V), the command voltage V_{dio} provided by the P regulator must be positive. This command voltage represents the error multiplied by K_p . When the bus voltage is lower than 3.35 V, the error is negative and the command voltage V_{dio} is null.

In order to use a minimum of components, the error calculation and the multiplication by K_p are carried out with the amplifier:

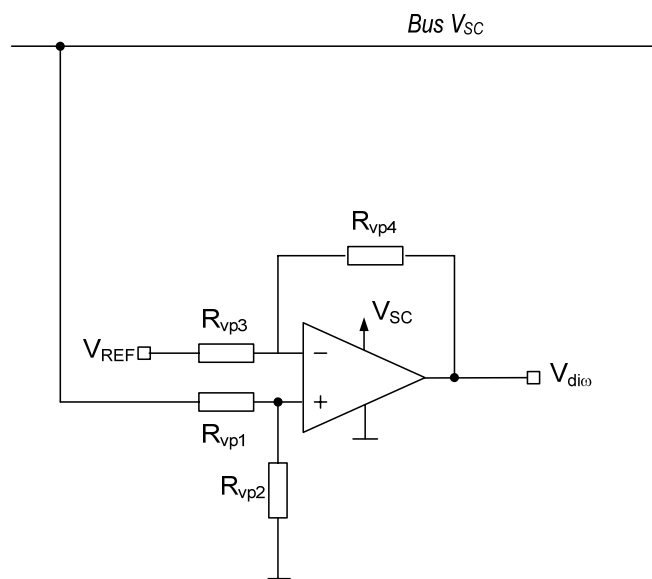


Figure 6-31 : P Regulator

The battery charge system works to control the bus voltage until 3.35 V. It is really important to guarantee that the dissipation system doesn't start before 3.35V. If it is not the case, the dissipation system will start below 3.35 V and energy will be wasted instead of inject it into the battery.

Equations of the circuit give the following relation:

$$V_{dio} = \frac{1 + \frac{R_{vp4}}{R_{vp3}}}{1 + \frac{R_{vp1}}{R_{vp2}}} \cdot V_{SC} - \frac{R_{vp4}}{R_{vp3}} \cdot V_{REF} \quad 6.83$$

V_{dio} represents the error between the bus voltage (V_{SC}) and the starting threshold (V_{SC_di}) of the dissipation system, and this error is multiplied by K_p :

$$V_{dio} = K_p (V_{SC} - V_{SC_di}) = K_p \cdot V_{SC} - K_p \cdot V_{SC_di} \quad 6.84$$

So it is possible to define K_p :

$$K_p = \frac{1 + \frac{R_{vp4}}{R_{vp3}}}{1 + \frac{R_{vp1}}{R_{vp2}}} \quad 6.85$$

When $V_{SC} = V_{SC_di} = 3.35$ V the command voltage must be null ($V_{dio} = 0$ V). The following equation is obtained from the relation 6.83:

$$V_{SC_di} = \frac{R_{vp4}}{R_{vp3}} \frac{1 + \frac{R_{vp1}}{R_{vp2}}}{1 + \frac{R_{vp4}}{R_{vp3}}} V_{REF} \quad 6.86$$

When V_{SC} reaches 3.4V the command voltage must be maximal ($V_{dio} = 2.35$ V). So, it is easy to calculate the gain K_p :

$$K_p = \frac{V_{dio_max}}{(V_{SC} - V_{SC_di})} = \frac{2.35}{(3.4 - 3.35)} = 47 \quad 6.87$$

To fix the V_{SC_di} at 3.35 V the ADR127 voltage reference is used again (1.25V).

It is necessary to calculate the resistors of the regulator taking into account the variation of the reference in order to guarantee that the dissipation doesn't start below 3.35 V.

Knowing K_p as well as the variation of the reference, we can determine R_{vp2} , R_{vp3} and R_{vp4} with relations 6.85 and 6.86.

In order to have a high precision, the selected resistors have a tolerance of 0.1%:

$$R_{vp1} = 620 \text{ k} \pm 0.1\%$$

$$R_{vp2} = 360 \text{ k} \pm 0.1\%$$

$$R_{vp3} = 4.3 \text{ k} \pm 0.1\%$$

$$R_{vp4} = 560 \text{ k} \pm 0.1\%$$

Here is plotted the variation of the starting threshold as a function of the reference voltage:

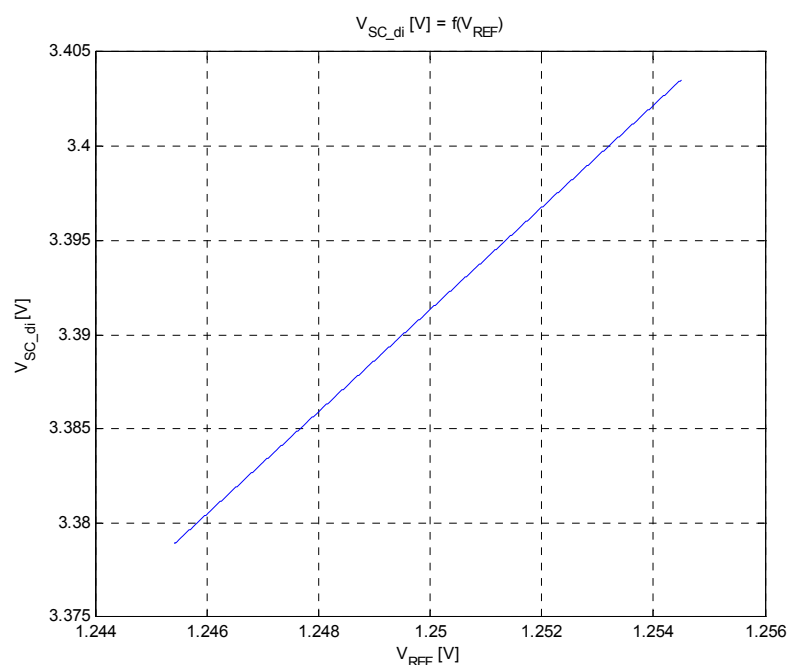


Figure 6-32 : Starting threshold voltage of the dissipation system

With $V_{REF_Min} = 1.2454$ V: $\mathbf{V_{SC_di} = 3.364 \text{ V}}$

With $V_{REF_Nom} = 1.2500$ V: $\mathbf{V_{SC_di} = 3.377 \text{ V}}$

With $V_{REF_Max} = 1.2545$ V: $\mathbf{V_{SC_di} = 3.389 \text{ V}}$

The transfer function of the P regulator is of course equal to K_p :

$$G_{Pdi}(s) = \frac{V_{di\omega}(s)}{V_{SC}(s) - V_{SC_di}(s)} = \frac{1 + \frac{R_{vp4}}{R_{vp3}}}{1 + \frac{R_{vp1}}{R_{vp2}}} \quad 6.88$$

6.10.5 Control Block diagram of the dissipation system

Here is the block diagram:

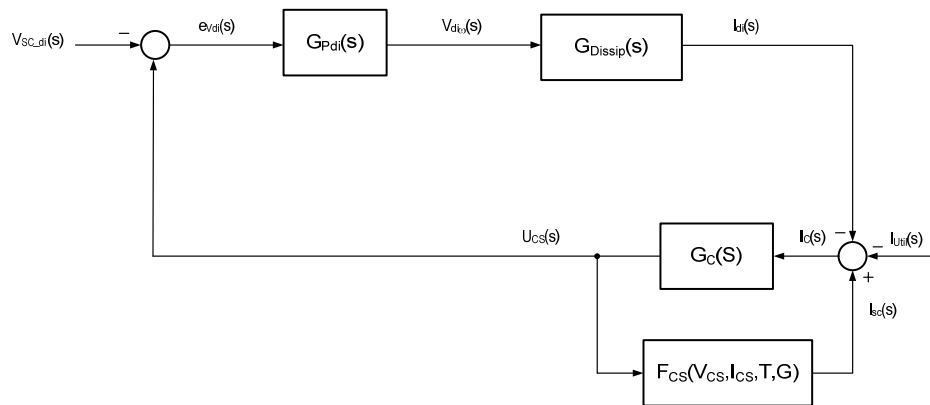


Figure 6-33 : Control block diagram of the dissipation system

And here is plotted a summary of the thresholds of charge and dissipation as a function of the reference:

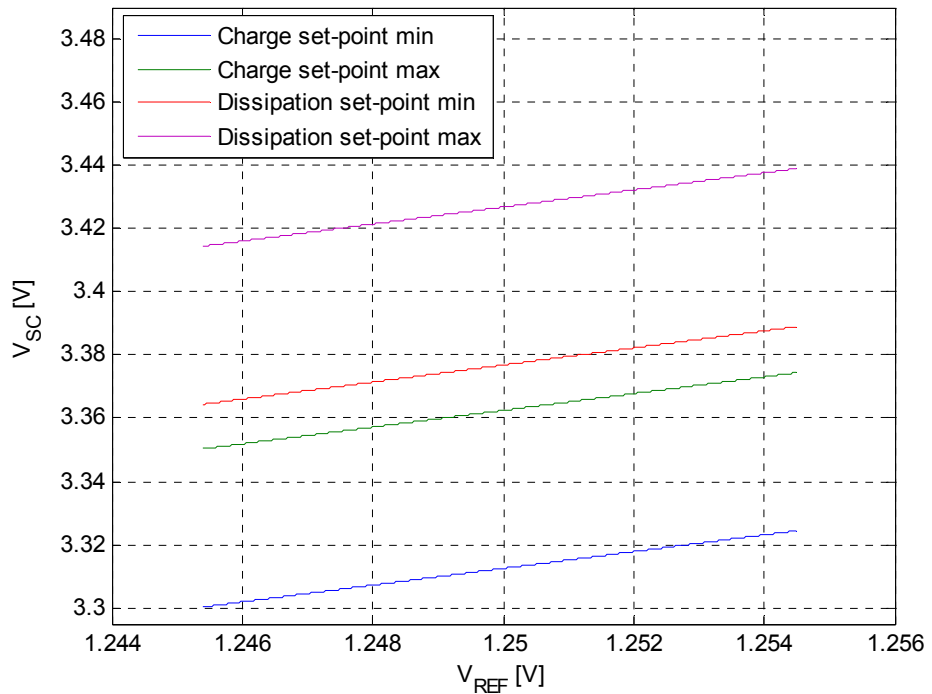


Figure 6-34 : Thresholds of charge and dissipation

6.11 Layout of the PCB

The PCB has four layers of 80 x 80 mm. The corners (10 x 10 mm) must not be used because this place is kept to fix the PCB in the satellite structure.

Here is the first layer:

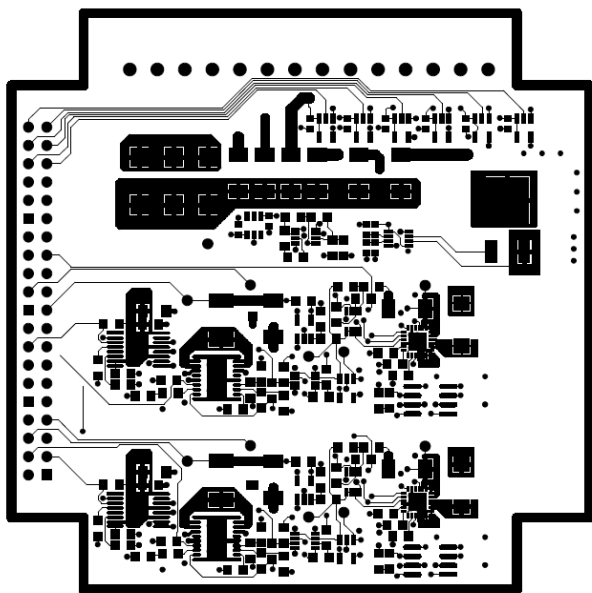


Figure 6-35 : First layer of PCB (scale 1:1)

The second layer is the plan of power and third layer is the plan of ground.

Here is the fourth layer:

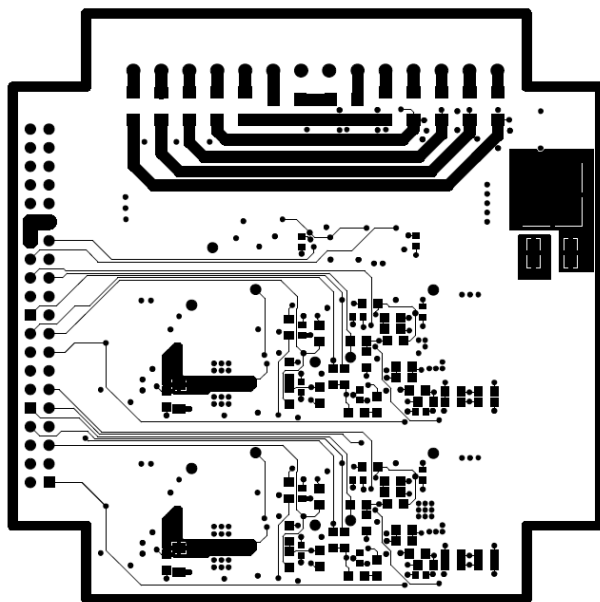


Figure 6-36 : Fourth layer of PCB (scale 1:1)

The thermal design of the sensitive components has been taken into consideration, in order to have a good repartition of the heat on the whole surface of the PCB.

When the system will be functional with all the components, thermal analyses will be carried out with a thermal camera in a vacuum chamber.

7 SIMULATIONS OF THE POWER SYSTEM

Abstract

Several simulations of the power system have been carried out. The regulation methodology has been validated by the simulation. The charge and discharge current control loops have been simulated and then the power bus voltage regulation too. This chapter presents only the simulation of the current control loops.

7.1 Charge Current Control Loop

First the charge current control loop is simulated. This loop is mainly formed by the step-up converter, the battery, the measure system and the regulator PI. Their transfer functions are described below. These transfer functions and their parameters are assumptions based on measurements.

7.1.1 Step-up converter

Transfer Function:

$$G_{Step-up}(s) = K_{Step-up} \frac{\omega_n^2}{s^2 + 2\xi\omega_n s + \omega_n^2} \quad 7.1$$

Parameters:

$$K_{Step-up} = 0.2$$

$$\omega_n = 2 \cdot \pi \cdot 8 \cdot 10^3 = 50.27 \cdot 10^3 \text{ [rad/s]}$$

$$\xi = 0.6$$

Bode diagram:

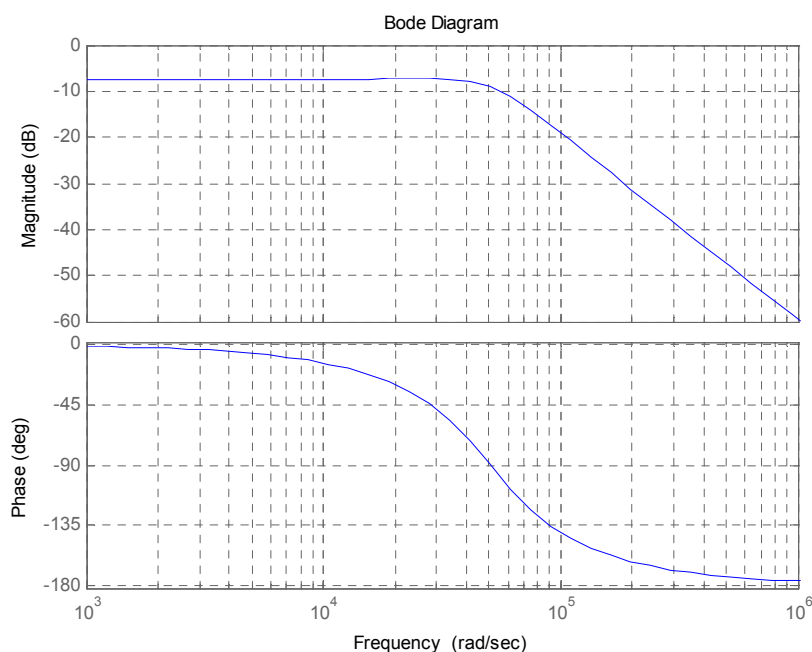


Figure 7-1 : Bode Diagram of the Step-up converter

Step response:

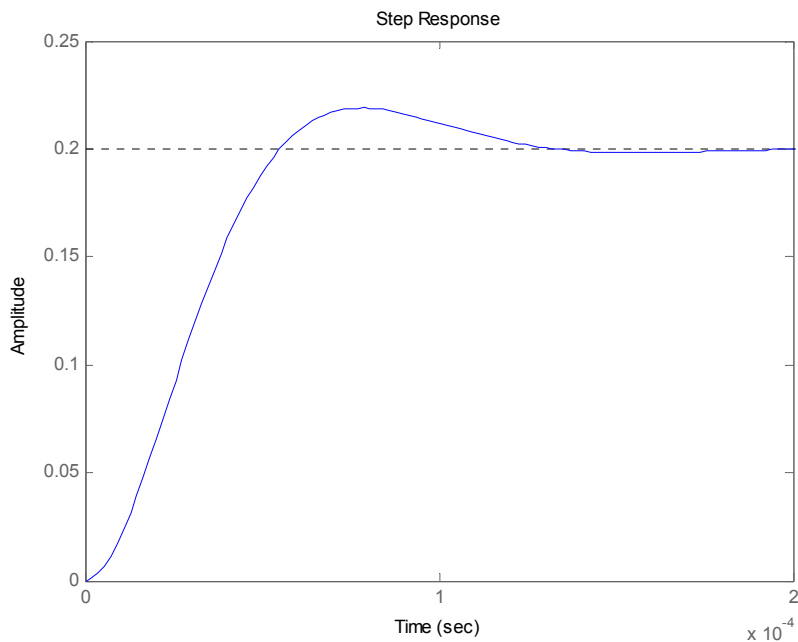


Figure 7-2 : Step response of the Step-up converter

7.1.2 Battery

Transfer function:

$$G_{Bat}(s) = \frac{sC_{Bat}}{1 + s(R_{sh} + R_{int})C_{Bat}} \quad 7.2$$

Parameters:

C_{Bat}	= 5082	[F]
R_{sh}	= 0.05	[Ω]
R_{int}	= 0.12	[Ω]

Bode diagram:

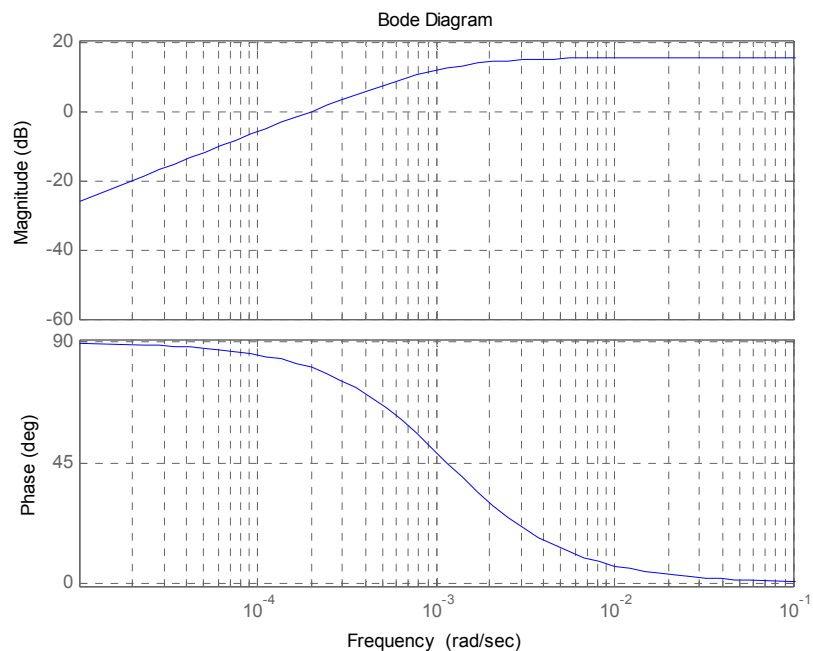


Figure 7-3 : Bode Diagram of the Battery

7.1.3 Measure System

Transfer function:

$$G_{mICh}(s) = 0.61$$

7.3

7.1.4 Gain of correction (input of the PI)

Transfer function:

$$G_{corCh}(s) = 3.3$$

7.4

7.1.5 System to control (open loop, without the regulator)

Transfer function:

$$G_{aCh}(s) = G_{Step-up}(s) \cdot G_{Bat}(s) \cdot G_{mICh}(s) \cdot G_{corCh}(s)$$

7.5

Bode diagram:

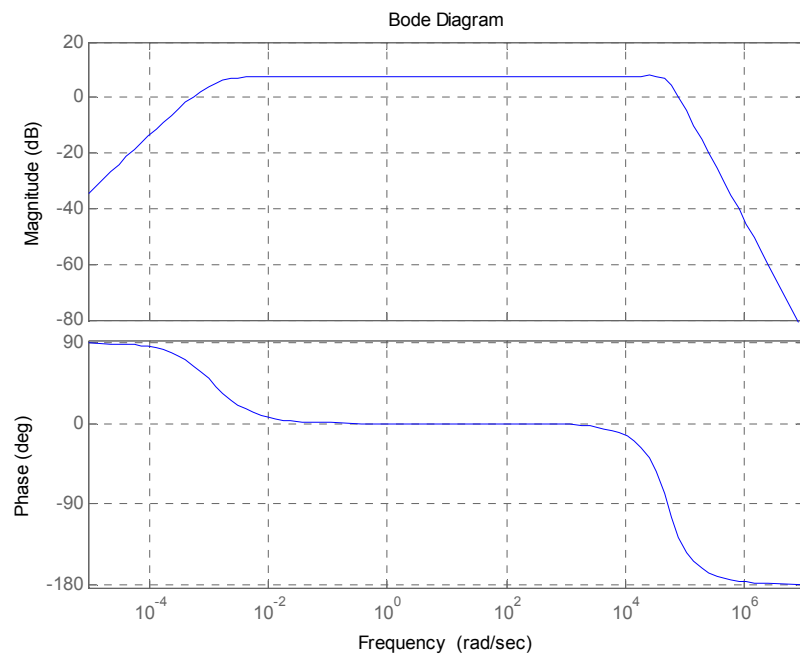


Figure 7-4 : Bode Diagram of $G_{aCh}(s)$

7.1.6 Synthesis of the PI Regulator

Transfer function of the PI regulator:

$$G_{PICh} = K_{pCh} \frac{1 + sT_{iCh}}{sT_{iCh}} \quad 7.6$$

Parameters choice:

$$K_{pCh} = 0.75$$

$$T_{iCh} = 10 \cdot (1 / \omega_n) \approx 200 \cdot 10^{-6}$$

Transfer function of the system in open loop with the regulator:

$$G_{oCh} = G_{PICh} \cdot G_{aCh} \quad 7.7$$

Bode diagrams of the system in open loop (with the PI regulator):

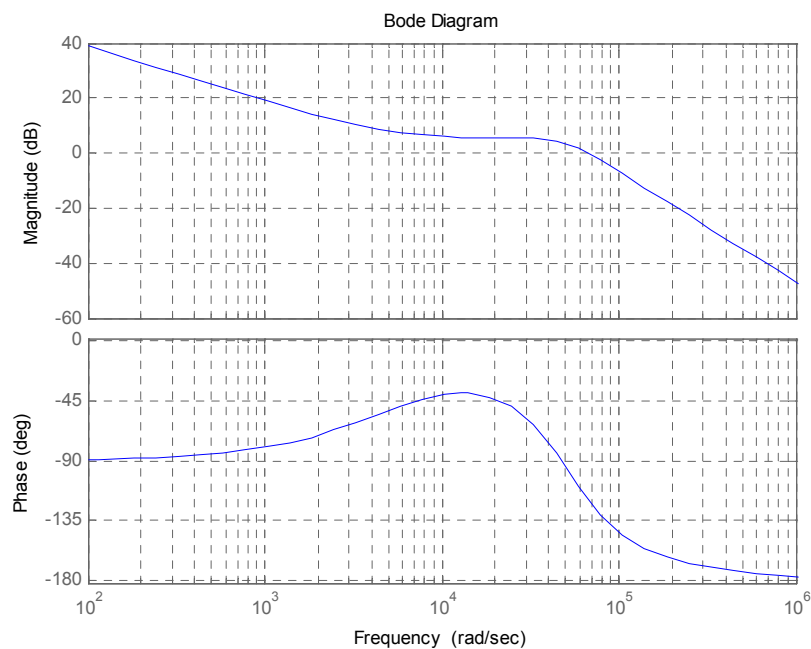


Figure 7-5 : Bode Diagram of $G_{oCh}(s)$

=> Phase margin = 60 °

Transfer function of the system in closed loop:

$$G_{wCh} = \frac{G_{oCh}}{1 + G_{oCh}} \quad 7.8$$

Bode diagrams of the system in closed loop:

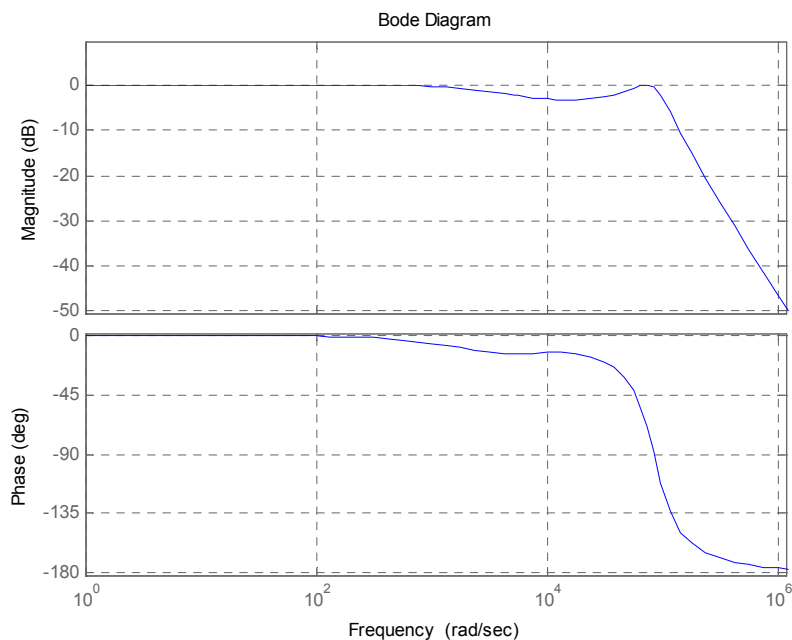


Figure 7-6 : Bode Diagram of $G_{wCh}(s)$

7.1.7 Results of the simulation with Simulink

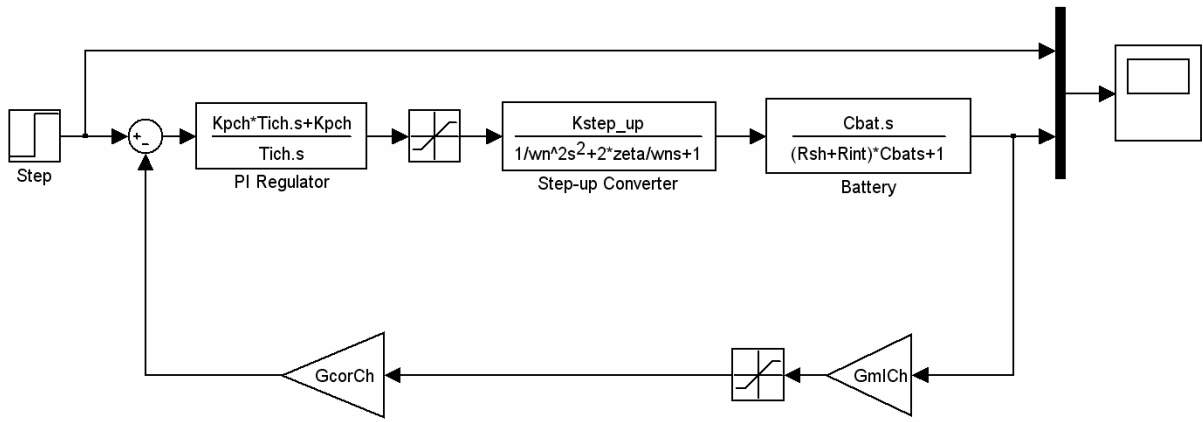


Figure 7-7 : Simulink Model of the Charge Current Control Loop

Step response:

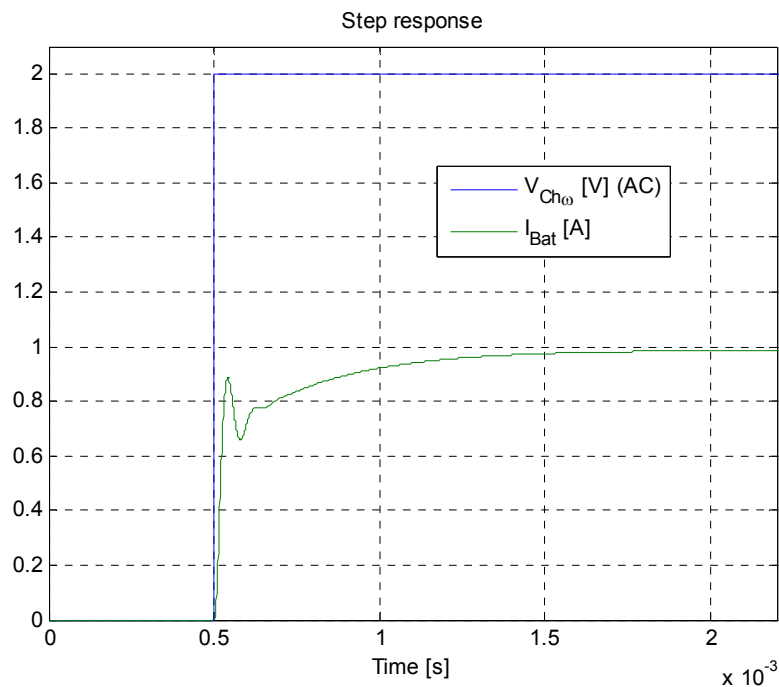


Figure 7-8 : Step response of the charge current control loop with the maximal $V_{Ch\omega}$ command

This response is satisfactory. Even if the command becomes maximal instantly, the charging current will not pass over 1A during the transient. The rise time to reach 95% of the final value is 0.8ms.

7.2 Discharge Current Control Loop

This loop is mainly formed by the step-down converter, the measure system and the regulator PI. Their transfer functions are described below.

For the moment, it is assumed that the battery is a constant voltage source whichever the current intensity provided. This assumption should be reconsidered in a future work because it is not really correct due to the internal resistance of the battery.

7.2.1 Step-down converter

The transfer function of the step-down converter is the same that the step-up one. Only the gain change a little bit:

$$\begin{aligned} K_{\text{Step-down}} &= 0.14 \\ \omega_n &= 2 \cdot \pi \cdot 8 \cdot 10^3 = 50.27 \cdot 10^3 \text{ [rad/s]} \\ \xi &= 0.6 \end{aligned}$$

7.2.2 Bus Capacitor

The transfer function of the bus capacitor is the same that the transfer function of the battery. However the capacity is really lower:

$$G_{\text{Cap}}(s) = \frac{sC_{\text{Cap}}}{1 + s(R_{\text{sh}} + R_s)C_{\text{Cap}}} \quad 7.9$$

Parameters:

$$\begin{aligned} C_{\text{Cap}} &= 440 \text{ [uF]} \\ R_{\text{sh}} &= 0.05 \text{ [\Omega]} \\ R_s &= 0.5 \text{ [\Omega]} \end{aligned}$$

7.2.3 Measure System

The measure system is also the same.

$$G_{mIDe}(s) = 0.61$$

7.10

7.2.4 Gain of correction (input of PI)

Given the fact that the maximal command of the system is different between charge system ($V_{Cho} = 2.05V$ (AC)) and discharge system ($V_{Deo} = 1.25V$ (AC)) the gains of correction will be different.

Transfer function:

$$G_{corDe}(s) = 2$$

7.11

7.2.5 System to control (open loop, without the regulator)

Transfer function:

$$G_{aDe}(s) = G_{Step-down}(s) \cdot G_{Cap}(s) \cdot G_{mIDe}(s) \cdot G_{corDe}(s)$$

7.12

Bode diagram:

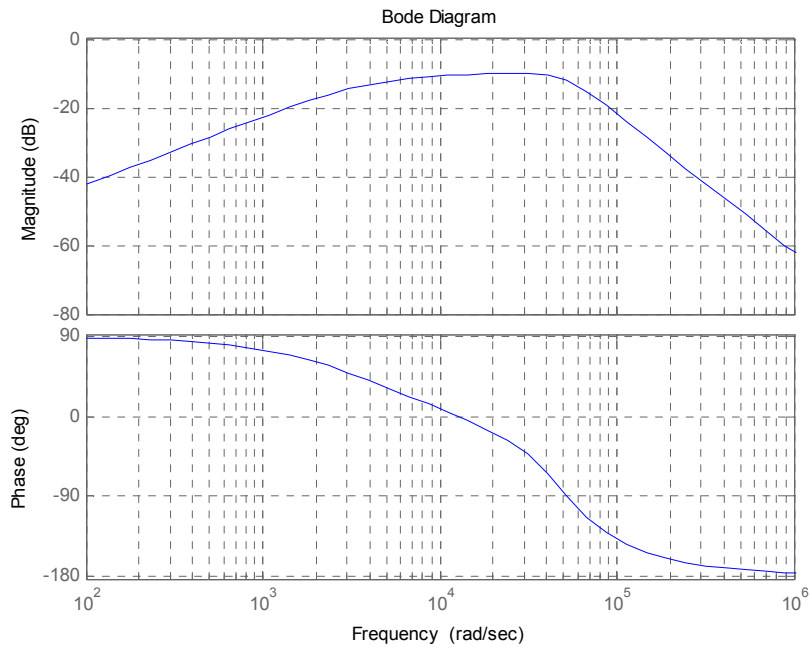


Figure 7-9 : Bode Diagram of $G_{aDe}(s)$

7.2.6 Synthesis of the PI Regulator

Transfer function of the PI regulator:

$$G_{PIDe} = K_{pDe} \frac{1 + sT_{iDe}}{sT_{iDe}} \quad 7.13$$

Parameters choice:

$$K_{pDe} = 6$$

$$T_{iDe} = 10 \cdot (1 / \omega_n) \approx 200 \cdot 10^{-6}$$

Transfer function of the system in open loop with the regulator:

$$G_{oDe} = G_{PIDe} \cdot G_{aDe} \quad 7.14$$

Bode diagrams of the system in open loop (with the PI regulator):

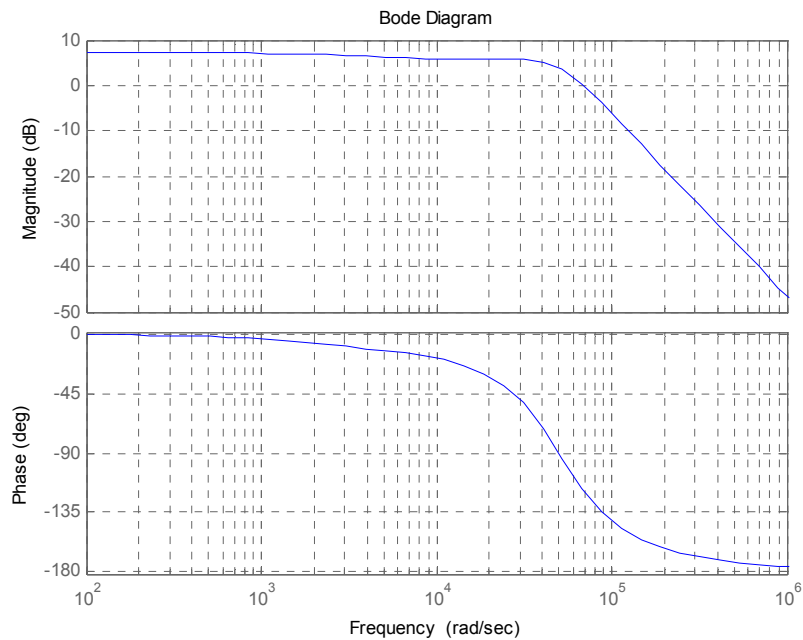


Figure 7-10 : Bode Diagram of $G_{oDe}(s)$

=> Phase margin = 60°

Transfer function of the system in closed loop:

$$G_{wDe} = \frac{G_{oDe}}{1 + G_{oDe}} \quad 7.15$$

Bode diagrams of the system in closed loop:

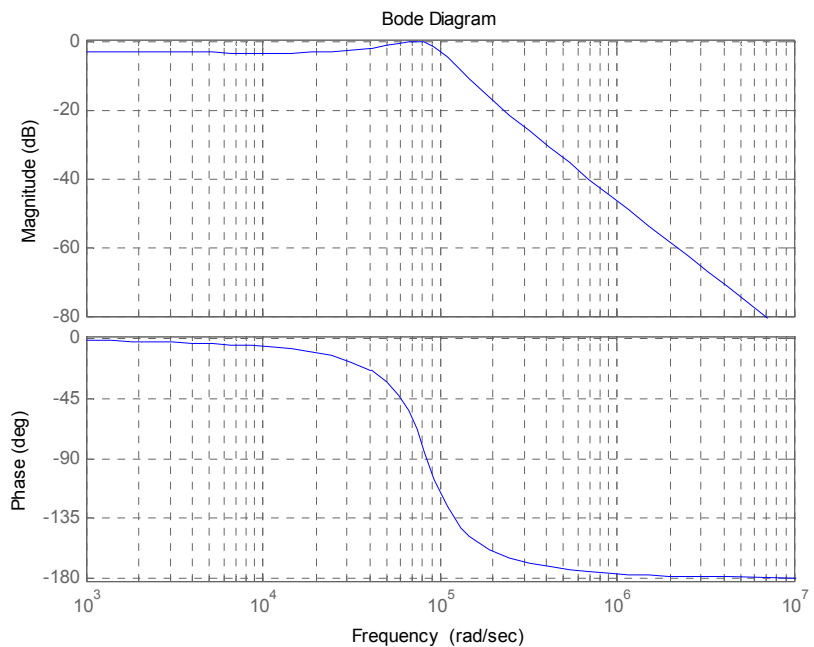


Figure 7-11 : Bode Diagram of $G_{wDe}(s)$

7.2.7 Results of the simulation with Simulink

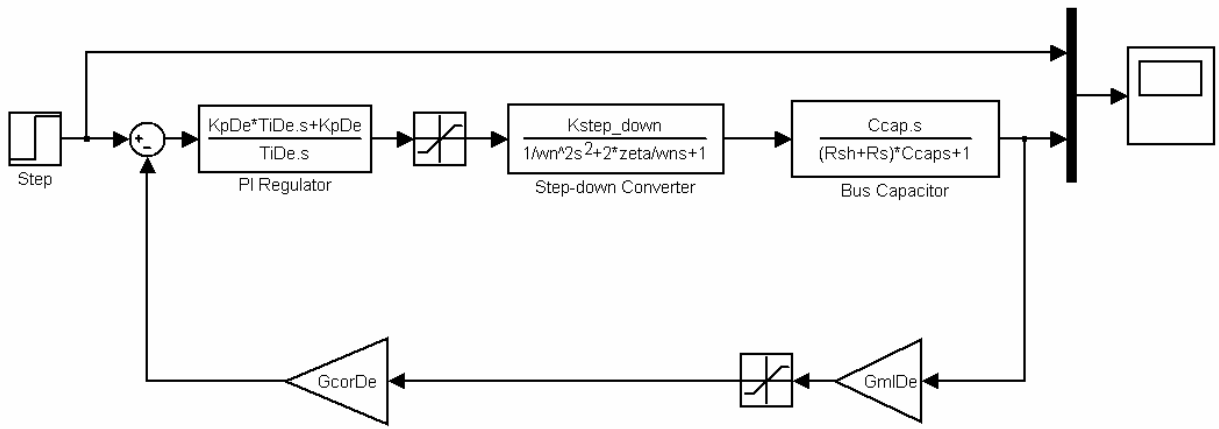


Figure 7-12 : Simulink Model of the Discharge Current Control Loop

Step response:

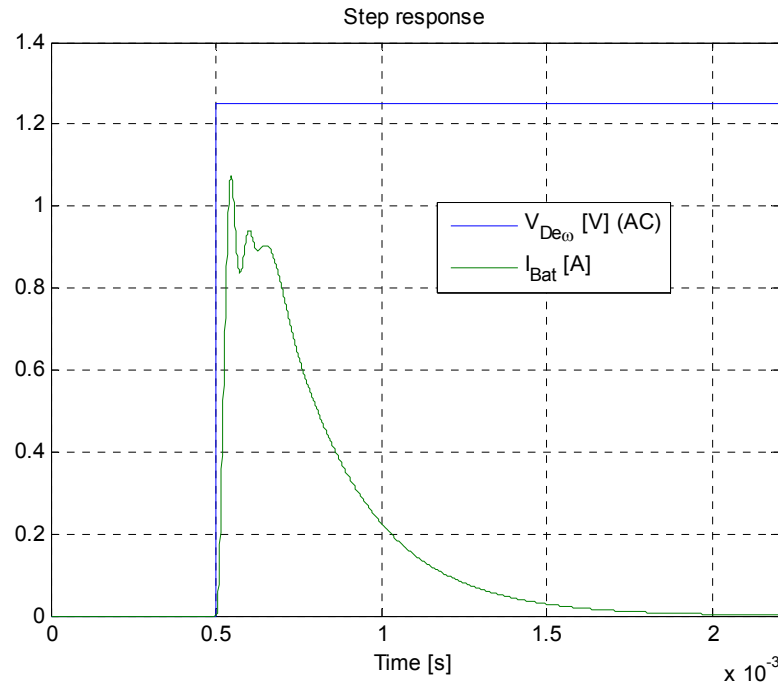


Figure 7-13 : Step response of the charge current control loop with the maximal $V_{Ch\omega}$ command

This response is satisfactory. It is very similar to the step response of the charge system. Given the fact that the capacity is very low in comparison with the equivalent capacity of the battery, it is

normal that the current decrease according to the RC constant. The capacity is full charged after 1.5ms.

7.3 Bus Voltage Control Loop

The charge and discharge current control loop will not work in the same time, but they will be controlled by the same PI regulator. This regulator will control the bus voltage by charging or discharging the battery. So the regulator must be synthesized on both closed loop transfer functions. This will be possible because they are very similar.

After synthesized the PI regulator correctly, the simulation of the bus voltage control loop is successful. There are already a lot of details to give about the results of the simulation but the model still must be improved. So this part will be developed in the final rapport of phase B.

All simulations show that the chosen regulation method is successful. Until end of phase B it will be necessary to prove that it is also possible in a practical design. It will be necessary to determine precisely the limits of the system (specifications).

8 PRELIMINARY TESTS

Abstract

Preliminary tests have been carried out on several devices:

- kill-switches: tests of the DC current limit;
- batteries : tests under vacuum;
- identification of the parameters of the step-up converter on the EPS prototype;
- validation of the first part of the EPS prototype;

8.1 Test of kill-switches

8.1.1 Test 1: DC current through the kill-switch in vacuum

Parameters of the test:

- $I_{\text{test}} = 3.5 \text{ A DC}$;
- $T_{\text{test}} = 25^\circ\text{C}$;
- $P_{\text{test}} = 10^{-2} \text{ mbar}$;
- $D_{\text{test}} = 2 \text{ h}$;

Results:

- Kill-switch unaffected;
- Temperature of the Kill-switch: has not increased;

8.1.2 Test 2: DC current limit (without commutation)

Parameters of the test:

- $I_{\text{test}} = 18 \text{ A DC}$;
- $T_{\text{test}} = 25^\circ\text{C}$;
- $P_{\text{test}} = 1 \text{ bar}$;
- $D_{\text{test}} = 5 \text{ min}$;

Results:

- Kill-switch apparently unaffected;
- Temperature of the Kill-switch has increased: $T_{\text{K-S}} = 50^\circ\text{C}$ after 5 min.

8.1.3 Test 3: DC current limit (with commutation)

Parameters of the test:

- $I_{\text{test}} = 5 \text{ A DC}$;
- $T_{\text{test}} = 25^\circ\text{C}$;
- $P_{\text{test}} = 1 \text{ bar}$;
- Number of commutations: 1

Results:

- Kill-switch breaks down (the contact melted);

Others tests must be carried out to more precisely determine the DC current limit of melting when the switch commutes (TBD).

8.2 Test of batteries

8.2.1 Test 1: Vacuum chamber (mechanical test)

Parameters of the test:

- $T_{\text{test}} = 25^\circ\text{C}$;
- $P_{\text{test}} = 10^{-4} \text{ mbar}$;
- $D_{\text{test}} = 24\text{h}$
- Battery without load

Results:

It appears a swelling of the envelope (on both sides of the battery) during the vacuum test. But this swelling disappears when the pressure is normal again.

The voltage of the cell hasn't change.

Photo of swelling:

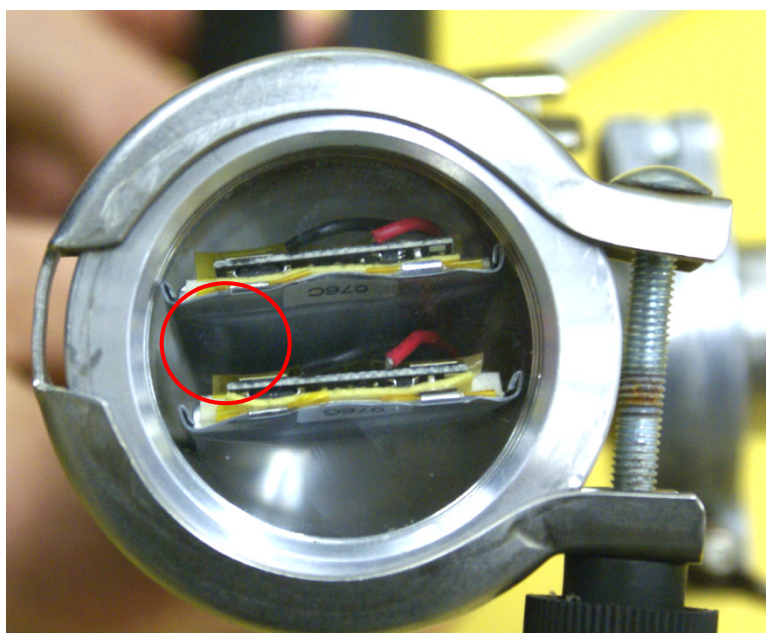


Figure 8-1 : Photo of the battery swelling

Note:

One step at the production of PoLiFlex cells is evacuation. At this step some gases are removed from the cell after formation. The vacuum is less than 100 mbar absolute for only a short time period (some seconds). The cell is open at this step. So, there is no pressure difference between inside and outside the cell. Thus, when putting a PoLiFlex cell under Vacuum it is normal that the envelope swells.

The problem appears if the organic electrolyte evaporates.

The only way that the cells will vent electrolyte is if the seal fails. The seal is designed to cope with variations in internal pressures as the cell charges and discharges. It should only vent when the differential between the internal and external pressure is significant (greater than 1bar).

So, for the moment it is considered that the battery supports the vacuum.

8.2.2 Electrical tests (Vacuum + Temperature variations)

Electrical tests will be carried out during next month.

Here is just an interesting recommendation from VARTA about the electrical characteristic of the battery charge if the temperature is less than 0°C (This situation could appear when the satellite just goes out of the eclipse and begin the charge):

“If you charge the cells at -10°C with higher current you will damage the cell. There will be an irreversible reaction of the Lithium. If you charge the cells at -10°C with a low current (0,2C) it is possible but it is outside our specification”.

8.3 Identification of the parameters of the DC/DC converters

It is important to know that the transfer function of DC/DC converters depends on the load. So it is necessary to identify the parameters of the converters for different loads.

8.3.1 Step-up converter

Parameters of identification:

- Method : Step response with the maximal command ($V_{cmCh} = 0$ to 3.3 V)
- $T_{test} = 25^\circ\text{C}$;

Measure with $I = 0.1$ A;

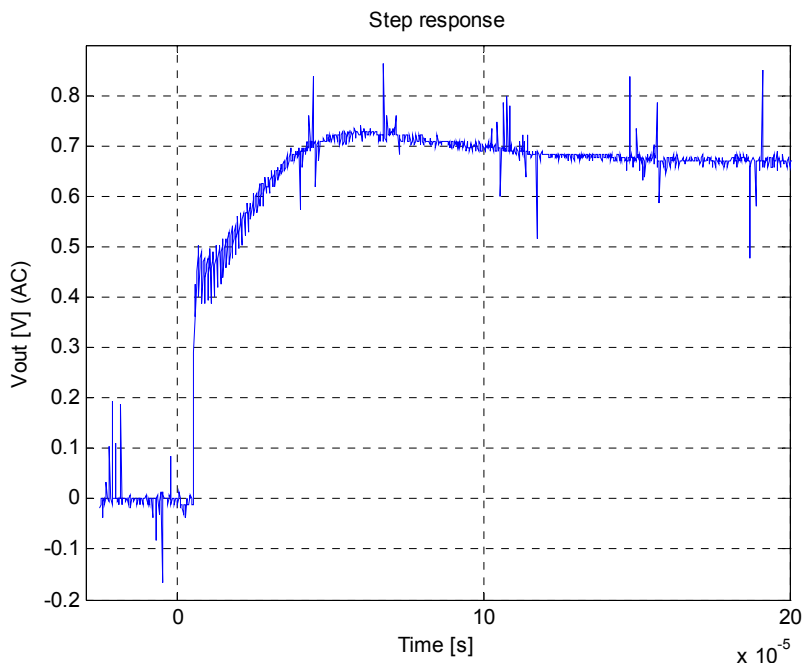


Figure 8-2 : Step response, $I_{test} = 0.1$ A

Measure with $I = 0.5 \text{ A}$;

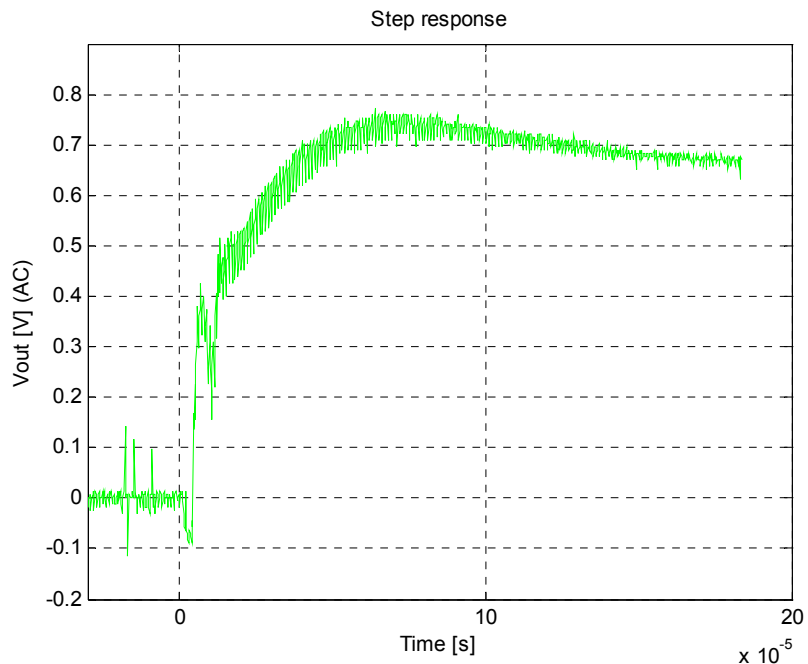


Figure 8-3 : Step response, $I_{\text{test}} = 0.5 \text{ A}$

Measure with $I = 1 \text{ A}$;

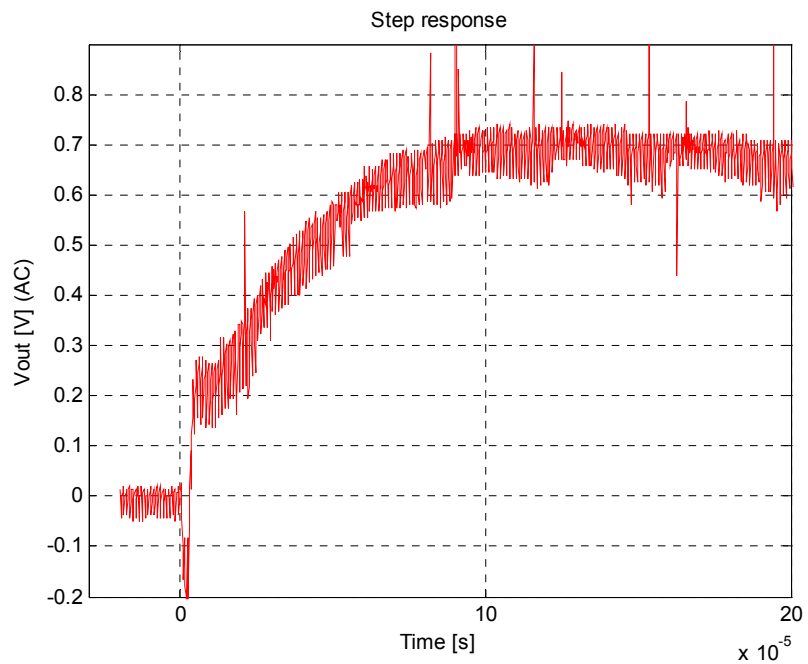


Figure 8-4 : Step response, $I_{\text{test}} = 1 \text{ A}$

In order to model the converter, the step response @0.5A has been taken. Two models have been considered: one model is of 1st order and the other model is of 2nd order.

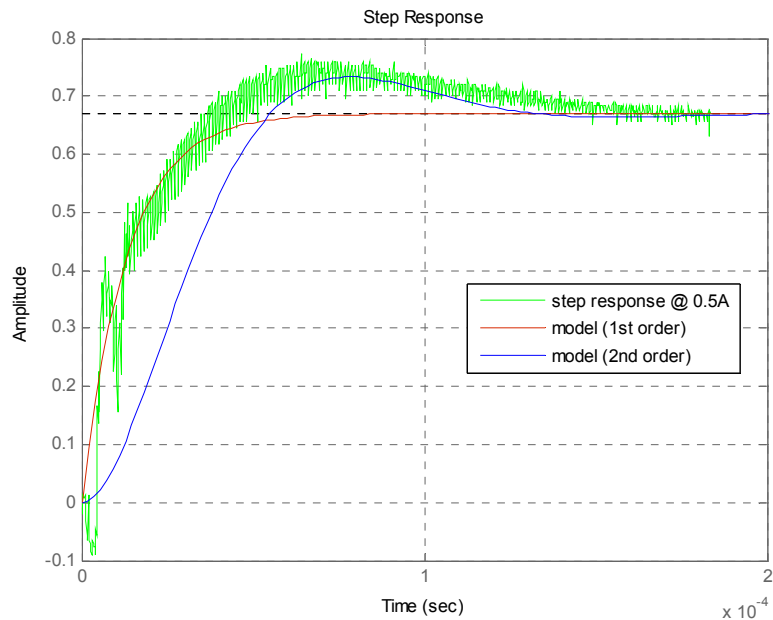


Figure 8-5 : Modelling of the step-up converter

The 2nd order model has been taken for the simulation. As described previously (in the simulation chapter), the parameters of this model are:

$$K_{\text{Step-up}} = 0.2$$

$$\omega_n = 2 \cdot \pi \cdot 8 \cdot 10^3 = 50.27 \cdot 10^3 \text{ [rad/s]}$$

$$\xi = 0.6$$

The real system is more rapid than the chosen model. On the face of it, this is not a problem because if the control loop works well with the model it should work still more rapidly with the real converter (the final value will be more rapidly reached and the ripple should not increase).

8.3.2 Step-down converter

The results are similar.



9 CONCLUSION AND FUTURE WORK

Abstract

This final chapter will present a summary of the results and difficulties of this work of diploma. There is still a large work until EPS is perfectly functional. It is the reason why this chapter will also give a list of the objectives to be carried out until the end of the phase B in order to have a functional engineering model which fits within the requirements.

9.1 Results and Difficulties

9.1.1 Solar Cells

- Three GaAs triple junctions solar cells from RWE have been bought and both of them have been mounted on a plastic support for preliminary test. It was difficult to connect wires on the cells. It will be probably necessary to use ultrasonic welding for the flight model;
- The electrical model is functional and efficient;
- Preliminary measurements have been done and extreme working points are known but it is necessary to make some better measurements with a solar generator and a temperature sensor in order to have a good identification of the cell;
- The preliminary comparison between model and measurements is satisfactory;

9.1.2 Batteries

- One type of VARTA PoLiFlex batteries has been selected and bought. The choice is justified by solid reasons (reliability, performances, etc.);
- The characterization is in progress. Electrical characteristics are well-known. Thermal characteristics are not determined and some tests must still be done (charge-discharge in vacuum);
- The protection module has been identified;
- Vacuum tests have been done: the ‘bag’ of the battery swells in vacuum.

9.1.3 Power management

- Simulations prove that the management strategy of the power system is theoretically functional and efficient;
- The hot redundancy guarantee a good reliability;
- Preliminary tests validate the model of DC/DC converters;
- The measure of the current is not enough precise, it must be improved in order to validate the current control loops;
- The strategy to guarantee a 15 min. delay after jettisoning has been study by another student of EPFL (this decision has been taken after the beginning of the diploma).

9.1.4 Design of electronics

- The electronics has been designed with high reliable components able to support thermal constraints.
- The electronics has been design with high efficient components in order to spare as much energy as possible;
- The PCB routing has been supervised;
- The PCB has been manufactured by Eurocircuit:

- The engineering model tests are in progress. For the moment only the functionalities are tested. In a second step the model will be tested under the conditions of use during the mission;

9.1.5 Kill-switches

- The kill-switches location and redundancy has been studied in order to guarantee the reliability. This part of the work has not been included in the rapport because it will be more developed by a student of EPFL.
- The kill-switches – selected by the “Structure and Configuration” designer – have been tested under the conditions of use during the mission.

9.2 Future Work

Here is a not exhaustive list of the future work:

- 1) Validate the current control loops;
- 2) Validate the bus voltage control loop;
- 3) Design the current limitations for each user.
- 4) Design the 5V step-up converter to supply the RF
The converter has been already selected : LT1613.
- 5) Find an OTP microcontroller also available in Flash.

In order to prevent failures due to the radiations it will be necessary to use an OTP microcontroller. But to develop the program it will be necessary to have the same microcontroller with a flash memory. The manufacturer NEC offers this possibility. This way must be explored.

- 6) Define a priority order to manage the enable of current limitations.
- 7) Define exactly what kinds of measure are made by the microcontroller.

At least:

- Temperature of the batteries (two sensors) => use the TMP35, 36 or 37 of ANALOG DEVICE;
- Voltage of the batteries (two measurements);
- Current generated by each face with two solar cells in series (6 sensors);
- 8) Program the microcontroller.
- 9) Do some analysis of the heat distribution on the PCB with a thermal camera;
- 10) Validate the engineering model (functioning, vacuum, temperature);
- 11) Test the thermal efficiency of the battery with the thermal designer;
- 12) ...



10 REFERENCES

10.1 Normative references

- [N1] ECSS-Q-70-02A
- [N2] Ryan Connolly, “The P-POD Payload Planner’s Guide”, 2000
- [N3] ECSS-Q-30-11A
- [N4] European Preferred Parts List
<https://escies.org/GetFile?rsrid=5280>

10.2 Informative reference

- [R1] James R. Wertz and Wiley J. Larson, “Space Mission Analysis and Design”, 1999
- [R2] Dan Olsson, “A Power System for a Micro-satellite”, Proceedings of the European Space Power Conference, ESA WPP-054, August 1993
- [R3] Edouard Perez, “VEGA launch vehicle User’s Manual”, ARIANESPACE, March, 2006
- [R4] “Power Supply for the AAU Cubesat”, Aalborg University, December, 2001
- [R5] “S3-A-SET-1-0-System_Description”, June, 2006
- [R6] Goeff Walker, “Evaluating MPPT converter topologies using a Matlab PV model”, Department of Computer Science and Electrical Engineering, University of Queensland, Australia
- [R7] Engin Karatepe, “Neural network based solar cell model”, Department of Electrical and Electronics Engineering, Faculty of Engineering, Ege University, Bornova, Izmir 35100, Turkey, September, 2005
- [R8] VARTA PoLiFlex, “Sales program and technical handbook”
- [R9] http://en.wikipedia.org/wiki/Lithium_polymer
- [R10] http://lss.mes.titech.ac.jp/ssp/cubesat/index_e.html
- [R11] <http://www.clyde-space.com/>
- [R12] J. Soler, “Analog Low Cost Maximum Power Point Tracking PWM Circuit for DC Loads”, 2005.
- [R13] F. Mudry, “Circuit à transistors bipolaires”, HEIG-VD, Yverdon-les-Bains, Switzerland, 2006.

11 TERMS, DEFINITIONS AND ABBREVIATED TERMS

11.1 Abbreviated terms

11.1.1 Subsystems abbreviations

ADCS	Attitude Determination and Control System
CDMS	Control and Data Management System
COM	Communication System
EPS	Electrical Power System
MECH	Mechanisms (Antenna deployment)
P/L	Payload

11.1.2 Technical abbreviations

BOL	Beginning Of Life
C	Capacity of the battery
DOD	Depth Of Discharge
DPA	Destructive Physical Analysis
EMC	Electromagnetic Compatibility
EMF	Electromotive Force
EOL	End Of Life
EPPL	European Preferred Parts List
ESR	Effective Series Resistance
GaAs	Gallium Arsenide
Li-Ion	Lithium-Ion
Li-Poly	Lithium-Polymer
LV	Launch Vehicle
MPP	Maximum Power Point
MPPT	Maximum Power Point Tracking
OTP	One Time Programmable
PCB	Printed Circuit Board
PCM	Protection Circuit Module (of VARTA PoLiFlex batteries)

SEL	Single Event Latch-up
SOC	State Of Charge
SSO	Sun-synchronous Orbit
TBC	To Be Confirmed
TBD	To Be Determined

11.1.3 Definitions

Albedo	Albedo is a measure of reflectivity of a surface or body. It is the ratio of total electromagnetic radiation reflected to the total amount incident upon it. The average albedo of Earth is about 30%.
Derating	Derating is the technique employed in power electrical and electronic devices wherein the devices are operated at less than their rated maximum power dissipation taking into consideration the case/body temperature, ambient temperature and pressure and the dissipation design used.
Hot redundancy	A system has a hot redundancy when it doesn't need a command from the Ground Station to be activated. The redundant system is automatically activated when the primary system is defective.
Insolation	Insolation is a measure of solar radiation power incident on a surface. The surface may be a planet or a terrestrial object inside the atmosphere, or any object exposed to solar rays including spacecraft. It may result in radiant heating of the object, or reflection, depending on the object's reflectivity or albedo.

DATE AND SIGNATURE

Yverdon December 19, 2006

Fabien Jordan



ANNEXES



[Annexe 1] RWE Space Solar Power GmbH, Cell Type : RWE3G-ID2/150-8040



[Annexe 2] Electrical schematic of EPS



[Annexe 3] Paper from ESA : “A Power System for a Micro-satellite”



[Annexe 4] PoLiFlex Battery Specifications